reactions

Review

Advances for Biorefineries: Glycerol Hydrogenolysis to 1,3-Propylene Glycol

Martin Nicolás Gatti *, Nora Nancy Nichio and Francisco Pompeo

Centro de Investigación y Desarrollo en Ciencias Aplicadas (CINDECA), Facultad de Ingeniería, Universidad Nacional de La Plata (UNLP)-Consejo Nacional de Investigaciones Científicas y Técnicas (CONICET), 47 No 257, La Plata 1900, Argentina

* Correspondence: martin.gatti@ing.unlp.edu.ar

Abstract: Humanity's growing dependence on non-renewable resources and the ensuing environmental impact thus generated have spurred the search for alternatives to replace chemicals and energy obtained from petroleum derivatives. Within the group of biofuels, biodiesel has managed to expand worldwide at considerable levels, going from 20 million tn/year in 2010 to 47 million tn/year in 2022, boosting the supply of glycerol, a by-product of its synthesis that can be easily used as a renewable, clean, low-cost raw material for the manufacture of products for the chemical industry. The hydrogenolysis of glycerol leads to the production of glycols, 1,2-propylene glycol (1,2-PG) and 1,3-propylene glycol (1,3-PG). In particular, 1,3-PG has the highest added value and has multiple uses including its application as an additive in the polymer industry, the manufacture of cosmetics, cleaning products, cooling liquids, etc. This review focuses on the study of the hydrogenolysis of glycerol for the production of 1,3-PG, presenting the main reaction mechanisms and the catalysts employed, both in liquid and vapor phase. Engineering aspects and the effect of the operating variables to achieve maximum yields are discussed. Finally, studies related to the stability and the main deactivation mechanisms of catalytic systems are presented.

Keywords: biorefinery; glycerol; hydrogenolysis; catalysts; 1,3-propylene glycol

Citation: Gatti, M.N.; Nichio, N.N.; Pompeo, F. Advances for Biorefineries: Glycerol Hydrogenolysis to 1,3-Propylene Glycol. *Reactions* **2022**, *3*, 451–498. https://doi.org/10.3390/reactions3030032

Academic Editor: Dmitry Yu. Murzin

Received: 30 July 2022
Accepted: 31 August 2022
Published: 19 September 2022

1. Introduction

For some years now, society has become aware of the environmental impact generated by the use of fossil resources to obtain energy sources and products for the chemical industry. Thus, the search for alternative sources has been encouraged to replace, in part, the current dependence on non-renewable sources.

In this context, the concept of biomass arises, defined by the technical specification of the European Committee for Standardization (CEN), as any material of biological origin except those belonging to the field of geology that have undergone a mineralization process. Biomass transformation processes, unlike fossil fuels, do not generate toxic residues or pollutants to the environment, and the CO_2 emissions derived from their combustion result in a neutral carbon balance.

Chemical products derived from biomass come from plant biopolymers such as cellulose, hemicellulose, lignin, and starch. From these products, it is possible to obtain different groups of monosaccharides (hexoses and pentoses), carboxylic acids, phenols, and alcohols, among others, depending on the nature of the polymer [1].

With respect to energy sources, they are based on biofuels that have been produced from plant crops (first-generation biomass), plant or animal waste derived from human activities (second-generation biomass), or by fermentative biological processes (third-generation biomass) [2]. For example, bioethanol and biodiesel have experienced increased production in the last decade [3].

In particular, for more than ten years now, biodiesel has undergone the greatest growth worldwide. The expansion of its production has been observed not only in developed

countries such as Germany, Italy, France, and the United States, but also in developing countries such as Brazil, Argentina, Indonesia, and Malaysia [4]. A recent report by the Food and Agriculture Organization of the United Nations (FAO) forecasts that by 2026, production could reach 40 million tons per year, 12% more than in 2016 [5].

In Argentina, biodiesel has been added as another link in the value-added chain of the national agro-industrial complex since 2007, placing Argentina as the fifth large-scale technology producer in the world and among one the most efficient in the world. [6].

From a chemical point of view, biodiesel consists of a mixture of esters from long-chain fatty acids, produced from a catalytic transesterification reaction, using virgin or used vegetable oils or animal fats and short-chain alcohols such as methanol (Scheme 1), ethanol (Scheme 2), or 1-propanol (Scheme 3). Alkali homogenous catalysts are conventionally used for biodiesel production such as NaOH, KOH, $NaOCH_3$, and $KOCH_3$, but also heterogeneous catalysts such as acid solid catalysts (e.g., zeolites, clays, mixed metal oxides, sulfated oxides, sulfonated carbon-based materials, and cation exchange resins) and alkali solid catalysts (e.g., alkali-earth metal oxides, hydrotalcites, alkali zeolites, and supported alkali metals) [7]. For every 10 kg of biodiesel produced, 10 kg of triglyceride source and 1 kg of alcohol are required, generating 1 kg of crude glycerol as a by-product with a purity that varies in the range of 55–90% due to the presence of triglyceride, alcohol, soaps, and catalyst residues, among others [8].

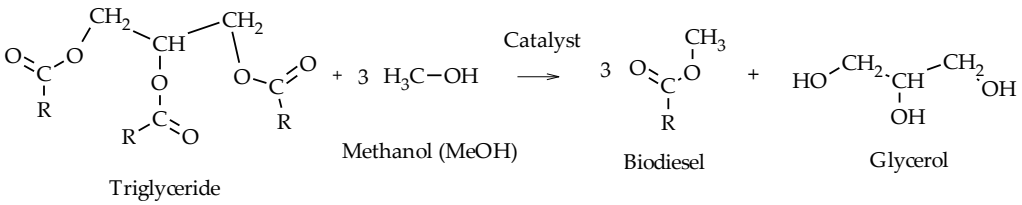

Scheme 1. The transesterification of triglycerides using methanol.

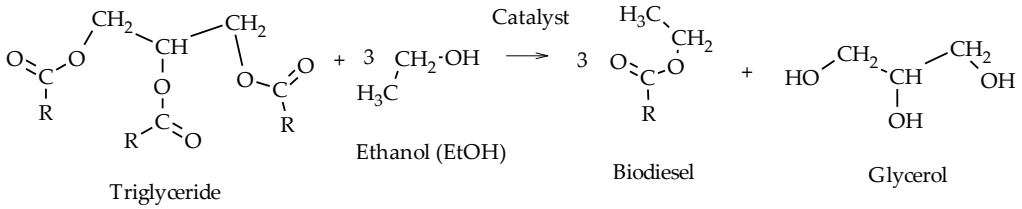

Scheme 2. The transesterification of triglycerides using ethanol.

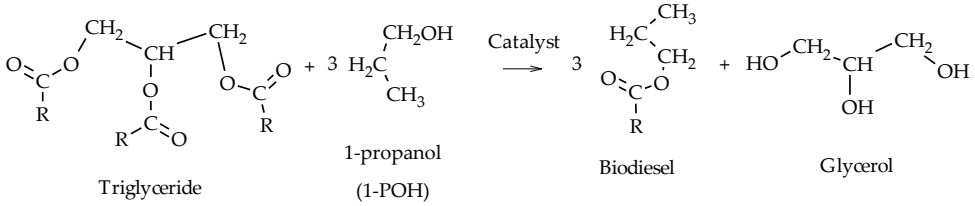

Scheme 3. The transesterification of triglycerides using 1-propanol.

Glycerol is a polyol with three hydroxyl groups and interesting physicochemical properties that allow its application in different industries. Its main application is in the pharmaceutical industry for the production of medicinal drugs (~18%), followed by its use in the cosmetics industry (~16%), polymers (~14%), food (~11%), and in the chemical industry for the manufacture of triacetin (~10%), alkyd resins (~8%), tobacco (~6%), detergents (~2%), cellophane (~2%), and explosives (~2%) (Figure 1) [9].

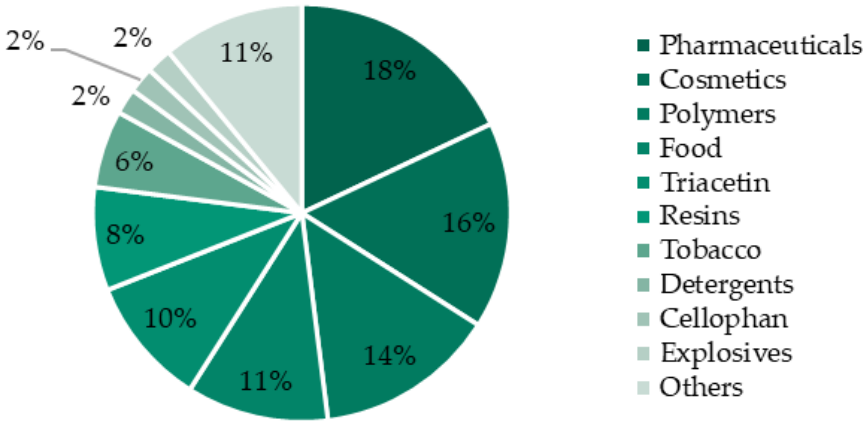

Figure 1. The main glycerol applications.

However, the crude glycerol obtained in biodiesel synthesis has a low level of purity and is not suitable for direct application in the above markets, thus requiring treatment and purification [10]. A fractional distillation process allows technical grade glycerol to be obtained but neither the pharmaceutical nor agri-food market can absorb the entire supply of glycerol. The surplus has oversaturated these markets, devaluing the price of crude glycerol. In the last 10 years, the price of crude glycerol has been between 200 and 400 USD/ton, with the current world average price being in the order of 480 USD/ton (Figure 2) [11].

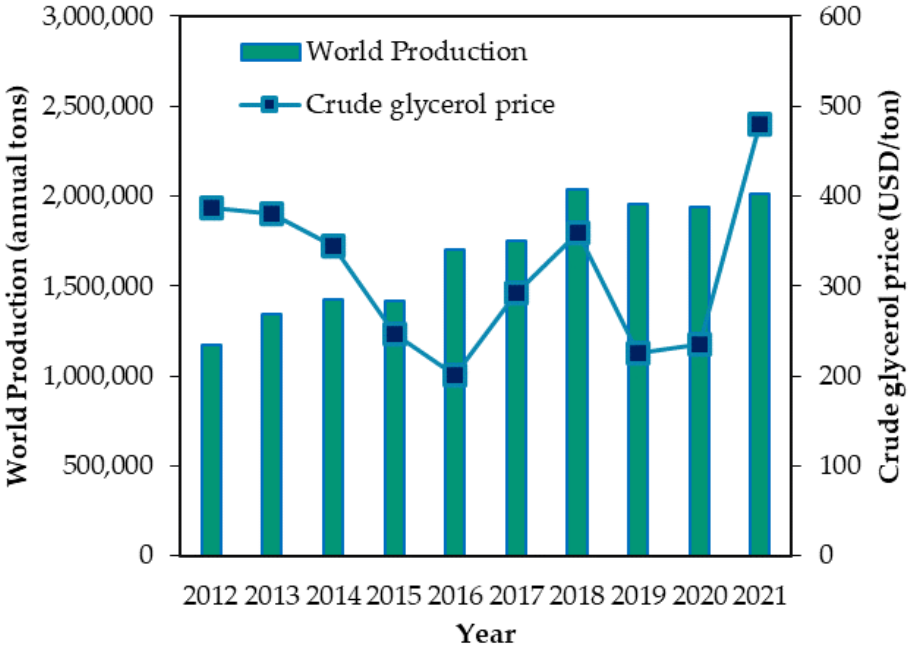

Figure 2. The annual crude glycerol production and market price (2012–2021).

Due to its wide availability and low cost, the search for new alternatives for the transformation of glycerol is very attractive [12]. The chemical functionality of the glycerol molecule makes it a platform molecule for obtaining chemical products and biofuels (Figure 3). Other chemical products can be obtained from glycerol through oxidation [6], nitration [9], polymerization [9], esterification [13], etherification [14], reforming [15], chlorination [16], carbonation [17], dehydration [18], and hydrogenolysis [19].

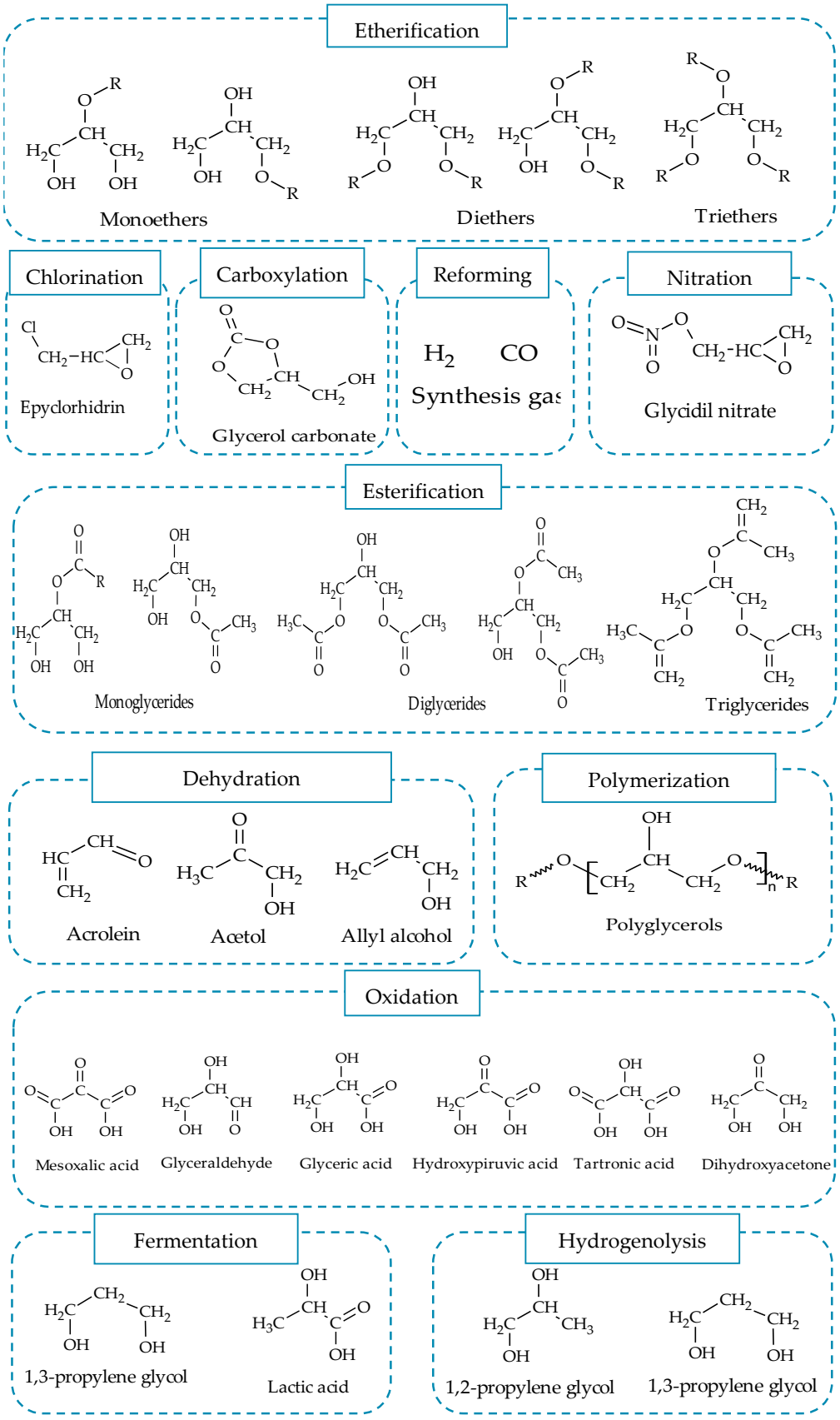

Figure 3. The processes for the transformation of glycerol into high value-added products.

Of all of the processes mentioned, catalytic hydrogenolysis is an interesting alternative due to the high oxygen content in the glycerol molecule (O/C = 1). In this sense, the breaking of C–O bonds of glycerol leads to the formation of glycols such as 1,2-propylene glycol (1,2-PG) and 1,3-propylene glycol (1,3-PG), and C3 alcohols such as 1-propanol (1-POH) and 2-propanol (2-POH), although the breaking of C–C bonds is also present, which allows for the generation of other low molecular weight alcohols such as ethanol (EtOH) and methanol (MeOH). Of these, glycols are the most valuable products, as shown in Figure 4 [20].

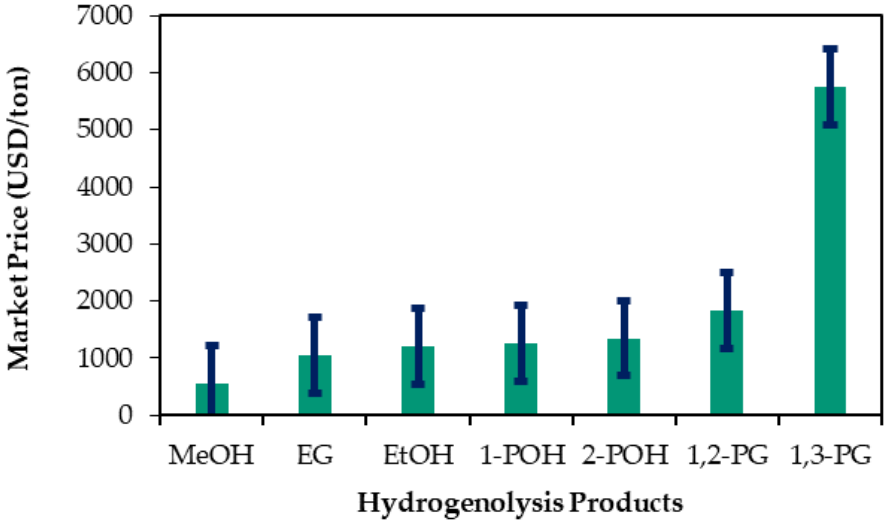

Figure 4. The market prices for the main products of glycerol hydrogenolysis.

From 1988 to the present, more than 450 research papers on glycerol hydrogenolysis have been reported, according to the Scopus database. The number of publications has grown exponentially given the growing interest in the search for an alternative from a renewable source (Figure 5). This growth also accompanies the increase in glycerol production worldwide (Figure 3).

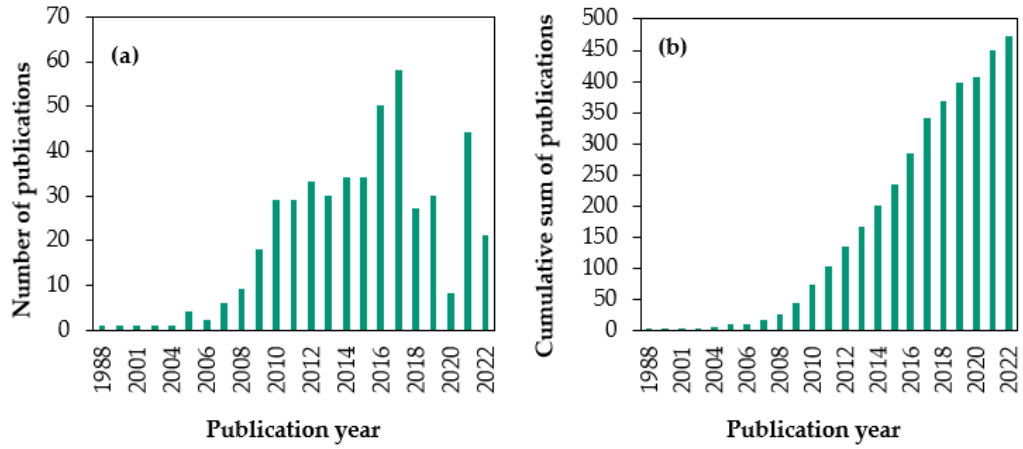

Figure 5. (**a**) The annual number of publications on the hydrogenolysis of glycerol obtained from the Scopus database ("hydrogenolysis of glycerol" as keywords). (**b**) Cumulative sum of publications from 1988 to the present (2022).

Of the total number of papers published to date that have studied the hydrogenolysis reaction of glycerol, 75% were directed to the production of 1,2-PG, while only 21% investigated the production of 1,3-PG and the remaining 4%, the production of 1-POH, 2-POH, and EG. In addition, 92% of this research amount have studied the production of 1,3-PG in the liquid phase, while only 8% studied it in the vapor phase (Figure 6).

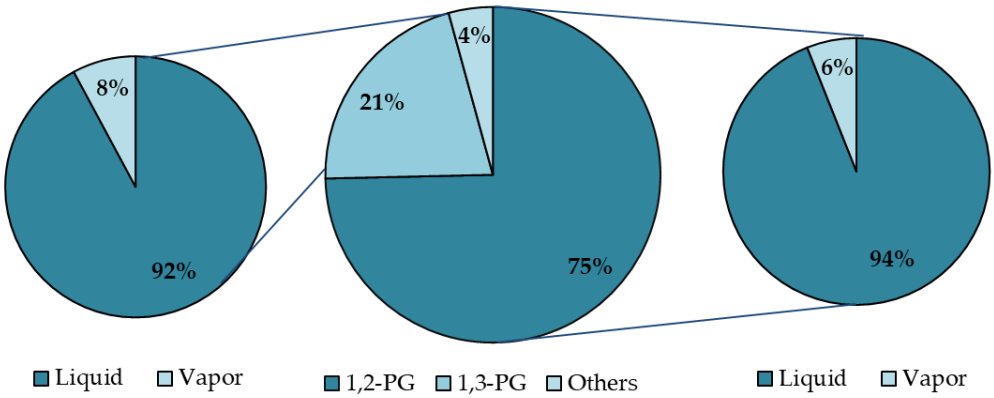

Figure 6. The percentage of publications by product of interest in the liquid and vapor phase.

According to the data presented, clearly the hydrogenolysis of glycerol to 1,3-PG in both the liquid and vapor phase has been the least explored in the literature, and due to its projection in the market, is an attractive option to be studied.

1,3-PG has multiple applications (Figure 7) such as the production of polyethers, polyesters, polycarbonates, and polyurethanes, which account for more than 50% of its productive application [21,22].

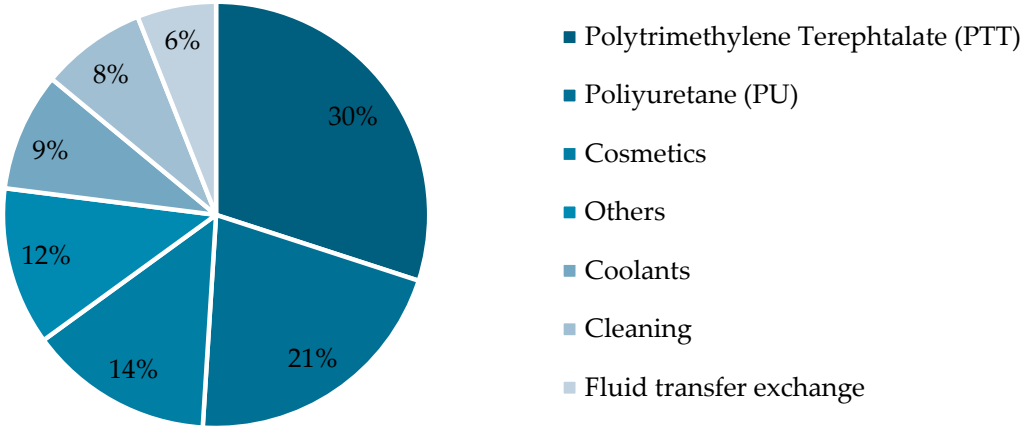

Figure 7. The main 1,3-PG applications.

Currently, 30% of 1,3-PG production is used to manufacture polytrimethylene terephthalate (PTT) from terephthalic acid (Scheme 4), a polymer used in the manufacture of textile fibers and carpets due to its chemical resistance, stability, elastic recovery, and dyeing capacity. In addition, this polymer could be used as a substitute for polyethylene terephthalate (PET) and polybutene terephthalate (PBT), both from the petrochemical industry [23–25].

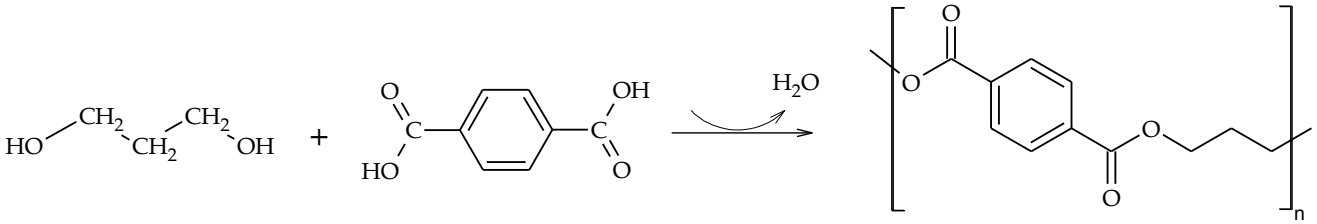

1,3-propylene glycol (1,3-PG) Terephthalic acid (TA) Polytrimethylene terphtalate (PTT)

Scheme 4. The polymerization of 1,3-PG in the presence of terephthalic acid to produce PTT.

About 21% of the 1,3-PG market is used in the manufacture of polyurethane (PU), which is used to make elastomers and plastics. It is also used in the manufacture of cosmetics (14%), as an antifreeze fluid (9%), in the manufacture of cleaning products (8%), and as a heat exchange fluid (6%). Other applications (12%) include its use as an intermediate in the pharmaceutical industry and as an organic solvent for the manufacture of printing inks [26–28].

At present, 1,3-PG is obtained mainly from petrochemical processes (Shell/Degussa-DuPont), although fermentative processes have also been employed (DuPont) [29–32].

In the petrochemical process developed by Shell, 1,3-PG is obtained from the hydroformylation of ethylene oxide (EO) in the presence of synthesis gas (CO + H_2). Initially, ethylene oxide reacts with the synthesis gas, preferably at 10 MPa and 100–150 °C in the presence of a Co–Ru complex dissolved in MTBE to obtain 3-hydroxypropionaldehyde (3-HPA), which is then hydrogenated to form 1,3-PG (Scheme 5) [29].

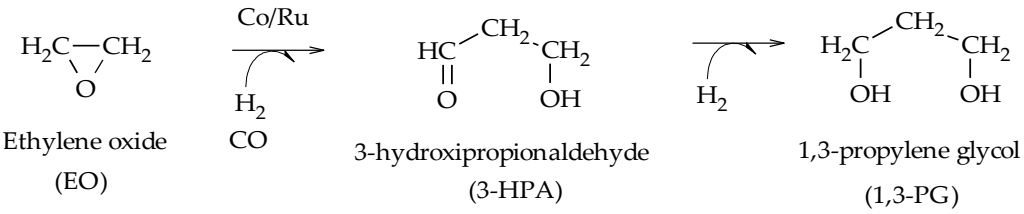

Scheme 5. The formation reaction of 1,3-PG from ethylene oxide (EO).

In the petrochemical process developed by Degussa and later acquired by DuPont, 1,3-PG is obtained by the hydration of acrolein (Acr) and its subsequent hydrogenation. Hydration takes place in an acidic medium at 150–250 °C and hydrogenation in the presence of hydrogen and a Ni Raney catalyst at 13.5 MPa in the range of 60–140 °C (Scheme 6) [30].

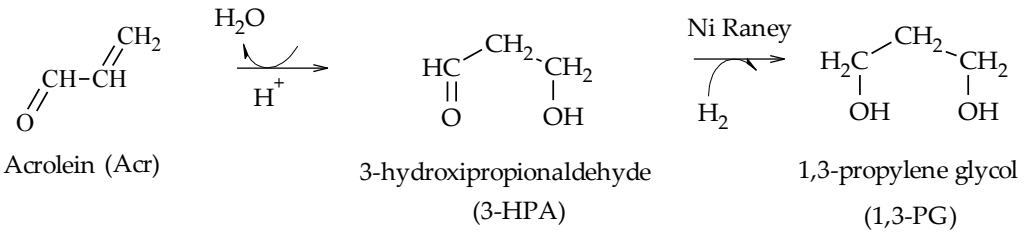

Scheme 6. The formation reaction of 1,3-PG from acrolein (Acr).

Although the petrochemical processes described above are the ones currently used for the production of 1,3-PG, their complexity and the toxicity of the substances involved (such as acrolein) have led us to considering other alternative routes to obtaining glycol.

On the other hand, in the fermentation process developed by Dupont, D-glucose in the presence of E. coli is used for the production of 1,3-PG [31,32]. Although this method has been able to obtain 1,3-PG with a lower content of impurities than those generated by the petrochemical route, the selectivity to 1,3-PG is low due to the generation of other fermentation by-products such as EtOH, ethyl acetate, butyrate, and CO_2. Several articles have been published using different microorganisms (Citrobacter, Clostridium, Enterobacter, Klebseilla, and Lactobacillus) to produce 1,3-PG from glycerol. The formation of secondary products such as succinic acid and acetic acid have also been observed in these studies. Moreover, since the water requirement for these processes is high, the formation of 1,3-PG proceeds very slowly, reaching high yields only at very large reaction times [33–38].

The production of 1,3-PG from the hydrogenolysis of glycerol offers a route based on the principles of green chemistry and is an alternative to the processes above-mentioned, since it would be possible to carry it out in a single reaction stage with the design of suitable catalysts. However, it has been reported that the activation energies for the removal of the primary and secondary –OH groups from the glycerol molecule are very similar

(70.9 kcal/mol and 73.2 kcal/mol, respectively) and their affinity for protons is almost identical (~195 kcal/mol). These characteristics, coupled with steric hindrance, make it more difficult to cleave the secondary C–O bond than the primary one in the glycerol molecule [39]. Thus, the design of catalysts for the formation of 1,3-PG from glycerol is a real challenge.

A number of review papers have so far been published on the subject, focusing their study on the properties of catalysts and their catalytic performance [40–45].

The first one dates back to 2013, published by Feng et al. who, after reviewing the literature data, concluded that catalysts based on Pt, Rh, or Cu in the presence of W chemical species were promising for the production of 1,3-PG, but the relationship between the metal phase and W species was unknown until that time [40]. In 2014, Nakagawa et al. published a review emphasizing the difficulty in selectively obtaining 1,3-PG in glycerol hydrogenolysis and punctuating the fact that noble metal-based catalysts such as Pt and Ir modified with W or Re are especially effective in the production of glycol. The authors elucidated that the hydrogenolysis of glycerol to 1,3-PG is a catalytic structure sensitive reaction and the catalyst composition must be cautiously designed to obtain high yields [41].

In 2020, Wang et al. reported the performance of different Pt–W catalysts and the properties of the catalysts that influence the activity and selectivity toward the formation of 1,3-PG [42]. In 2021, Wu et al. complemented the review by focusing in detail on the relationship between W species and the metal phase to selectively produce 1,3-PG from glycerol [43].

A review article has also reported on the current 1,3-PG market and its growth prospects in future years, considering the current chemical production routes and the development of the latest heterogeneous catalysts aiming at new economically competitive industrial processes [44].

Recently, Zhang et al. published an article about the key factors for the design of active and selective catalysts toward the production of 1,3-PG. They performed a critical review on the electronic effects and steric hindrances at the metal–acid interfaces of catalytic surfaces. Their results provide important insights for manipulating the spatial structure of a given catalyst to produce 1,3-PG selectively [45].

The present review paper proposes to review the articles reporting the hydrogenolysis of glycerol for the production of 1,3-PG focusing on engineering aspects, describing and comparing the catalytic systems used in liquid phase batch reactors and continuous flow reactors, both in the liquid and vapor phase. As an introduction, the main reaction mechanisms and the performance of the main catalysts used are presented, classifying them according to their metallic phase and support. Since the reactor configuration has an impact on the product distribution and catalytic stability, the effect of the operating conditions in the reactors was analyzed and concluded with a review of the stability of the catalytic systems. The novel aspect of this review, in contrast to previously reported works, is the incorporation of a section dedicated to engineering aspects and the effect of reactor parameters, which will serve as a tool to design new effective catalysts and determine their ideal operating conditions to maximize 1,3-PG production.

2. Mechanisms of Glycerol Hydrogenolysis for the Production of 1,3-PG

Hydrogenolysis is a type of reduction reaction in which the breaking of C–O and C–C bonds occurs with the addition of hydrogen, often using catalysts of different natures (Scheme 7). While the breaking of C–C bonds decreases the length of a molecule and fragments it into smaller molecules, the breaking of C–O bonds decreases the oxygen content in the starting molecule, maintaining its total number of carbon atoms.

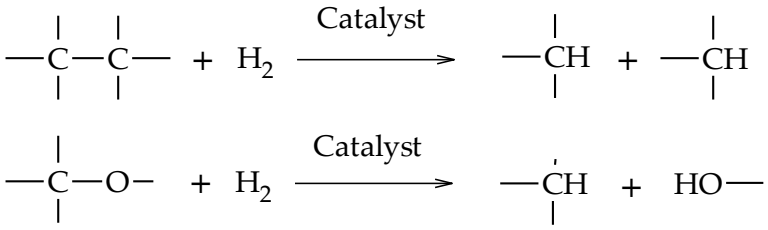

Scheme 7. The C–C and C–O bond cleavage in the catalytic hydrogenolysis reaction.

In particular, the hydrogenolysis of glycerol can lead to the formation of 1,2-PG, 1,3-PG, 1-POH, 2-POH, and propane by the C–O bond cleavage, while the C–C bond cleavage can lead to the formation of EG, MeOH, EtOH, methane, and ethane (Scheme 8) [9].

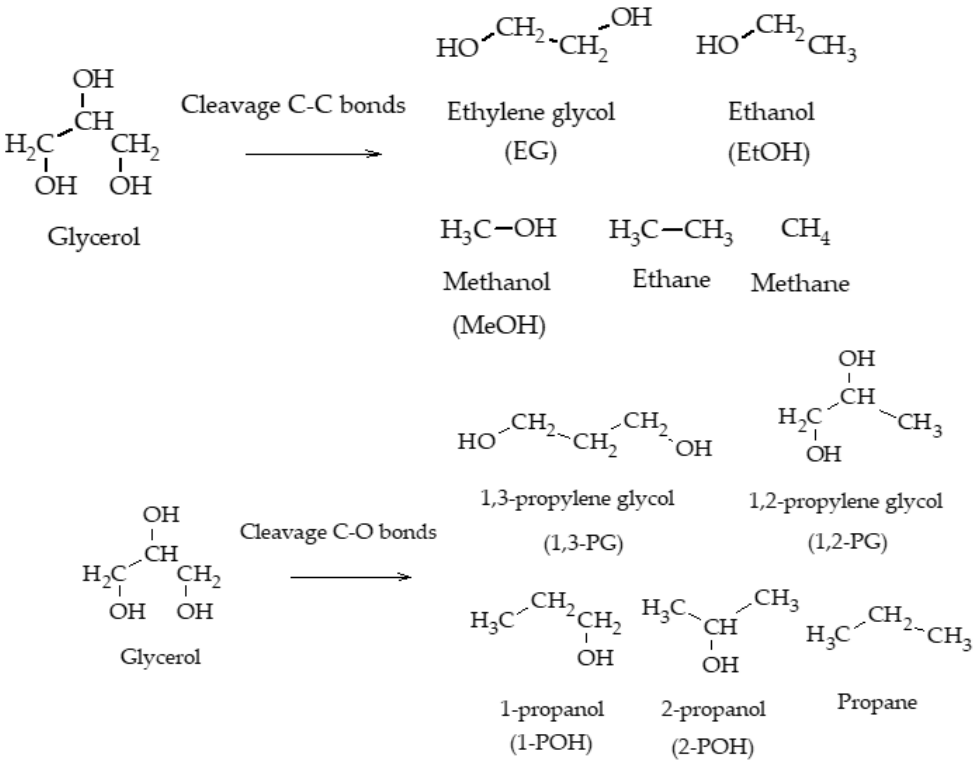

Scheme 8. The formation reaction of 1,3-PG from acrolein (Acr).

The mechanism of the hydrogenolysis of glycerol varies depending on the operating conditions and catalysts employed.

The first of the reports was published by Montassier et al., who studied the selective hydrogenolysis of glycerol solutions at very low concentrations (1–4 wt.%) using a Ru/C catalyst, moderate temperatures (180–260 °C), and high pressures (3–4 MPa) [46]. Their results showed the presence of glyceraldehyde (GLA), 2-hydroxyacrolein (2-HA), and 1,2-PG, suggesting that the reaction proceeded via a mechanism involving the dehydrogenation of glycerol to produce GLA at the metal sites of the catalyst, followed by the dehydration of GLA to produce 2-HA in the presence of a slightly basic aqueous medium, and finally, the hydrogenation of 2-HA to produce 1,2-PG at the metal sites of the catalyst (Scheme 9). Both dehydrogenation and hydrogenation processes take place on the metal sites of the catalyst (Ru particles), while dehydration process occurs because of the basic medium.

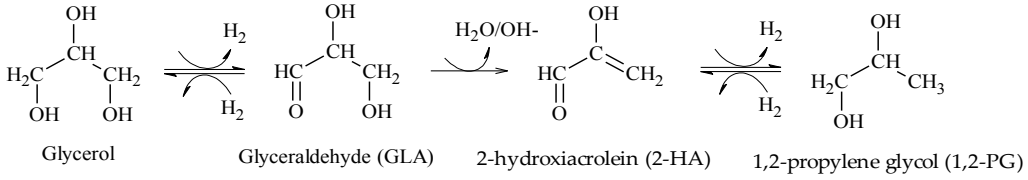

Scheme 9. The reaction mechanism proposed by Montassier et al. for the formation of 1,2-PG.

The dehydrogenation step of glycerol to GLA is thermodynamically disadvantaged due to the presence of H_2, especially when the reaction is carried out at high H_2 pressures. In these cases, GLA can be rapidly hydrogenated back to glycerol. Therefore, to favor the Montassier mechanism, the dehydration step must be very fast, and this can occur in the presence of bases in the reaction medium or basic catalysts.

Montassier et al. proposed two different routes for the formation of side products from C–C bond cleavage reactions.

When a Ru catalyst is employed, they proposed that the formation of EG and MeOH comes from a retro-aldol reaction, as indicated in Scheme 10a. Subsequently, MeOH could be further hydrogenated to generate CH_4 and H_2O. The higher tendency for C–C bond cleavage allows for low molecular weight hydrocarbons such as methane using the Ru catalyst to be obtained.

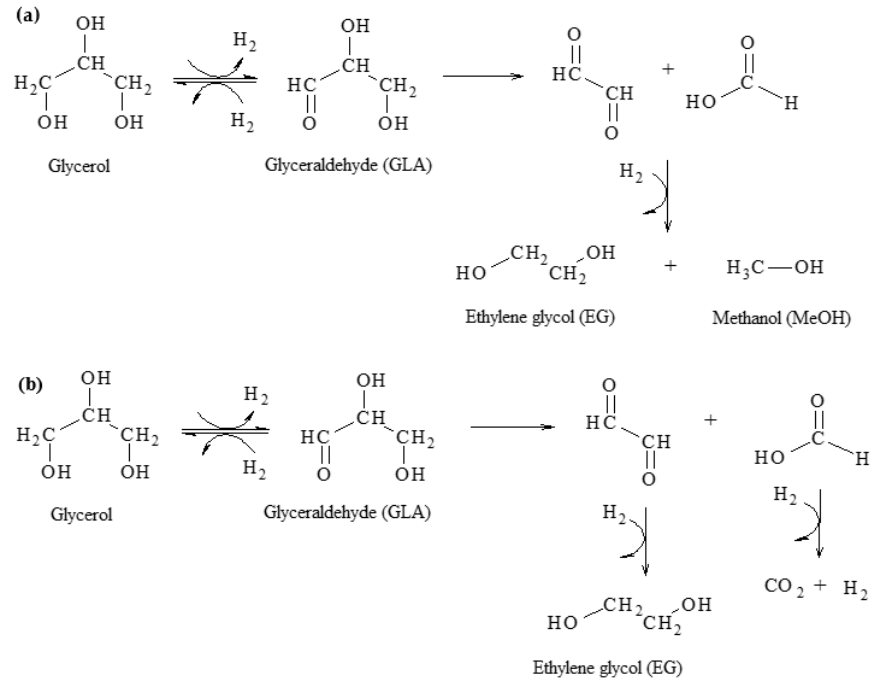

Scheme 10. The reaction mechanism proposed by Montassier et al. for the formation of EG, MeOH, and CO_2 by the (**a**) retro-aldol reaction and (**b**) retro-Claisen reaction.

When a Cu catalyst is used, the authors proposed that the formation of EG comes from a retro-Claisen reaction, as indicated in Scheme 10b. In this case, the ability to cleave C–O bonds with respect to C–C bonds is higher for the Cu catalyst, leading to a lower selectivity to EG and MeOH.

These first results, although not focused on the mechanism of obtaining 1,3-PG, show that the selective conversion of glycerol to propanediols requires bifunctional catalysts that promote both dehydration and hydrogenation reactions.

In this section, each of the reported reaction mechanisms for the formation of 1,3-PG are presented in order of chronological occurrence.

2.1. Mechanism of Dehydration-Hydrogenation

Dasari et al. carried out tests in a liquid phase batch reactor at 200 °C and 1.4 MPa H_2, using a Cu/Cr_2O_4 catalyst with 80 wt.% analytical glycerol solutions and 24 h of reaction time. From their results, they proposed the formation of 1,2-PG from acetol (AcOH) as a reaction intermediate [47]. In this mechanism, glycerol is first dehydrated to AcOH, which is then hydrogenated to form 1,2-PG (Scheme 11). The presence of acid sites in Cu/Cr_2O_4 favor the dehydration step to form AcOH from glycerol, and the presence of the metallic phase of Cu makes the hydrogenation step possible to occur.

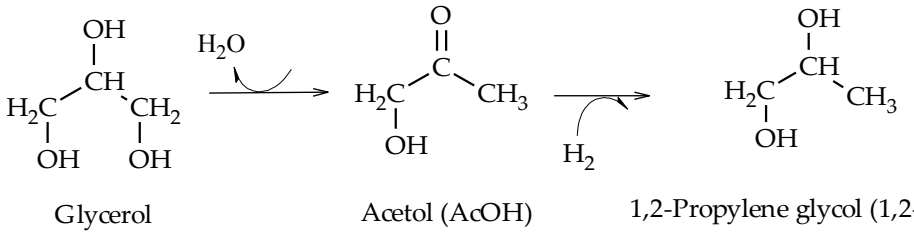

Scheme 11. The reaction mechanism proposed by Dasari et al. for the formation of 1,2-PG.

From the thermodynamic point of view, it has been reported that the formation of 1,2-PG from AcOH is a reversible process in which the direct reaction rate (AcOH → 1,2-PG) is higher than the reverse reaction rate (1,2-PG → AcOH), so it is expected that in the presence of H_2, the route of transformation of AcOH to 1,2-PG is the most favorable one [48]. Recently, Yfanti et al., making use of the in situ IR spectroscopy technique, reported that the formation of 1,2-PG from glycerol occurs via AcOH, and such formation is favored at a higher availability of hydrogen in the reaction medium [49].

Although the reaction mechanism proposed by Dasari et al. includes the formation of neither 1,3-PG nor the 1-POH and 2-POH propanols, their work was important as it was a breakthrough in the study of the reaction mechanism of hydrogenolysis [50].

In 2006, Miyazawa et al. proved that the dehydration of glycerol to AcOH was catalyzed by the use of acidic materials (H_2SO_4, HCl, and Amberlyst resin), and the subsequent hydrogenation of AcOH over the metal sites of the catalyst (Ru, Pt, Rh, Pd) led to the formation of 1,2-PG. Additionally, the results of their tests showed the presence of 1,3-PG for the first time, and a route to obtain it in two stages was proposed by analogy to the formation of 1,2-PG. According to this route, glycerol is first dehydrated to 3-hydroxypropionaldehyde (3-HPA), which is then hydrogenated to generate 1,3-PG (Scheme 12) [51].

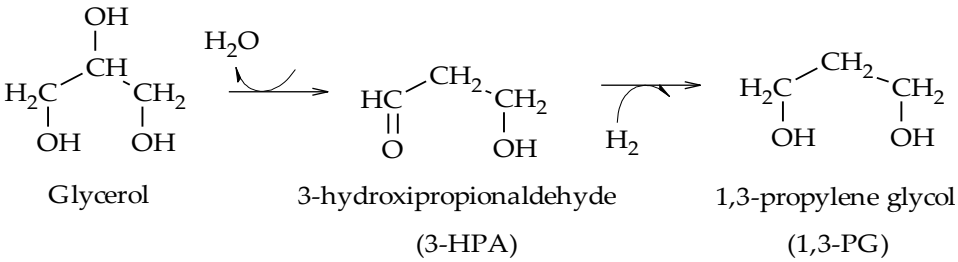

Scheme 12. The reaction mechanism proposed by Miyazawa et al. for the formation of 1,3-PG.

From a thermodynamic point of view, AcOH is a more stable intermediate than 3-HPA, being identified in most scientific reports [40], and the formation of 1,2-PG predominates over the formation of 1,3-PG [52].

Hydrogenation can lead to secondary products such as 1-POH and 2-POH. Miyazawa et al. also proposed the formation of EG and MeOH and the subsequent hydrogenation of EG to produce EtOH (Scheme 13) [51].

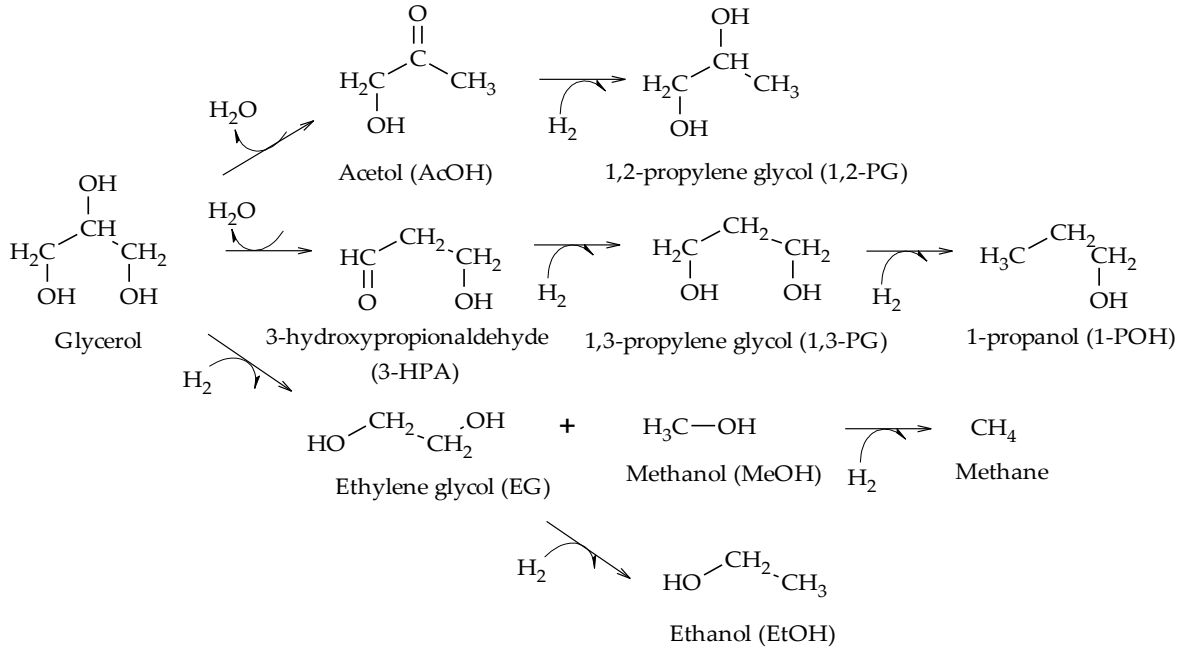

Scheme 13. The mechanism of dehydration–hydrogenation reported by Miyazawa et al.

Maglinao et al. calculated the vapor phase equilibrium K_p constants for several of the reactions involved in this hydrogenolysis mechanism. Regarding the first dehydration step, the reactions were reported to be thermodynamically favorable, both the dehydration of glycerol to AcOH (K_p (190 °C) ~ 7.3×10^9) and the dehydration of glycerol to 3-HPA (K_p (190 °C) ~ 8.2×10^7). These values confirm that the formation of AcOH is more favorable than the formation of 3-HPA. With respect to the second stage, the hydrogenation of the formed intermediates is limited by thermodynamic equilibrium, both the hydrogenation of AcOH to 1,2-PG (K_p (190 °C) ~ 10^{-1}), and the hydrogenation of 3-HPA to 1,3-PG (K_p (190 °C) ~ 2.6×10^{-2}) [53].

The formation of propanols from 1,2-PG and 1,3-PG was reported by Perosa et al. who, using a Ni–Raney catalyst, detected the formation of secondary products. In their reaction scheme, they established the formation of 1-propanol (1-POH) and 2-propanol (2-POH) from 1,3-PG and 1,2-PG, respectively, which in turn can be further hydrogenated to form propane (Scheme 14) [54]. The presence of 1-POH, 2-POH and propane could be explained because of a certain tendency of Ni–Raney to cleave C–O bonds.

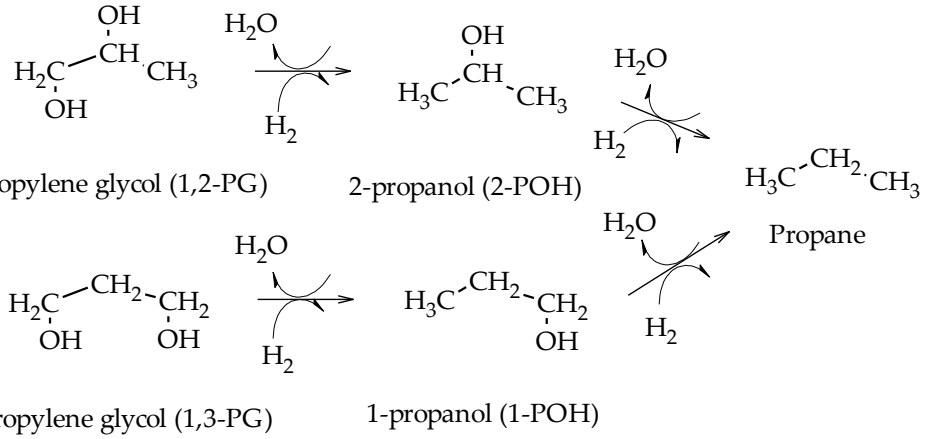

Scheme 14. The process of obtaining 1-POH, 2-POH, and propane from glycols, according to Perosa et al.

Furikado et al. found that the formation of propanols followed a different reaction pathway for Rh/C catalysts with respect to the Ru/C catalysts. In the case of Rh/C, 2-POH is formed from 1,2-PG, whereas for Ru/C, only 1-POH is present, which could come from 1,2-PG [55]. Kunosoki et al. suggested the formation of 1-POH by both 1,2-PG and 1,3-PG hydrogenation, and additionally proposed the formation of MeOH and EtOH from both glycols (Scheme 15) [56].

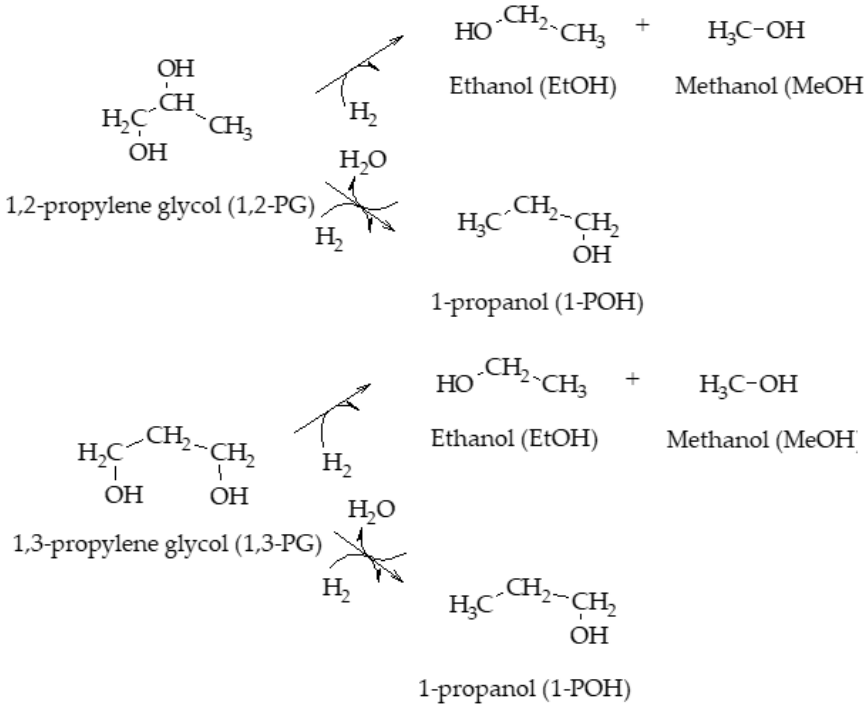

Scheme 15. The reaction pathways for obtaining 1-POH, EtOH, and MeOH from glycols, as proposed by Kunosoki et al.

With respect to EtOH formation, Magliano et al. indicated that although it could occur by the hydrogenolysis of either 1,2-PG or AcOH, the former thermodynamically predominated over the latter. However, as both equilibrium constant values are high, the design and properties of the catalyst determine which of the two reactions has an impact on EtOH formation [48].

2.2. Mechanism of Chelation–Hydrogenation

Chaminand et al. employed Cu, Pd, and Rh catalysts supported on C, ZnO, and Al_2O_3 to carry out the hydrogenolysis reaction at 180 °C and 8 MPa H_2. Of the catalysts studied, Rh/C, promoted by H_2WO_4, allowed 1,2-PG and 1,3-PG to be obtained. By replacing water with different solvents (sulfolane and dioxane), they were able to increase the glycerol conversion and make the reaction more selective to each of these glycols. Based on their results, these authors proposed a mechanism with three probable routes for the formation of glycols. One of them consisted of a chelation step on the metal sites and subsequent hydrogenation in the presence of H_2 (Scheme 16) [57].

The chelation of glycerol on the metal sites of the catalyst (M) and its subsequent hydrogenation suggest that the formation of 1,3-PG is favored over the formation of 1,2-PG due to the stability of the intermediate formed. However, this was the only work that proposed chelation as an intermediate process in the formation of 1,3-PG.

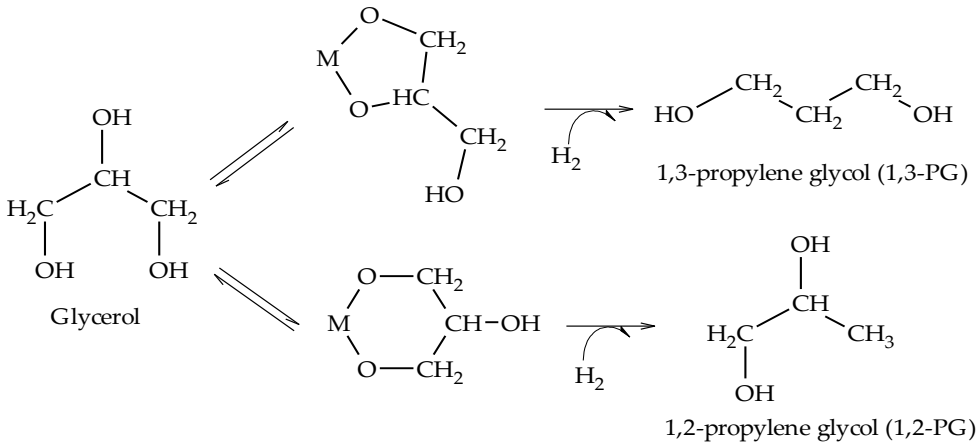

Scheme 16. The mechanism of chelation–hydrogenation as reported by Chaminand et al.

2.3. Direct Mechanism of Hydrogenolysis

Some articles have reported the hydrogenolysis of glycerol through a direct mechanism.

Tomishige et al. reported Ir-MO_x/SiO_2 and Rh-MO_x/SiO_2 (M = Re, Mo, V) catalysts that were studied in the liquid phase reaction, in the range of 100–180 °C and pressures between 2 and 8 MPa of H_2, employing aqueous glycerol solutions between 20 and 100 wt.%. Taking as reference the Ir-ReO_x/SiO_2 and Rh-ReO_x/SiO_2 catalysts, they formulated a direct mechanism of hydrogenolysis based on the formation of hydroxypropoxides on the catalytic surface, leading to the formation of 1,2-PG or 1,3-PG depending on the intermediate formed.

According to this mechanism, as represented in Scheme 17, glycerol adsorbs on the surface sites of the ReO_x species forming 1,3-dihydroxypropoxide or 2,3-dihydroxypropoxide (1st step). Then, H_2, dissociatively adsorbed on the metal surface (Ir or Rh), attacks the tertiary or secondary carbon of the intermediate species, forming 1-hydroxypropoxide or 3-hydroxypropoxide, respectively (2nd step). Finally, these species are hydrolyzed to give rise to the formation of 1,2-PG or 1,3-PG, respectively (3rd step) [58–60].

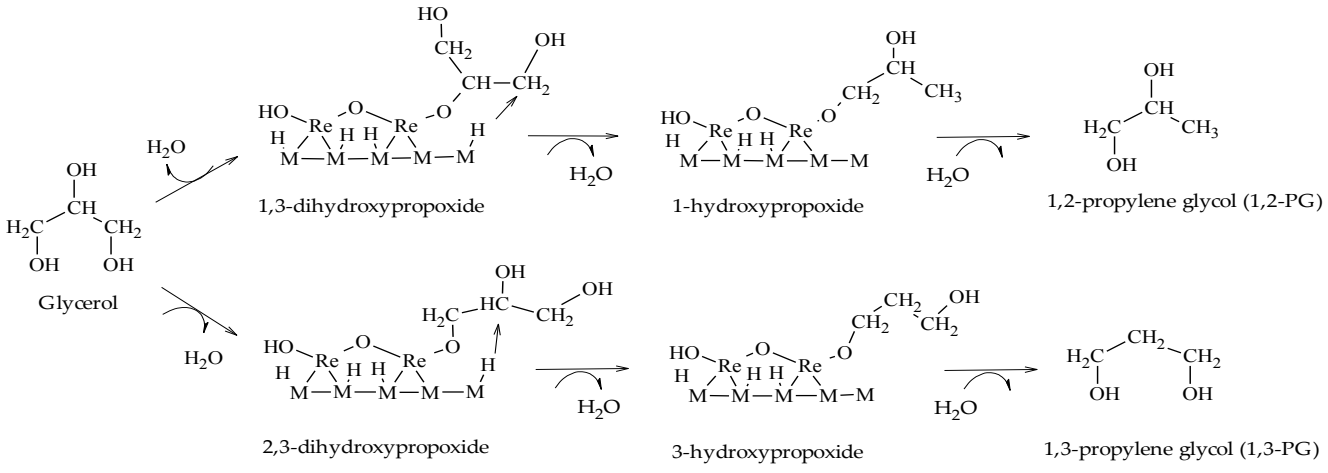

Scheme 17. The direct mechanism of hydrogenolysis over M-ReO_x (M = Ir, Rh) catalysts.

Guan et al. employed Ir-ReO_x/ZrO_2 catalysts and DFT calculations that allowed them to conclude that the formation of 1,3-PG proceeded by a direct reaction mechanism via alkoxide species formed on the ReO_x particles. In this regard, the results showed that the formation of terminal alkoxide species (2,3-dihydroxypropoxide) prevailed over the formation of secondary alkoxide species (1,3-dihydroxypropoxide), whereby the formation of 1,3-PG was favored over the formation of 1,2-PG [61]. These results agree with the catalytic performance of Ir-Re/SiO_2 reported by Tomishige's group [58–60].

Another direct mechanism of glycerol hydrogenolysis was proposed for the $Pt/WO_3/ZrO_2$ [62], Pt/WO_x [63], $Pt/WO_x/AlOOH$ [64], $Pt/WO_x/Al_2O_3$ [65,66], and $Pt/WO_x/SBA\text{-}15$ [67] systems. It has been proposed that on these catalysts, the formation of glycols occurs through an ionic mechanism involving proton and hydride transfer steps on the catalytic surface [62]. Although the mechanism presents variations depending on the support employed, the formation of glycols (1,2-PG or 1,3-PG) starts with the adsorption of glycerol on the support and the adsorption of H_2 through a heterolytic cleavage into H_+ and H^- on the metal sites of the active phase (1st step). Next, protonation and dehydration of the adsorbed glycerol occurs to form a primary (I) or secondary (II) oxocarbenium type intermediate, depending on the attack of the H^+ on the primary or secondary –OH group of the adsorbed glycerol (2nd step). Finally, the H^- ions are transferred to the oxocarbenium (I) or (II) ions to form 1,2-PG or 1,3-PG, respectively (3rd step) (Scheme 18).

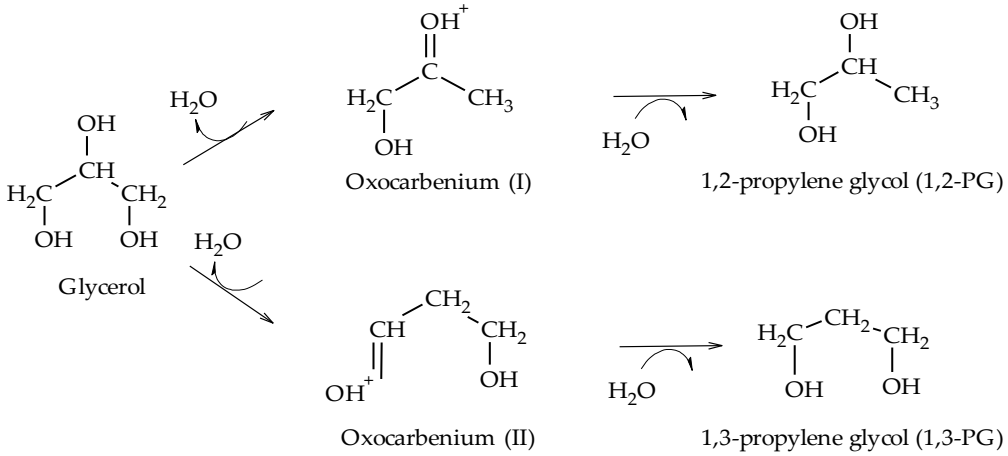

Scheme 18. The direct mechanism of hydrogenolysis over the $Pt/WO_x/S$ catalysts.

It has been reported that the choice of support (S) in the $Pt/WO_x/S$ catalysts plays a fundamental role in the reaction mechanism since it disperses and stabilizes the Pt metal particles and WO_x species [63]. The presence of WO_x species is fundamental because they allow for a better dispersion of Pt, which facilitates the heterolytic cleavage of H_2 molecules into H^+ and H^- [63,65], and on the other hand, they provide sites for the adsorption of glycerol and the stabilization of intermediate carbocations [66]. According to recent reports, WO_x species have the character of Brønsted acids and favor the formation of 1,3-PG [67].

Theoretical studies based on DFT calculations have shown that oxocarbenium-type intermediates are relatively stable and that the formation of other enol-type intermediates from oxocarbeniums is therefore unlikely [68].

2.4. Mechanism of Etherification–Hydrogenation

Wang et al. proposed the formation of glycidol as a reaction intermediate for the formation of 1,2-PG, although no other authors have mentioned the presence of this intermediate. They employed Cu–ZnO catalysts, prepared by the coprecipitation method, at 180–240 °C and 4.2 MPa H_2. The results showed that the hydrogenolysis of glycerol occurred via a bifunctional mechanism involving the dehydration of glycerol to AcOH and glycidol on the surface of ZnO particles and the hydrogenation of these intermediates on Cu particles. Both glycerol conversion and selectivity to 1,2-PG depend on the sizes of the ZnO and Cu particles. The authors proposed a new pathway for the formation of 1,2-PG, which is presented in Scheme 19 [69].

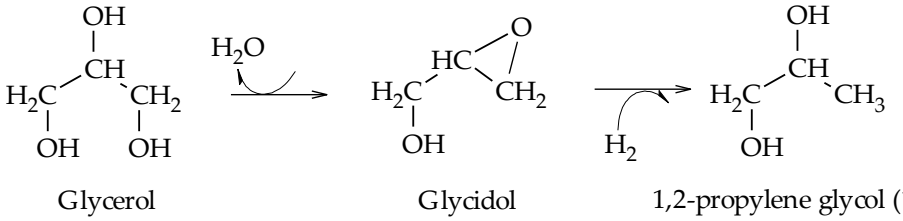

Scheme 19. The etherification–hydrogenation mechanism to obtain 1,2-PG.

Recently, Gebretsadik et al. employed Ni, Cu, and Ni–Cu catalysts supported on saponite and modified with transition metal oxides (V, Mo, W, Re), thus completing the etherification–hydrogenation mechanism by incorporating the formation of 1,3-PG. Their results showed that Cu–ReO_x allows obtaining 1-POH via deoxygenation–hydrogenation reactions, while Ni–ReO_x mainly favors the formation of 1,3-PG. On the other hand, the ReO_x-modified saponite support favors the formation of condensation products (Scheme 20) [70].

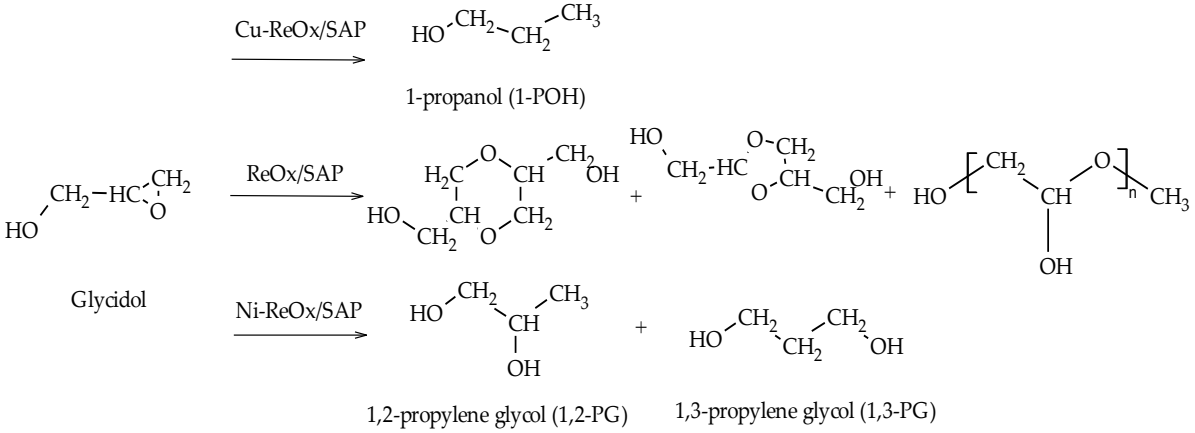

Scheme 20. The mechanism of etherification–hydrogenation via glycidol.

3. Catalysts for 1,3-PG Production

This section presents the most relevant results of the activity and catalytic properties of the catalysts used for the production of 1,3-PG, differentiating them according to the metal phase and the type of reactor, both in the liquid and vapor phase.

3.1. Pd, Ru, and Rh Catalysts

The first results with a certain tendency to form 1,3-PG were obtained using homogeneous phase catalysts based on Pd, Ru, and Rh as the active phase. Table 1 summarizes the results obtained in the liquid phase batch reactors.

Table 1. The hydrogenolysis of glycerol to 1,3-PG using homogeneous Pd, Ru, and Rh catalysts operating in liquid phase batch reactors.

Catalyst	T (°C)	P (MPa)	m_{gly}/m_{Me}	t (h)	X (%)	$S_{1,3\text{-PG}}$ (%)	$Y_{1,3\text{-PG}}$ (%)	Ref.
Rh + H_2WO_4	200	31.6	335.1	24	47.7	43.9	20.9	[71]
Pd-BCPE	140	NR	1420.7	10	7.8	30.8	2.4	[72]
Ru complex	110	5.2	100	19	NR	42.0	3.0	[73]

m_{gly}/m_{Me}—glycerol/metal mass ratio; NR—not reported; X—glycerol conversion; $S_{1,3\text{-PG}}$—selectivity to 1,3-PG; $Y_{1,3\text{-PG}}$—yield to 1,3-PG.

One of the first references dates back to a patent developed by Che, who reported that by employing a catalyst composed of Rh and H_2WO_4 in the presence of 1-methyl-2-pyrrolidinone as the solvent, it is possible to achieve a glycerol conversion of 47% with a

selectivity to 1,3-PG of 43% at 200 °C and 31.6 MPa of a CO/H_2 (1:2) mixture after 24 h of reaction [71].

In another patent, Drent et al. employed a Pd-1,2-bis(1,5-cyclooctylenphosphino) ethane (Pd-BCPE) catalyst in a water/sulfolane (10:10) medium at 140 °C and 6 MPa of a CO/H_2 mixture (20:40) and obtained selectivity values to 1,3-PG of about 30% with glycerol conversions of about 7%, leading to low yields of 1,3-PG (~2%) [72].

Bullock et al. reported the use of homogeneous Ru catalysts in a sulfolane medium for the production of 1,3-PG. Under moderate temperature and pressure conditions, 110 °C and 5.2 MPa H_2, they obtained very low yields to 1,3-PG (~3%) [73].

The difficulty in separating the homogeneous catalyst and recovering it from the reaction product mixture has led to the consideration of heterogeneous phase catalytic systems.

Given the superior activity of Rh-based homogeneous catalysts, the first supported catalysts used Rh as the active phase. Table 2 summarizes the main results obtained with these catalysts used in liquid-phase batch reactors.

Table 2. The hydrogenolysis of glycerol to 1,3-PG using Rh catalysts operating in liquid phase batch reactors.

Catalyst	T (°C)	P (MPa)	m_{gly}/m_c	t (h)	X (%)	$S_{1,3\text{-PG}}$ (%)	$Y_{1,3\text{-PG}}$ (%)	Ref.
Rh/SiO_2	120	8.0 (H_2)	2.7	10	14.0	9.8	1.3	[55]
Rh/SiO_2 + Amberlyst	120	8.0 (H_2)	2.7	10	29.3	5.4	1.5	[55]
$Rh/C + H_2WO_4$	180	8.0 (H_2)	28.0	10	1.3	20.9	0.2	[56]
$Rh/C + H_2WO_4$	180	8.0 (H_2)	2.5	168	32.0	12.0	3.8	[57]
$Rh/Cs_{2.5}H_{0.5}[PW_{12}O_{40}]$	180	0.5 (H_2)	5.2	10	6.3	7.1	0.4	[74]
$Rh\text{-}ReO_X/SiO_2$	120	8.0 (H_2)	400.0	96	61.3	19.7	12.0	[75]

m_{gly}/m_c—glycerol/catalyst mass ratio; X—glycerol conversion; $S_{1,3\text{-PG}}$—selectivity to 1,3-PG; $Y_{1,3\text{-PG}}$—yield to 1,3-PG.

Chaminand et al. tested Rh/C catalysts in the presence of H_2WO_4 and found very low activity levels for the formation of 1,3-PG. However, their work revealed that, unlike other acids such as HCl, the addition of H_2WO_4 favored the first stage of development of the intermediate in the formation of 1,3-PG [57]. Later, Kunosoki et al. tested the activity of Ru/C, Pt/C, Pd/C, and Rh/C catalysts in the hydrogenolysis of glycerol to 1,2-PG and 1,3-PG [56]. With respect to the hydrogenating activity, they found the following order of activity:

$$Ru/C > Pt/C > Rh/C > Pd/C$$

Following the work of Chaminand et al., the results by Kunosoki et al. confirmed that Rh is an interesting metal for obtaining 1,3-PG due to the selectivity values obtained with respect to Ru, Pt, and Pd. By also adding H_2WO_4 to the reaction medium in the presence of Ru/C and Rh/C, they obtained a marked increase in the selectivity to 1,3-PG in the presence of Rh/C, suggesting the existence of a Rh–W bond that favors the production of glycol [56]. Surprisingly, there have been no studies following up on this idea.

Furikado et al. tested Rh/SiO_2 catalysts that were equally selective to 1,3-PG as Rh/C catalysts. In the presence of an Amberlyst resin in the reaction medium, the activity levels improved, but there was no substantial change in selectivity to 1,3-PG [55]. Other Rh-based systems on heteropolyacids, $Cs_{2.5}H_{0.5}[PW_{12}O_{40}]$, also showed some tendency to form 1,3-PG [74]. However, in all cases, the yield to 1,3-PG was very low (<4%).

Higher, but still low yields (12%) were obtained by employing a ReO_x-modified Rh/SiO_2 catalyst. The results indicated that the acidic properties of the ReO_x particles favored the formation of the reaction intermediate, leading to the formation of 1,3-PG following the direct mechanism of hydrogenolysis [75].

These results, although showing low yields to 1,3-PG, proved that the presence of an active hydrogenating phase and acidic chemical species such as H_2WO_4 or ReO_x particles is promising for the development of improved catalysts for the production of 1,3-PG.

3.2. Ir Catalysts

Ir catalysts and their bimetallic combinations with Ni, Co, Re, and Ru have been reported with some activity for the formation of 1,3-PG. Reports have employed these catalysts in the liquid phase using batch reactors (Table 3).

Table 3. The hydrogenolysis of glycerol to 1,3-PG using Ir catalysts operating in liquid phase batch reactors.

Catalyst	T (°C)	P (MPa)	m_{gly}/m_c	t (h)	X (%)	$S_{1,3\text{-PG}}$ (%)	$Y_{1,3\text{-PG}}$ (%)	Ref.
Ir-ReO_x/SiO_2	120	8.0 (H_2)	26.7	36	81.0	47.0	38.0	[60]
Ir/γ-Al_2O_3	200	2.5 (H_2)	6.6	12	6.6	6.5	0.4	[76]
Ir-Ni/γ-Al_2O_3	200	2.5 (H_2)	6.6	12	23.0	3.0	0.7	[76]
Co-Ir nanorods	200	3.0 (H_2)	66.7	12	82.4	23.1	20.8	[77]
Ir-ReO_x/SiO_2	120	8.0 (H_2)	26.7	24	33.7	46.2	15.6	[78]
Ir-ReO_x/SiO_2	120	8.0 (H_2)	25.0	24	69.0	47.0	32.4	[79]
Ru-Ir-ReO_x/SiO_2	120	8.0 (H_2)	26.7	24	77.9	38.9	30.3	[80]
Ir-ReO_x/TiO_2	120	8.0 (H_2)	26.7	8	69.0	52.0	36.0	[81]
IrO_x/H-ZSM-5	180	8.0 (H_2)	2.4	24	63.0	38.0	23.9	[82]
Ir-ReO_x/H-ZSM-5	220	4.0 (H_2)	42.0	8	14.9	19.0	2.8	[83]
Ir-Re/KIT-6-R	120	8.0 (H_2)	26.7	12	39.7	37.1	14.7	[84]
Ir-Re/SiO_2-Al_2O_3 (-Al)	120	8.0 (H_2)	26.7	12	54.5	38.9	21.2	[85]

m_{gly}/m_c—glycerol/catalyst mass ratio; X—glycerol conversion; $S_{1,3\text{-PG}}$—selectivity to 1,3-PG; $Y_{1,3\text{-PG}}$—yield to 1,3-PG.

Low yields (<1%) were obtained by employing Ir/γ-Al_2O_3 catalysts and their modification with Ni, Ir-Ni/γ-Al_2O_3, even though the presence of the metal produced an increase in glycerol conversion. For these catalysts, the species responsible for the activity were IrO_2 and $IrCl_x$ coming from the decomposition of the precursor $H_2IrCl_6.xH_2O$ [76]. In contrast, Co–Ir nanorods (Co:Ir = 100) were shown to be more active toward the formation of 1,3-PG, essentially due to the morphology of these structures and the exposure of their {10-10} crystalline planes [77].

Ir–Re based catalytic systems such as Ir-ReO_x/SiO_2 showed even higher yields due to a promoting effect by Re [59–61,78,79,86,87]. The presence of ReO_x particles results in the formation of 2,3-dihydroxypropoxide from glycerol. Then, gaseous hydrogen, activated on the metal sites of Ir under the hydride form, attacks the 2-position of 2,3-dihydroxypropoxide to form 3-hydroxypropoxide, which finally hydrolyzes to lead to the formation of 1,3-PG (Figure 8) [59].

Modifying the Ir/SiO_2 catalyst with other oxides based on W, Mo, V, Cr, Mn, and Ag, Amada et al. found that the selectivity to 1,3-PG varied in the following order:

$$Re > W > V > Mo > Cr > Mn \sim Ag$$

Their study determined that the cleavage of the C–O bond occurred at the interface between the metal surface of the Ir and the ReO_x particles, where the substrate was adsorbed [60]. Unlike other promoters, ReO_x allows for the formation of a terminal alkoxide, leading to the formation of 1,3-PG instead of a secondary alkoxide that would favor the formation of 1,2-PG [61].

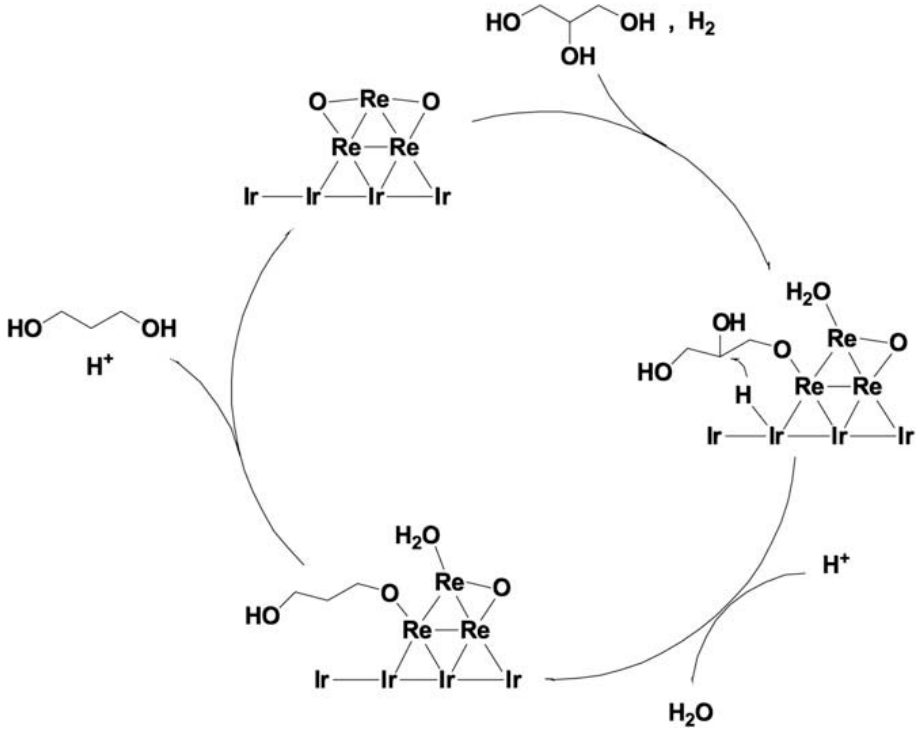

Figure 8. The mechanism for the formation of 1,3-PG in the presence of Ir-ReO_x/SiO_2. Reproduced from [59] with permission from Elsevier.

In their study, they further proved that by keeping the Re promoter but changing the metal phase to Rh, Ru, and Pt, the order of activity was as follows:

$$Ir > Pt > Rh > Ru > Pd$$

Finally, they concluded that the performance of Ir-ReO_x/SiO_2 was superior to that presented by the Ir/SiO_2 and ReO_x/SiO_2 monometallic catalysts [60].

To understand a little more about their promoter effect, Gilkey et al. studied the structural properties of ReO_x particles on the Ir-ReO_x/SiO_2 catalysts. During preparation, the catalyst precursor is in the form of IrO_2-ReO_x/SiO_2 with Ir having a +4 oxidation state that is reduced to Ir^0 after reduction. The ReO_x species, on the other hand, are partially reduced and remain with an average oxidation state of +2.6 after reduction [86]. Amada et al. demonstrated that, once reduced, the surface of such catalysts was covered by metallic Ir particles forming cube-octahedrons covered by ReO_x particles. The presence of Re improved the reducibility of the catalyst due to the interaction between Re and IrO_2 during the calcination process. In addition, the performance of the Ir-ReO_x/SiO_2 catalysts was attributed to the active sites formed by metal bonds between metallic Ir and ReO_x species (Figure 9) [87].

In the presence of another metal such as Ru, the Ir-ReO_x/SiO_2 catalysts showed enhanced activity levels toward the formation of 1,3-PG. The presence of Ru at a given concentration dissociates H_2 molecules and transfers H species via a spillover mechanism toward the Ir-ReO_x particles. These species form protons and facilitate the formation of 1,3-PG (Figure 10) [80]. Surprisingly, Ru-Re/SiO_2 catalysts were found to be less active and selective than the Ir-ReO_x/SiO_2 catalysts, reinforcing the idea that Ru acts as a promoter in the hydrogenolysis reaction [88].

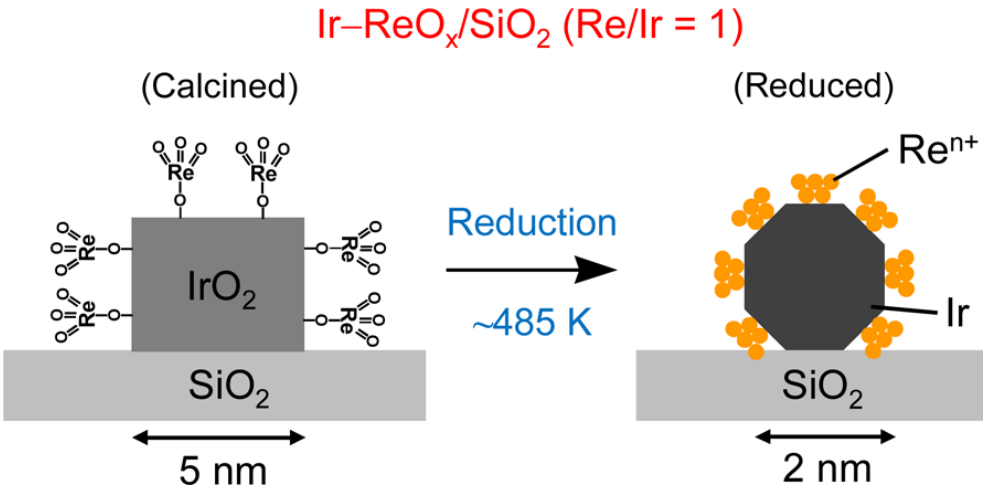

Figure 9. The formation of metallic Ir particles covered by Re oxides. Reproduced from [87] with permission from American Chemical Society (ACS).

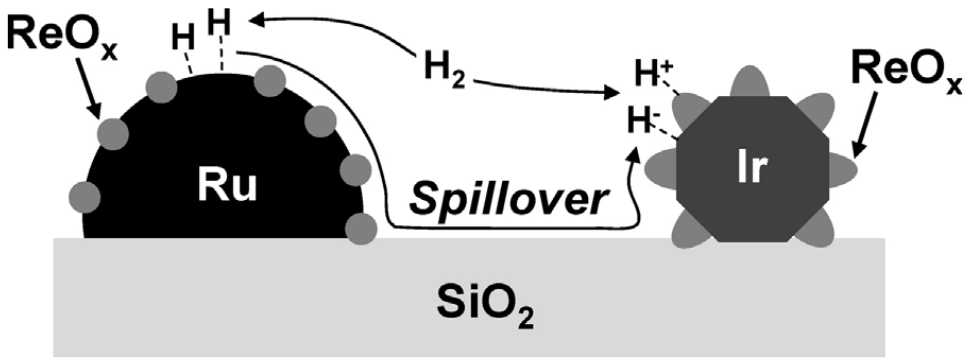

Figure 10. The hydrogen spillover on the Ru-Ir-ReO_x catalysts. Reproduced from [80] with permission from Elsevier.

In order to explore the reaction mechanism of hydrogenolysis using Ir-ReO_x/SiO_2 catalysts, Varghese et al. carried out an experimental and simulation study in liquid phase batch reactors. The characterization of the catalysts by photoelectron spectroscopy (XPS) revealed the presence of metallic Ir and ReO_x particles with multiple oxidation states (0, +4, +7). A catalyst structural model was developed based on this study, considering that on metallic Ir, nanoparticles are dispersed ReO_x particles with an average oxidation state of +4 for Re. Their results also revealed that once the catalyst was reduced, the ReO_x particles constituted Brønsted acid sites with Ir-$H_3Re_3O_6$ type clusters [89].

In addition to SiO_2, other supports were studied to support the Ir-ReO_x couplet. In this regard, Liu et al. investigated Ir-ReO_x catalysts supported on anatase TiO_2, rutile TiO_2, C, ZrO_2, CeO_2, SiO_2, Al_2O_3, and MgO. Of all the materials used as supports, rutile TiO_2 was found to be the most active. The results were attributed to the stabilization and dispersion of the Ir-ReO_x particles on the rutile TiO_2 surface, which allowed for an increase in the number of active sites. In these, the Ir particles interacted with the partially oxidized ReO_x clusters (average Re oxidation state: +3) covering almost the entire rutile TiO_2 surface [81].

From the zeolite group, Wan et al. prepared IrO_x/H-ZSM-5 catalysts in the absence of ReO_x. Their results showed that the activity is a function of Ir dispersion, Ir (0)/Ir (III) ratio, and Brønsted acid site content. The activity was found to be linear as a function of the content of Brønsted acid sites while the selectivity to 1,3-PG increased with the presence of this type of site, denoted as Ir-O(H)-H-ZSM-5. These sites are generated by the synergistic interaction between IrO_x and H-ZSM-5 species through a hydrogen spillover. The authors proposed a direct mechanism for the formation of 1,3-PG on IrO_x/H-ZSM-5, considering

that glycerol adsorption occurs on IrO_x particles and H_2 activation takes place on the Si–Al sites of the H-ZSM-5 zeolite (Figure 11) [82].

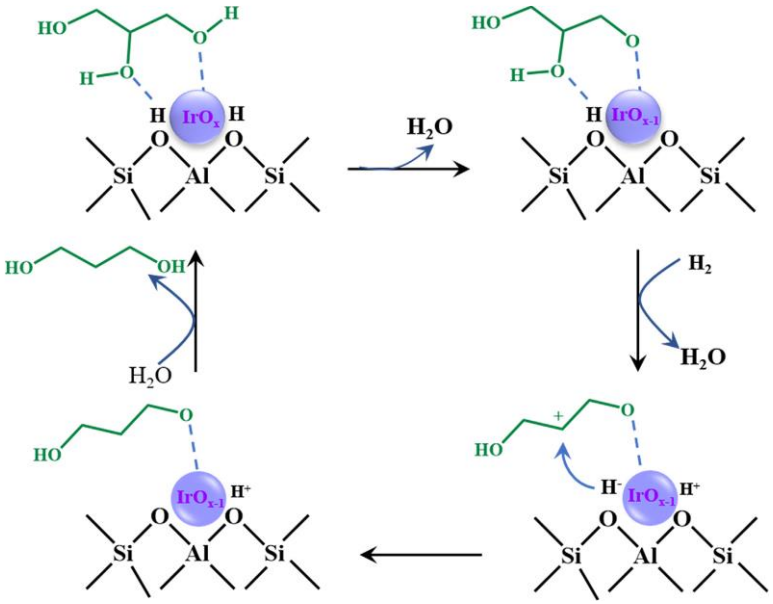

Figure 11. The mechanism for the formation of 1,3-PG in the presence of IrO_x/H-ZSM-5. Reproduced from [82] with permission from Elsevier.

Recently, Chanklang et al. prepared Ir-ReO_x catalysts supported on H-ZSM-5, which showed high metal dispersion with a decrease in the Ir particle size by the addition of Re. The results indicated that the activity is a function of the Ir metal content and Re/Ir molar ratio. However, even by optimizing the reaction conditions (temperature, reaction time, and catalyst concentration), the catalysts were found to be poorly selective at 1,3-PG (~19%) with very low yields (~2.8%) due to excessive hydrogenolysis of the glycol to form 1-POH. The authors proposed a mechanism similar to the direct mechanism of hydrogenolysis used to explain the results in Ir-ReO_x/SiO_2 (Figure 12) [83].

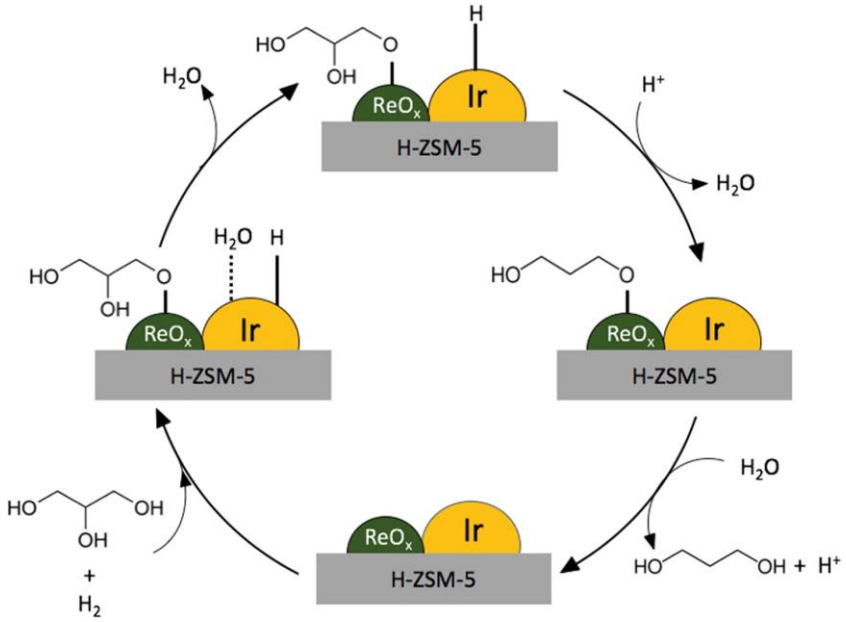

Figure 12. The mechanism for the formation of 1,3-PG in the presence of Ir-ReO_x/H-ZSM-5. Reproduced from [83] with permission from Elsevier.

Other Ir–Re systems on mesoporous silica and SiO_2–Al_2O_3 supports were also studied from the structural point of view.

Deng et al. studied the reduction of Ir–Re (Ir:Re = 1) catalysts supported on a mesoporous silica of the KIT-6 type in the range of 400 to 700 °C. Their results showed an improvement in glycerol conversion with an increasing reduction temperature up to 600 °C due to an increase in the number of acid sites that produced a higher Ir–Re interaction. For temperatures between 600 and 700 °C, a decrease in the activity of these catalysts was observed due to a growth in the size of the metal particles [84]. In another work by these authors, they compared the Ir-Re/KIT-6 catalyst prepared by direct reduction at 500 °C of (Ir-Re/KIT-6-R) with the same precursor, but previously calcined in air at 500 °C (Ir-Re/KIT-6-CR). The results showed that the direct reduction in a H_2 atmosphere allowed for the generation of metallic Re particles that together with Ir formed a much more active Ir–Re alloy than the Ir-ReO_x phase formed during calcination, because the ReO_x particles cannot be easily reduced once the oxide is formed. In the presence of an Amberlyst-15 type resin, it is possible to reach the maximum yield to 1,3-PG [90].

In Ir–Re catalysts supported on silica-alumina, Ir-Re/SiO_2-Al_2O_3, it has been reported that the presence of Al promotes the dispersion of Re particles and facilitates the formation of large Ir crystals, leading to low Ir–Re interaction and, consequently, low activity levels. When the Al content in the support, SiO_2–Al_2O_3 (–Al), is reduced, the Re particles form an alloy with the Ir particles due to the proximity between them and their interaction, which promotes higher activity levels and selectivity to 1,3-PG (Figure 13) [85].

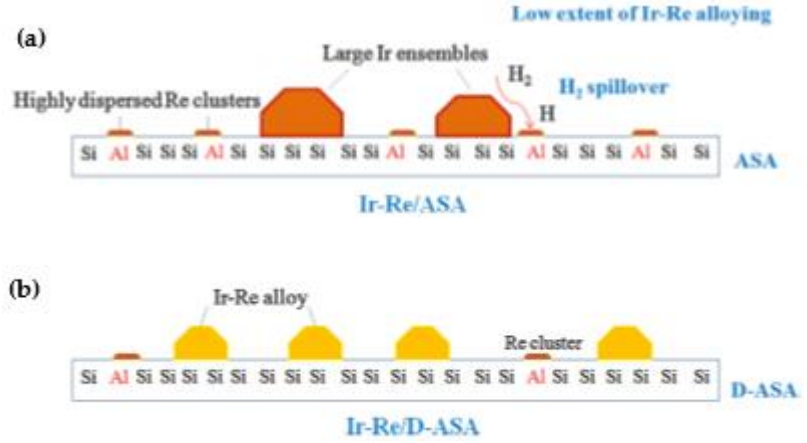

Figure 13. The formation of Ir and Ir–Re species on (**a**) SiO_2–Al_2O_3 (ASA) and (**b**) SiO_2–Al_2O_3 (–Al) (D–ASA). Reproduced from [85] with permission from Elsevier.

Despite the efforts made with these higher complexity supports, the results show that the highest yields to 1,3-PG (~38%) were obtained with Ir-ReO_x/SiO_2 catalysts at moderate temperature (120 °C) and pressure (8 MPa) conditions operating in liquid phase batch reactors.

3.3. Pt Catalysts

Pt catalysts were used for the production of 1,3-PG in both the liquid and vapor phases. Tables 4 and 5 summarize the main catalysts tested in the liquid phase using batch and continuous flow reactors, respectively.

Of the set of noble metals, Ru, Pd, Rh, Ir, and Pt, the latter has shown to be the most promising one for obtaining 1,3-PG, since, unlike the other metal phases, Pt acts not only as an active site for hydrogenation, but also facilitates the cleavage of the secondary C–O bond in the glycerol molecule [91].

Studies have mainly focused on the modification of traditional supports to prepare Pt catalysts, leading to the formation of 1,3-PG. The modification of supports was carried out using W and Re species, but, even so, the yields achieved were less than 70%.

The first studies were based on the modification of Pt catalysts using Re. In this sense, the Pt-Re/C catalysts were found to be more active and selective toward the formation of 1,3-PG than monometallic Pt/C and Re/C catalysts due to the formation of a Pt–Re alloy with an average metal particle size smaller than 2 nm [92]. The same Pt–Re combination was supported on SiO_2, C, and SiO_2 modified with W. The study revealed that, although Pt was completely reduced in the alloy, Re was oxidized with a distribution of oxidation states, conferring a Brønsted-type acidity to the Pt–Re particles, which influenced the selectivity to 1,3-PG [93].

With the aim of generating Brønsted acid sites, other authors have prepared Pt catalysts modified with heteropolyacids (HTPA) and tungsten oxides (WO_x).

Table 4. The hydrogenolysis of glycerol to 1,3-PG using Pt catalysts operating in liquid phase batch reactors.

Catalyst	T (°C)	P (MPa)	m_{gly}/m_c	t (h)	X (%)	$S_{1,3\text{-PG}}$ (%)	$Y_{1,3\text{-PG}}$ (%)	Ref.
Pt/WO_x	180	5.5 (H_2)	4.0	12	18.0	39.3	7.0	[63]
$Pt/WO_x/AlOOH$	180	5.0 (H_2)	0.9	12	100.0	66.0	66.0	[64]
$Pt/WO_x/Al_2O_3$	200	9.0 (H_2)	6.0	4	62.5	61.5	38.5	[66]
Pt/WO_x/SBA-15	150	4.0 (H_2)	3.0	30	86.8	70.8	61.5	[67]
$Pt/WO_3/ZrO_2$	170	8.0 (H_2)	2.7	18	85.8	28.2	24.2	[91]
Pt-Re/C	170	4.0 (H_2)	NR	8	45.0	29.0	13.0	[92]
$Pt/Al_2O_3 + H_4SiW_{12}O_{40}$	200	4.0 (H_2)	0.5	18	49.0	28.0	13.7	[94]
$Pt/H_4SiW_{12}O_{40}$-Al_2O_3	240	6.0 (H_2)	25.0	8	45.3	10.5	4.8	[95]
$Pt/H_4SiW_{12}O_{40}$-m-Al_2O_3	200	4.0 (H_2)	0.9	15	60.5	33.3	20.1	[96]
$Pt/WO_3/TiO_2/SiO_2$	180	5.5 (H_2)	2.0	12	15.3	50.5	7.7	[97]
Pt/Al-WO_x	160	3.0 (H_2)	2.0	30	79.0	40.6	32.1	[98]
Pt/WO_x	140	1.0 (H_2)	2.0	12	37.4	35.1	13.1	[99]
Pt-La/WO_x	140	1.0 (H_2)	2.0	12	39.9	41.3	16.4	[99]
Pt-Au/WO_x	140	1.0 (H_2)	1.0	12	81.4	51.6	42.0	[100]
$Pt/Au/WO_3$	155	5.0 (H_2)	2.0	12	55.0	41.0	22.5	[101]
$Pt/WO_x/ZrO_2$	140	8.0 (H_2)	6.0	24	76.2	64.8	49.4	[102]
$Pt/WO_x/Al_2O_3$	140	0.5 (H_2)	0.6	6	35.8	29.0	10.4	[103]
$Pt/WO_x/Al_2O_3$	220	6.0 (H_2)	12.0	5	78.0	42.0	32.8	[104]
$Pt/WO_x/\gamma$-Al_2O_3	200	5.5 (H_2)	3.3	4	65.0	50.0	32.5	[105]
$Pt/WO_x/\alpha$-Al_2O_3	180	5.0 (H_2)	9.0	24	59.5	43.9	26.1	[106]
Pt/W+Al/SBA-15	160	6.0 (H_2)	1.5	12	66.0	50.0	33.0	[107]
Pt/WO_x/T-Ta_2O_5	160	5.0 (H_2)	0.9	24	87.0	45.6	39.7	[108]
$Pt/WO_x/Ta_2O_5$	160	5.0 (H_2)	9.0	24	78.0	38.0	29.6	[109]
Pt/sulfated ZrO_2	170	7.3 (H_2)	NR	24	66.5	83.6	55.6	[110]
$Pt/Mn/WO_x/ZrO_2$	180	8.0 (H_2)	8.0	18	56.2	42.0	23.6	[111]
$Pt/WO_x/SiO_2/ZrO_2$	180	5.0 (H_2)	5.0	12	90.1	44.5	40.1	[112]
$Pt/WO_3/ZrP$	200	4.0 (H_2)	1.0	12	92.3	20.9	19.3	[113]
Pt-Ru/WO_x/Al_2O_3	170	9.0 (H_2)	3.0	36	90.4	43.0	38.9	[114]
Pt-Au/WO_x/Al_2O_3	180	5.0 (H_2)	4.0	12	57.0	41.4	23.5	[115]
Pt/W-MCFs	150	4.0 (H_2)	3.0	24	100.0	65.0	65.0	[116]
Pt/WO_x/S-TiO_2	120	4.0 (H_2)	1.3	8	100.0	36.0	36.6	[117]
$Pt/WO_x/TiO_2$	120	4.0 (H_2)	1.3	8	57.0	66.0	37.0	[117]

m_{gly}/m_c—glycerol/catalyst mass ratio; NR—not reported; X—glycerol conversion; $S_{1,3\text{-PG}}$—selectivity to 1,3-PG; $Y_{1,3\text{-PG}}$—yield to 1,3-PG.

Table 5. The hydrogenolysis of glycerol to 1,3-PG using Pt catalysts operating in liquid phase continuous flow reactors.

Catalyst	T (°C)	P (MPa)	SV (h^{-1})	X (%)	$S_{1,3\text{-PG}}$ (%)	$Y_{1,3\text{-PG}}$ (%)	Ref.
$Pt/WO_3/ZrO_2$	130	4.0 (H_2)	0.25 (LHSV)	70.2	45.6	32.0	[62]
$Pt/H_4SiW_{12}O_{40}$-SiO_2	200	6.0 (H_2)	0.045(WHSV)	81.2	38.7	31.4	[118]
Pt-$H_2Li_2SiW_{12}O_{40}/SiO_2$	180	5.0 (H_2)	0.09 (WHSV)	43.5	53.6	23.3	[119]
Pt-$H_3PMo_{12}O_{40}/SiO_2$	180	5.0 (H_2)	0.09 (WHSV)	27.1	7.8	2.1	[120]
Pt-$H_3PW_{12}O_{40}/SiO_2$	180	5.0 (H_2)	0.09 (WHSV)	25.5	32.9	8.4	[120]
Pt-$H_4SiW_{12}O_{40}/SiO_2$	180	5.0 (H_2)	0.09 (WHSV)	24.1	48.1	11.6	[120]
$Pt/WO_x/Al_2O_3$	160	5.0 (H_2)	0.09 (WHSV)	64.2	66.1	42.4	[121]
$Pt/WO_x/Al_2O_3$	160	5.0 (H_2)	1.02 (WHSV)	75.2	44.0	33.1	[122]
$Pt/WO_x/Al_2O_3$	160	5.0 (H_2)	1.02 (WHSV)	80.5	47.4	38.2	[123]
$Pt/WO_x/SiO_2/ZrO_2$	180	5.0 (H_2)	1.00 (WHSV)	54.3	52.0	28.2	[124]
Pt/WO_x-ZrO_2-TiO_2	140	5.0 (H_2)	0.50 (WHSV)	75.0	33.7	25.3	[125]
Pt-$Li_2B_4O_7/WO_x/ZrO_2$	150	4.0 (H_2)	0.20 (WHSV)	90.0	47.4	42.7	[126]
$Pt/Mg/WO_x/ZrO_2$	150	4.0 (H_2)	0.20 (WHSV)	52.6	60.7	32.1	[127]
$Pt/WO_x/Al_2O_3$	180	5.0 (H_2)	1.00 (LHSV)	80.4	35.3	28.8	[128]

SV—space velocity; X—glycerol conversion; $S_{1,3\text{-PG}}$—selectivity to 1,3-PG; $Y_{1,3\text{-PG}}$—yield to 1,3-PG.

With respect to the use of HTPA, $H_4SiW_{12}O_{40}$ was found to be the most effective in producing 1,3-PG, either by the addition to the reaction medium in the presence of Pt/Al_2O_3 catalysts [94], or by the modification of supports such as SiO_2 [118], ZrO_2 [119,120], Al_2O_3 [95], and ordered mesoporous Al_2O_3 (m-Al_2O_3) [96]. The results indicated that the modification of these supports with the heteropolyacid enhanced the dispersion of Pt and conferred the appropriate acidity for the formation of the intermediate in the production of 1,3-PG. In this respect, it has been verified that there is a linear correlation between the yield to 1,3-PG and the surface concentration of Brønsted acid sites provided by the heteropolyacids. This trend was verified using Pt-$H_4SiW_{12}O_{40}/ZrO_2$ [119], Pt-$H_3PW_{12}O_{40}$-ZrO_2 [120], and Pt-$H_3PMo_{12}O_{40}/ZrO_2$ [120].

With respect to modification with tungsten oxides (WO_x), it has been shown that the presence of these oxides endows the support with Brønsted acid sites for the adsorption of glycerol and the subsequent formation of an alkoxide intermediate in the formation of 1,3-PG, following the direct mechanism of hydrogenolysis [97]. The tungsten redox cycle, $W^{+6} \leftrightarrow W^{+5}$, further allows in situ regeneration of the surface sites after the formation of 1,3-PG [129]. In the Pt/WO_x catalysts, the interaction between Pt particles and metallic H_2 produces a hydrogen spillover from Pt to WO_x. The presence of oxygen vacancies in the WO_x facilitates the mechanism of heterolytic cleavage of H_2 into H^+ and H^- ions, which are necessary in hydrogenolysis for the formation of 1,3-PG from the alkoxide intermediate (Figure 14) [63].

In situ ATR-IR studies revealed that WO_x plays three fundamental roles in the formation of 1,3-PG: (1) adsorption of the primary –OH group of glycerol; (2) provision of H+; and (3) stabilization of the intermediate carbocation in the formation of 1,3-PG [66].

Recently, Yang et al. carried out characterization studies by photoelectron spectroscopy and hydrogen chemisorption and determined that the catalytic activity of Pt/WO_x was from the oxygen vacancies found in the WO_x species. By preparing Pt/Al-WO_x catalysts, they determined that by modulating the content of atomically dispersed AlO_x species on the WO_x support, it was possible to generate a higher content of oxygen vacancies and thus promote the formation of 1,3-PG (Figure 15) [98].

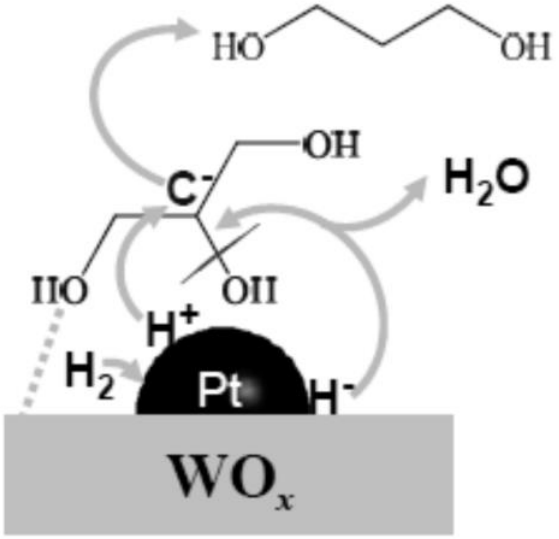

Figure 14. The reaction mechanism on the Pt/WOx catalysts. Reproduced from [63] with permission from Elsevier.

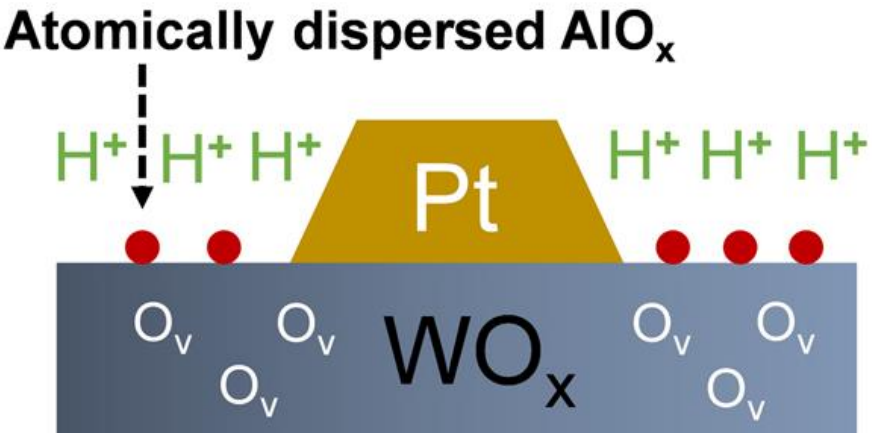

Figure 15. The generation of oxygen vacancies in WO_x by the incorporation of atomically dispersed AlO_x species. Reproduced from [98] with permission from Elsevier.

In order to promote the activity of the Pt/WO_x catalysts, studies on the addition of promoters such as La [99] and Au [100] have been reported. Both strategies improved the activity and selectivity toward 1,3-PG due to the extra generation of Brønsted acid sites. In the case of Pt-Au/WO_x, the presence of Au enhanced the dissociative adsorption of H_2 [100]. Yang et al. characterized Pt/Au/WO_3 catalysts prepared by a surface-modified deposition method and determined that the presence of Au promotes the reduction of Pt and W at low temperatures while making the dispersion of Pt uniform on the WO_3 support. These changes in the electronic properties allow for an improvement in the activity and selectivity of the catalyst [101].

To increase the dispersion of WO_x particles and improve the catalytic properties, Pt/WO_x catalysts supported on ZrO_2 [62,91,102], Al_2O_3 [103–106,121–123], AlOOH [64], SBA-15 [67,107], and Ta_2O_5 [108,109] were prepared.

With respect to the Pt/WO_x/ZrO_2 catalysts, their activity in the isomerization of alkanes is well-known [130–133]. On the surface of these catalysts, H_2 molecules are transformed into protons (H^+) and hydrides (H^-) via heterolytic cleavage [134,135]. The hydrogenolysis reaction of glycerol to form 1,3-PG consists of a substitution reaction, in which an H atom replaces the secondary –OH group in the glycerol molecule. For this reason, a possible sequence is the two-step reaction of glycerol with H^+ and H^-, which produces water and the substitution of the secondary –OH group by H [136,137]. Following

this idea, $Pt/WO_x/ZrO_2$ catalysts [62,91,102] were used for the hydrogenolysis of glycerol to 1,3-PG.

Compared to other traditional supports, ZrO_2 is one of the most interesting to combine with Pt as the metal phase and to generate Brønsted acid sites. For example, the modification of ZrO_2 with sulfonic groups allows for the preparation of Pt catalysts that showed yields of 55% to 1,3-PG due to the generation of Brønsted acid sites [110]. It has also been indicated that the tetragonal phase of ZrO_2 is more active than the monoclinic phase to be used as a support, since it generates higher metal dispersion and Brønsted acid sites of higher acidic strength [102].

In comparison to catalysts such as $Pt/WO_3/TiO_2$, $Pt/WO_3/HY$, and $Pt/WO_3/AlMCM$-41, the $Pt/WO_3/ZrO_2$ catalyst proved to be the best alternative, reaching the maximum yield to 1,3-PG [91]. In these catalysts, the formation of 1,3-PG is structurally sensitive to the degree of polymerization of WO_x species. The Pt-$(WO_x)_n$-H type active sites provide a strong Brønsted acidity that promotes the formation of 1,3-PG [111].

With the aim of improving the catalytic properties, modifications of $Pt/WO_x/ZrO_2$ catalysts including the use of SiO_2 [112,124], TiO_2 [125], $Li_2B_4O_7$ [126], Mn [111], Mg [127], and P [113] have been reported.

$Pt/WO_x/SiO_2/ZrO_2$ catalysts resulted in being more active and selective to 1,3-PG due to a promoting effect of SiO_2 that favors not only the dispersion of Pt, but also of the WO_x species [124]. This effect has been observed in similar $Pt/WO_x/TiO_2/SiO_2$ catalytic systems [97]. The presence of an adequate SiO_2 content favors the transformation of crystalline WO_3 species into polytungstate species, which are more active and allow for an increase in the yield to 1,3-PG. When the SiO_2 content exceeds the optimum, the polytungstate species are transformed into monotungstate species that decrease the yield to 1,3-PG (Figure 16a). This leads to obtaining a maximum yield to 1,3-PG as a function of the SiO_2 content (Figure 16b) [124].

Zhao et al. proved that the presence of bibridged (OH_{II}) and tribridged hydroxyl groups (OH_{III}) on the SiO_2/ZrO_2 support could react with WO_x species forming Zr–O–W bands and retarding the agglomeration of WO_x species. The high dispersion of WO_x species in conjunction with Zr–O–W bonds benefit the formation of Brønsted acid sites that promote the formation of 1,3-PG [112].

Xi et al. prepared a series of Pt/WO_x-ZrO_2-ZrO_2-TiO_2 catalysts from an evaporative assembly method using different Ti/Zr molar ratios. The authors detected the presence of $ZrTiO_4$ and Ti_2ZrO_6 phases, responsible for the activity in the hydrogenolysis of glycerol. For a Ti/Zr = 7:3 molar ratio, the catalyst showed the maximum yield to 1,3-PG (~25.3%) [125].

The modification of $Pt/WO_x/ZrO_2$ catalysts with $Li_2B_4O_7$ in the 0.5–2 wt.% range allowed for a better dispersion of the Pt particles and increased the total number of acid sites, thus increasing the interaction between the metal phase and the support. At 150 °C and 4 MPa H_2, the catalyst with 2 wt.% $Li_2B_4O_7$ allowed for obtaining the maximum yield to 1,3-PG (~42.7%), being stable for more than 200 h [126].

Doping Mn into the $Pt/WO_x/ZrO_2$ catalysts allowed for the generation of a large number of WO_x species with some intermediate degree of polymerization, which increased the number of Pt-$(WO_x)_n$-H sites promoting the formation of 1,3-PG [111]. The same effect was found with the incorporation of Mg to the $Pt/WO_x/ZrO_2$ catalysts. In this case, the formation of small WO_x species with some degree of polymerization was active for the formation of 1,3-PG [127].

The preparation of $Pt/WO_3/ZrP$ catalysts also led to good yields to 1,3-PG, but lower in comparison to $Pt/WO_x/ZrO_2$ catalysts. The co-presence of Pt and W in the catalyst composition led to a synergistic enhancement in the catalytic activity and 1,3-PDO selectivity. Highly dispersed Pt nanoparticles in contact with polytungstate-like WO_x species were active centers for the hydrogenolysis reaction [113].

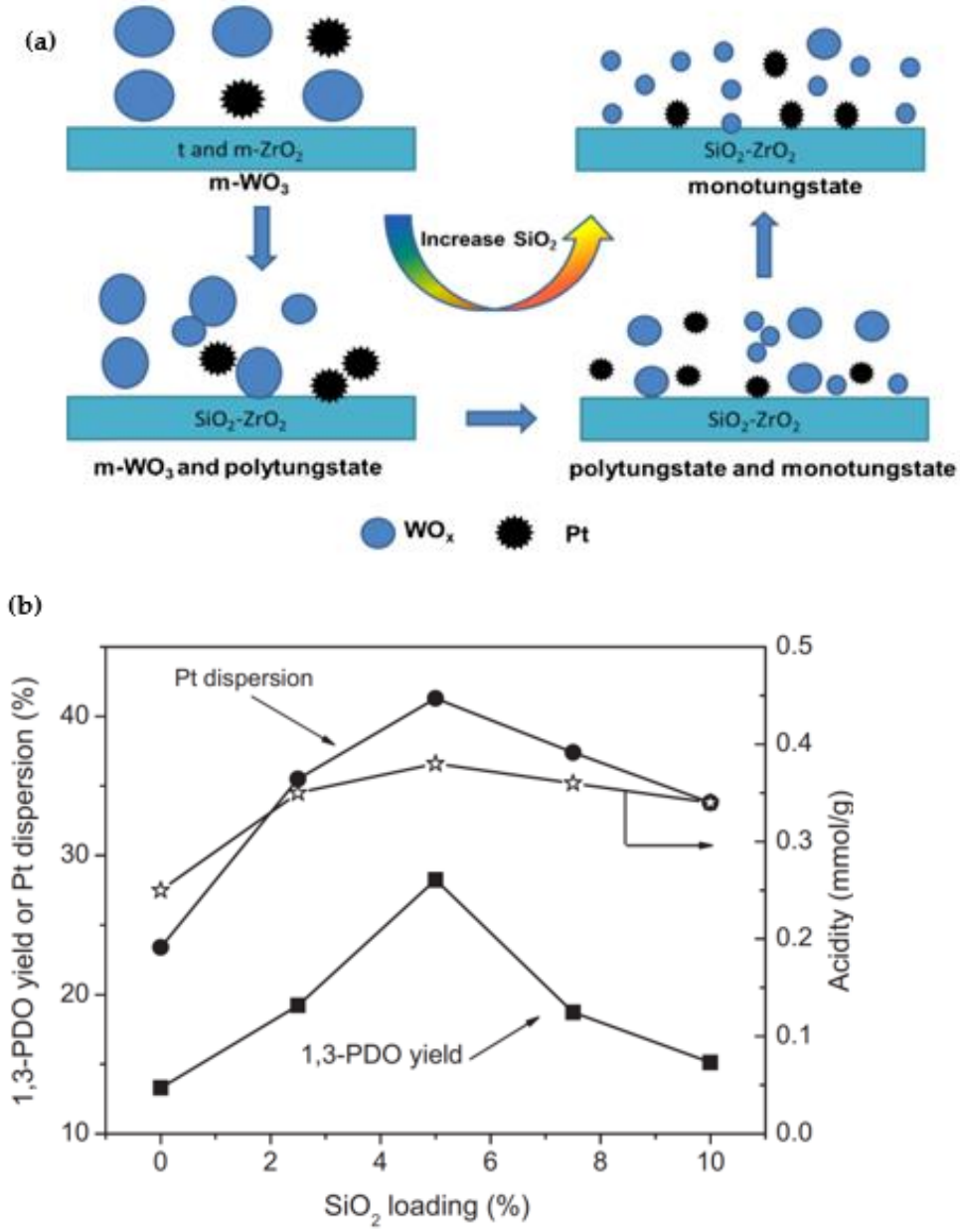

Figure 16. (**a**) The generation of polytungstate and monotungstate species on the $Pt/WO_x/SiO_2/ZrO_2$ catalysts [124] (**b**) The yield to 1,3-PG as a function of the SiO_2 content. Reproduced from [124] with permission from Elsevier.

With respect to the modification of Al_2O_3 with WO_x, it has been reported that the surface density of W determines the type of W species on the support surface and thus the selectivity to 1,3-PG. In the $Pt/WO_x/Al_2O_3$ catalysts, the presence of monotungstate, polytungstate, and mesoporous WO_3 species generates the Brønsted acid sites necessary for the cleavage of the secondary C–O bond of the glycerol molecule [121]. In this regard, it has been reported that the transformation of WO_3 to polytungstate is required to achieve the highest yields to 1,3-PG [124]. The combination of polytungstate species with highly dispersed Pt particles leads to the formation of alkoxide intermediates and their subsequent hydrogenation to form 1,3-PG (Figure 17) [65].

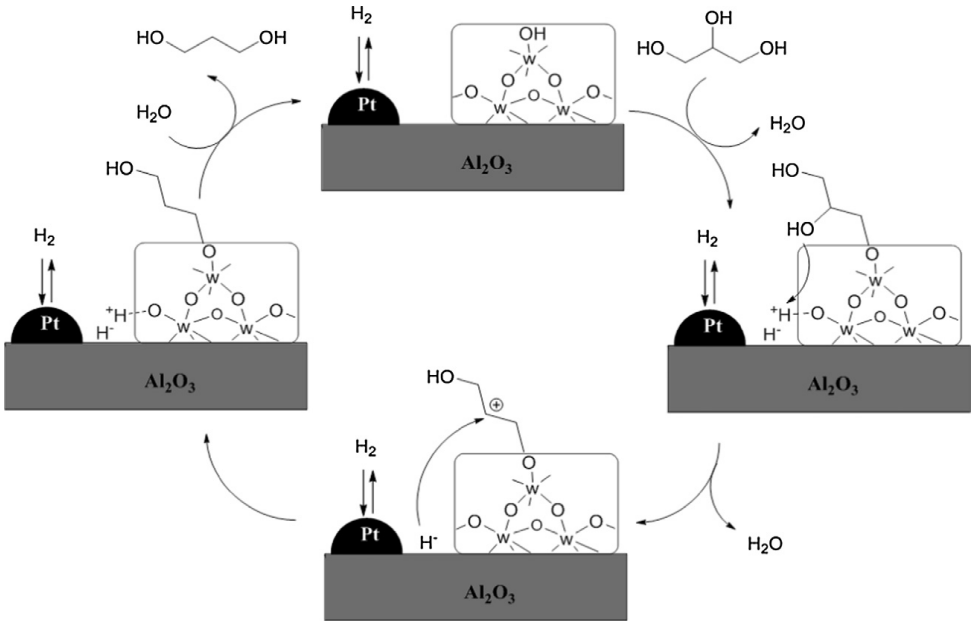

Figure 17. The reaction mechanism on the $Pt/WO_x/Al_2O_3$ catalysts. Reproduced from [65] with permission from Elsevier.

It has also been reported that an excessive number of tungsten species can lead to the formation of undesired products such as 1-POH, 2-POH, MeOH, and gases [138]. Thus, a proper balance between Pt, W species, and support is required, leading to the need for an optimization of the W content in the catalyst. In this regard, Lei et al. studied various compositions of Pt and WO_x species on Al_2O_3. Their results determined that for a fixed Pt content (2 wt.%), an increase in the W concentration up to 7.5 wt.% causes an increase in the selectivity to 1,3-PG; if the W concentration continues to increase, the selectivity to 1,3-PG decreases by the generation of products such as 1-POH. Similarly, maintaining a fixed W content (12.9 wt.%), an increase in the Pt concentration up to 6 wt.% causes an increase in glycerol conversion, while for higher contents of the metal, there is a drop in activity due to a decrease in the metal dispersion. The results of this work indicate that for each W content and optimum Pt content (or vice versa), it is required to achieve the highest levels of glycerol conversion and selectivity to 1,3-PG, which implies maximizing the yield to the glycol of interest, as shown in Figure 18 [128].

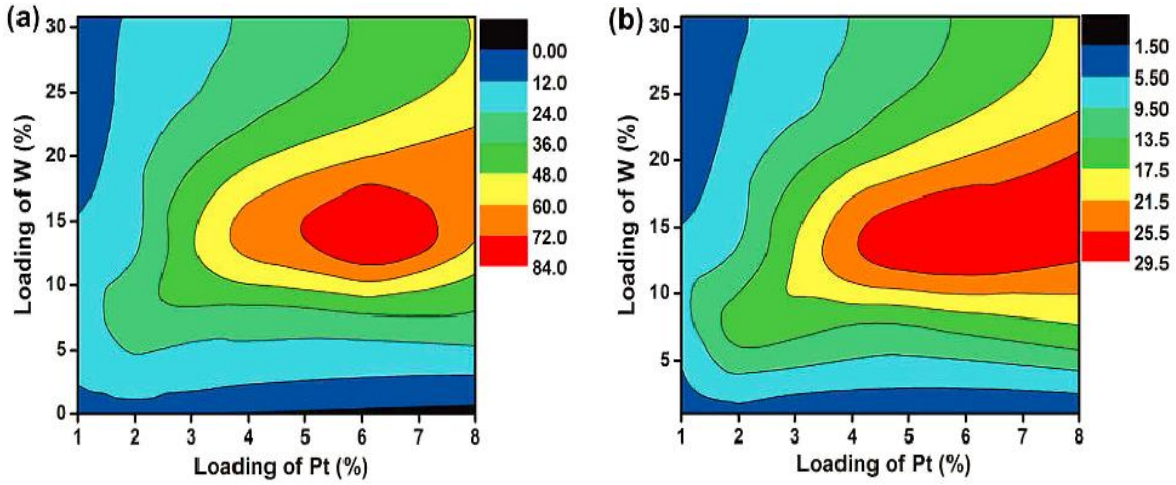

Figure 18. (**a**) The conversion of glycerol. (**b**) Yield to 1,3-PG as a function of Pt and W content in the $Pt/WO_x/Al_2O_3$ catalysts. Reproduced from [128] with permission from Wiley.

Zhao et al. developed a strategy to prepare Pt catalysts supported on Al_2O_3 containing highly dispersed WO_x species by employing high-temperature heat treatment. In their work, these authors attributed the catalytic efficiency to the strong interaction between isolated WO_4 species and the Pt metal phase, which would be responsible for generating Brønsted acid sites in situ, according to the results of the IR spectroscopy and NH_3 adsorption–desorption [106].

In order to improve the properties of the $Pt/WO_x/Al_2O_3$ catalyst, Wen et al. studied the modification of the metal phase with Ru. The authors found that the presence of Ru favored the redox cycle $W^{+6} \leftrightarrow W^{+5}$, which allowed for an improvement in the adsorption of H_2 and an increase in the number of Brønsted acid sites of medium acidic strength, leading to the attainment of a higher yield to 1,3-PG [114].

Similar results were obtained with the $Pt\text{-}Au/WO_x/Al_2O_3$ catalysts. In these systems, the addition of Au, which exists on the catalytic surface mostly as single atoms, enhances the hydrogen spillover capacity, decreasing the interaction between the Pt and WO_x species, promoting Pt dispersion (~2 nm) and increasing its exposed area. Since the spillover capacity is directly linked to the number of Brønsted acid sites, the presence of Au favors the production of 1,3-PG [115].

For catalysts of similar characteristics, but based on bohemite (AlOOH), a reaction mechanism through alkoxide type intermediate species has been proposed, in whose formation Pt, WO_x, and AlOOH type oxides are cooperatively involved. Initially, glycerol is adsorbed on the surface sites of the bohemite through the primary –OH group, forming alkoxide species of the $HOCH_2CH(OH)CH_2OAlO_x$ type. Next, the secondary –OH group of the alkoxide species is protonated on the acid sites of the WO_x and dehydrates, producing a secondary carbocation. This carbocation is attacked by hydride species generated on the WO_x sites due to the H_2 spillover produced by the interaction between the Pt particles and the metallic H_2. Finally, the alkoxide species are hydrolyzed to generate 1,3-PG and the catalytic cycle is completed. On the other hand, the surface of the bohemite plays a fundamental role as it stabilizes the Pt particles and the W oxides [64]. With this catalyst, it is possible to reach a 66% yield to 1,3-PG, which is the highest yield reported to date.

Recently, yields very close to that value (~65%) have been reported by Cheng et al., who prepared Pt catalysts (Pt/W-MCFs) supported on tungsten-doped siliceous mesocellular foams (W-MCFs). The synergy between the Pt nanoparticles and the tetrahedral sites of W^VO_4 species at the oxide–metal interface were responsible for the catalyst activity as well as the 3-dimensional continuous large pore structure of the W-MCFs, which facilitates the entry of the reactant and the escape of the product [116].

With respect to the $Pt/WO_x/SBA\text{-}15$ catalysts, the addition of W produces WO_4, which is incorporated into the SBA-15 matrix as a Lewis acid site. The H_2 adsorbed on Pt is transferred by spillover to the W oxide, which is transformed into a Brønsted acid site, allowing for the formation of the intermediate and then of 1,3-PG [67].

Feng et. al. also prepared Pt/SBA-15 catalysts, but modified with W and Al, which were homogeneously incorporated into the SBA-15 matrix using a one-step synthesis method under an acidic medium. The joint presence of W and Al allowed for an increase in the synergism effect between the Lewis and Brønsted acid sites, which were tightly related to the incorporation of W and Al species on the modified SBA-15. According to these authors, glycerol adsorbs on the catalytic surface at the WO_x sites to form a terminal alkoxide, which then dehydrates and hydrogenates to finally form 1,3-PG. Naturally, the adsorption and activation of H_2 takes place on the Pt metal sites (Figure 19) [107].

Recently, Zhou et al. tested $Pt/WO_x/TiO_2$ catalysts that were found to be active and selective to 1,3-PG, showing 37% yields for 57% glycerol conversions at 120 °C and 4 MPa H_2 after 8 h of reaction. Modification of these catalysts with sulfate ions allowed them to achieve full glycerol conversion while maintaining the overall yield to 1,3-PG under the same reaction conditions. The result was attributed to the increase in Brønsted acid sites as well as a better dispersion of Pt particles and WO_x species [117].

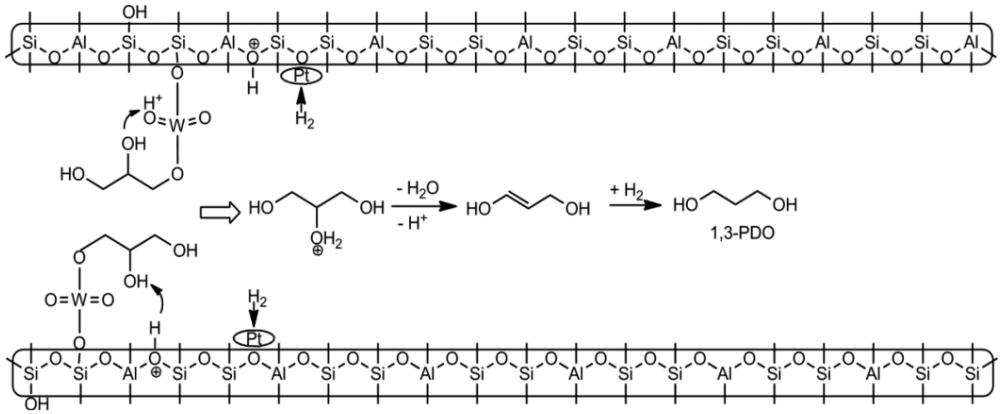

Figure 19. The reaction mechanism on the Pt/W+Al/SBA-15 catalyst. Reproduced from [107] with permission from the American Chemical Society (ACS).

Other more current systems based on Pt-WO_x have been supported on Ta_2O_5. The calcination of these catalysts at high temperature (900 °C) has allowed for high dispersions of tungsten oxides to be obtained with a low degree of polymerization, increasing the oxygen vacancies on their surface. This generates a higher dispersion of the Pt particles, maximizing the Pt–O–W interfacial bonding, and leads to obtaining higher yields to 1,3-PG [108,109].

With respect to obtaining 1,3-PG in the vapor phase, Table 6 summarizes the main Pt catalysts employed in continuous flow reactors.

Table 6. The hydrogenolysis of glycerol to 1,3-PG using Pt catalysts operating in liquid phase continuous flow reactors.

Catalyst	T (°C)	P (MPa)	SV (h^{-1})	X (%)	$S_{1,3\text{-PG}}$ (%)	$Y_{1,3\text{-PG}}$ (%)	Ref.
Pt/WO_3/Al_2O_3	260	0.1 (H_2)	0.10 (WHSV)	99.0	14.0	13.8	[139]
Pt-WO_3/SBA-15	210	0.1 (H_2)	1.02 (WHSV)	86.0	42.0	36.1	[140]
Pt/$AlPO_4$	260	0.1 (H_2)	1.02 (WHSV)	100.0	35.4	35.4	[141]
Pt/H-MOR	225	0.1 (H_2)	1.02 (WHSV)	94.9	48.6	46.1	[142]
Pt-Cu/H-MOR	215	0.1 (H_2)	1.02 (WHSV)	90.0	58.5	52.6	[143]
Pt/S-MMT	200	0.1 (H_2)	1.02 (WHSV)	94.0	62.0	58.2	[144]

SV—space velocity; X—glycerol conversion; $S_{1,3\text{-PG}}$—selectivity to 1,3-PG; $Y_{1,3\text{-PG}}$—yield to 1,3-PG.

The Pt/WO_3/Al_2O_3 catalysts that had demonstrated yields to 1,3-PG close to 40% in the liquid phase showed low yields to 1,3-PG in the vapor phase (14%), probably due to the thermal level in combination with the surface acidity, which promotes the formation of undesired products. In this regard, the activity results indicated that the reaction proceeds via an initial dehydration of glycerol to form acrolein, which is then rehydrated to form 3-HPA, an intermediate of 1,3-PG [139].

Surprisingly, the modification of SBA-15 with WO_3 allowed for the preparation of Pt catalysts that showed higher yields to 1,3-PG than Pt/WO_3/Al2O_3 (36%), probably due to lower acidity and less severe reaction conditions. In these systems, the activity of the Brønsted acid sites present in WO_3 is combined with the hydrogenation activity of Pt [140]. Similar yields were obtained with Pt/$AlPO_4$ catalysts due to the presence of weak Brønsted acid sites in $AlPO_4$ and the dispersion of Pt particles [141].

Other Pt [142] and Pt–Cu [143] based catalysts on protonated mordenite supports (Pt/H-MOR, Pt-Cu/H-MOR) showed superior performance for the formation of 1,3-PG with yields of 46–52% at 0.1 MPa H_2 and 1 h^{-1} (WHSV) in the 225–215 °C range, respectively. In these systems, the dispersion of Pt combined with the concentration of Brønsted acid sites of the support promote the selective formation of 1,3-PG [142]. In the case of the

bimetallic catalyst, the presence of Cu decreases the C–C cleavage side reactions promoted by Pt [143]. The highest yields to 1,3-PG were obtained with a Pt catalyst on sulfuric acid activated montmorillonite (Pt/S-MMT) (~58%) at 200 °C and 0.1 MPa H_2 [144].

4. Engineering Aspects and Effect of Reactor Parameters

The glycerol hydrogenolysis reaction to 1,3-PG can be carried out in either the liquid or vapor phase. The liquid phase condition requires moderate temperatures (120–240 °C) and high pressures (2–10 MPa) of H_2 or N_2 depending on the case. Generally, a H_2 atmosphere is used due to the requirement in the hydrogenation stage, although there are some studies where N_2 is used and H_2 donor substances are included [145–147]. The liquid phase condition involves higher fixed costs associated with the reaction equipment due to the high pressures used, but has the advantage of not requiring vaporization of the reaction mixture [47].

Batch reactors and continuous flow reactors can be used to carry out the hydrogenolysis reaction in the liquid phase. The use of batch reactors allows for experimental data to be obtained for the future formulation of kinetic models, the study of temperature, pressure, reaction time, and the concentration of reagents and the catalyst being of relevance as operating variables. One of the disadvantages of batch reactors is the increase in the concentration of secondary products as the reaction time increases, which affects the yield to glycols [148]. Recently, Jean et al. recommended the use of continuous flow trickle bed reactors to carry out liquid phase hydrogenolysis [149]. This type of reactor offers several advantages, mainly due to the low contact times between the glycerol and the active sites of the catalyst [150–152], and thus the catalysts show higher stability.

On the other hand, the vapor phase condition requires low pressures (0.1–0.5 MPa) and higher temperatures (200–260 °C) and fixed-bed continuous flow reactors have been used to carry this out. Disadvantages include the need to vaporize the fed glycerol solution, which requires high temperatures and high energy consumption. Since the crude glycerol is in a concentration ranging from 50 to 80 wt.%, the temperatures required for vaporization could lead to the decomposition of the glycerol. Because lower H_2 pressures are used, higher selectivity values to dehydration intermediates are obtained and polymerization reactions can also be favored [153]. In these reactors, the study of temperature, pressure, space velocity, and H_2 flow rate are the main operating variables.

A detailed study is presented below of the different operating variables studied in batch reactors and in continuous flow reactors in both the liquid and vapor phase using different catalytic systems.

4.1. Effect of the Initial Glycerol Concentration

Since glycerol from biodiesel synthesis is found in aqueous solutions in the range of 50–80 wt.%, it is of relevance to study its effect on catalyst performance. Once the catalyst mass is fixed, the effect of the glycerol content has been reported for both the liquid phase condition (Table 7) and the vapor phase condition (Table 8).

Table 7. The effect of glycerol concentration in the liquid phase using batch reactors.

Catalyst	Range (wt.%)	Operative Value (wt.%)	T (°C)	P (MPa)	t (h)	m_{gly}/m_c	$Y_{1,3\text{-PG}}$ (%)	Ref.
Ru/C	2–40	20	120	8.0 (H_2)	10	2.7	0.08	[55]
Rh/SiO_2	2–40	20	120	8.0 (H_2)	10	2.7	1.0	[55]

m_{gly}/m_c—glycerol/catalyst mass ratio; $Y_{1,3\text{-PG}}$—yield to 1,3-PG.

In general, the results indicate that increasing the glycerol concentration produces a decrease in conversion, regardless of the catalytic system considered and the operating condition of the liquid phase [55] or vapor phase [140,141]. This effect is due to the lower availability of active sites at high glycerol concentrations, since the catalyst mass does not change but the glycerol content does. On the other hand, selectivity to 1,3-PG depends on

the glycerol concentration and decreases with an increasing concentration in the presence of Ru [55] and Pt [141,142] based catalysts.

Table 8. The effect of glycerol concentration in the vapor phase using continuous flow reactors.

Catalyst	Range (wt.%)	Operative Value (wt.%)	T (°C)	P (MPa)	SV (h^{-1})	$Y_{1,3\text{-PG}}$ (%)	Ref.
Pt-WO_3/SBA-15	5–20	10	210	0.1 (H_2)	1.02 (WHSV)	36.1	[140]
Pt/$AlPO_4$	5–20	10	260	0.1 (H_2)	1.02 (WHSV)	35.4	[141]

SV—space velocity; $Y_{1,3\text{-PG}}$—yield to 1,3-PG.

4.2. Effect of Initial Water Concentration

Due to the presence of water in crude glycerol (20–50 wt.%), its effect has also been studied for different catalytic systems.

Regarding the initial water content in the glycerol solution, there are several aspects to consider. It has been reported that a minimum water content in the starting glycerol solution is necessary, since its presence inhibits side reactions of glycerol dehydration to undesired products [154] such as the dehydration of 1,3-PG to allyl alcohol [155] as well as condensation reactions between the glycerol and side products such as EG, EtOH, and MeOH [156]. Moreover, in continuous flow steam-phase reactors, it is desirable to minimize the water content to produce energy savings in vaporization [155], but its presence allows for vaporization of the glycerol solution to be achieved at lower temperature.

Several studies have reported that when the water content is very high, the hydrogenolysis of glycerol can lead to the formation of C–C bond cleavage products such as EtOH [154]. From another point of view, a techno-economic study has been reported to carry out the purification of 1,2-PG by distillation in stages. The first stage consists in separating the water from the liquid products, then separating the unreacted glycerol and finally the 1,2-PG from the rest of the products, especially EG. The economic study determined that the separation of water in the first distillation stage was the costliest step of the whole purification [157].

Regarding the performance of the catalysts, since water is generated as a by-product during hydrogenolysis, it is better to work with low water contents in the starting solution to shift the equilibrium toward product formation.

In this regard, Nakagawa et al. studied the effect of increasing the glycerol concentration from 5 to 80 wt.% by decreasing the water content from 95 to 20 wt.% using Ir-ReO_x/SiO_2 catalysts in the presence of H-ZSM-5. Their results showed an increase in glycerol conversion from 31% to 51% with a slight increase in selectivity to 1,3-PG [78]. The same effect was reported by Varghese et al. who, employing the Ir-ReO_x/SiO_2 catalyst, observed an increase in glycerol conversion from 40 to 53% with a maintenance in selectivity at 1,3-PG (~40%) when the water content decreased from 98 to 80 wt.% at 120 °C, 8 MPa, and 24 h reaction [89].

4.3. Effect of the Solvent

Since water has a negative effect on the activity of the catalysts and their selectivity to 1,3-PG, the replacement of water by other solvents has been a focus of study. Among the solvents used in the hydrogenolysis reaction, aprotic and aprotic solvents have been used.

Regarding the use of aprotic solvents, sulfolane, N-methylimidazole, and 1,3-dimethyl-2-imidazolidinone (DMI) have been mainly employed in the production of 1,3-PG [57,66,110,138]. Chaminand et al. carried out tests to obtain 1,3-PG using a Rh/C catalyst in the presence of H_2WO_4 and sulfolane as the solvent. After 168 h of reaction, they obtained a glycerol conversion of 32% with a selectivity to 1,3-PG of 12%, reaching low yields of this product (~4%) [57]. Kurosaka et al. prepared catalysts from Pt, Pd, Rh, and Ru supported on different traditional oxides such as ZrO_2, TiO_2, Al_2O_3, and zeolites such as HY and AlMCM-41, all modified with WO_3. After 18 h of reaction, they obtained 24% yield to 1,3-PG, employing 65 wt.% glycerol solutions in 1,3-dimethyl-2-imidazolidinone (DMI) at 170 °C and 8 MPa H_2 [66]. Oh et al. employed Pt catalysts supported on sulfated ZrO_2 in the

presence of 1,3-dimethyl-2-imidazolidinone (DMI), obtaining 66% glycerol conversion with a selectivity to 1,3-PG of 83% at 170 °C and 7.3 MPa H_2 after 24 h of reaction [110]. Low yields to 1,3-PG were obtained in the presence of N-methylimidazole and sulfolane as solvents employing a $Pt/WO_3/TiO_2/SiO_2$ catalyst at 180 °C and 5.5 MPa H_2 [97].

The use of protic solvents, on the other hand, has the advantage that many of them are H_2 donor substances that allow H_2 to be generated in situ and thus improve the performance of the catalysts. Moreover, it has been reported that in the presence of protic solvents such as MeOH and EtOH, the H_2 solubility is much higher than in water [158]. There are, however, some drawbacks. Since glycerol and hydrogen donor substances compete for the same active sites in the hydrogenolysis process, there should be a balance between the amount of glycerol and the amount of hydrogen donor substance to achieve high conversion and selectivity to the desired product [146]. In addition, the use of protic solvents such as EtOH and MeOH favors the formation of condensation products such as glyceryl ethers [152].

For the production of 1,2-PG, MeOH, EtOH, 2-POH, formic acid [145–147,157,159,160], and EG [161] have been used as protic solvents. Strikingly, in the production of 1,3-PG, only the use of MeOH [152], water, and EtOH [97,152,162,163] have been evaluated. Of all of them, water and EtOH have been shown to be the best solvents due to their ability to ionize and generate H^+, which favor the formation of, 1,3-PG, since they act as Brønsted acid sites on the surface of the catalysts, as it is in the case of Pt/WO_3-ZrO_2. These sites allow for the anchoring of the central –OH group on the glycerol molecule and its subsequent cleavage to produce 1,3-PG. The generation of H^+ on the catalytic surface avoids steric hindrance of the anchoring of the central –OH group on the glycerol molecule unlike other acidic sites, which benefits the formation of 1,3-PG [162,163]. In this regard, Gong et al. reported improved glycerol conversion and selectivity to 1,3-PG in the presence of water and EtOH as solvents, employing a $Pt/WO_3/TiO_2/SiO_2$ catalyst at 180 °C and 5.5 MPa H_2 [97]. Cai et al. reported similar results employing a Co–Al catalyst, obtaining the best selectivity to 1,3-PG in the presence of water due to the H^+ transfer capacity of water and its high polarity [152].

4.4. Effect of Temperature

The kinetics of the hydrogenolysis reaction is a function of temperature and, therefore, the formation of 1,3-PG, 1,2-PG and other products such as MeOH, EtOH, and EG depends on this operating variable.

It has been found that an increase in temperature causes an increase in glycerol conversion with a loss in selectivity to 1,3-PG due to the formation of side products such as 1-POH, EG, EtOH, MeOH, and gases.

It is worth mentioning that temperature is also a critical parameter in reactor operation, and severe thermal conditions can lead to high energy demands, which increases the operating costs of the hydrogenolysis process [164].

Tables 9 and 10 show the thermal effect study for different catalysts. For each of them, the tables also show the thermal range studied, the operating conditions under which the study was carried out, and the optimum temperature that maximizes the yield to 1,3-PG.

Table 9. The thermal effect studied in batch reactors using different catalysts.

Catalyst	Range (°C)	$T_{optimum}$ (°C)	P (MPa)	m_{gly}/m_c	t (h)	$Y_{1,3\text{-PG}}$ (%)	Ref.
Ir-ReO_x/H-ZSM-5	180–240	220	4.0 (H_2)	42.0	4	2.0	[83]
Ir-ReO_x/SiO_2	100–200	120	8.0 (H_2)	20.0	24	17.5	[89]
Pt/WO_3/TiO_2/SiO_2	160–190	180	5.5 (H_2)	2.0	12	7.7	[97]
Pt/Au/WO_3	140–180	155	5.0 (H_2)	2.0	12	22.5	[101]
Pt-Ru/WO_x/Al_2O_3	140–180	170	4.0 (H_2)	3.0	36	38.9	[114]
Pt/WO_x/S-TiO_2	100–130	120	4.0 (H_2)	1.3	8	36.0	[117]
Ni-Zr/H-β	150–250	200	4.1 (H_2)	40.0	10	10.8	[165]
Pt-WO_x/SAPO-34	170–210	210	6.0 (H_2)	5.0	80	12.0	[166]

m_{gly}/m_c—glycerol/catalyst mass ratio; $Y_{1,3\text{-PG}}$—yield to 1,3-PG.

Table 10. The thermal effect studied in continuous flow reactors using different catalysts.

Catalyst	Range (°C)	$T_{optimum}$ (°C)	P (MPa)	SV (h^{-1})	$Y_{1,3\text{-PG}}$ (%)	Ref.
Pt/WO_3/ZrO_2	110–140	130	4.0 (H_2)	0.25 (LHSV)	32.0	[62]
Pt-$H_4SiW_{12}O_{40}$/SiO_2	180–210	200	5.0 (H_2)	0.045 (WHSV)	22.0	[118]
Pt-$H_2Li_2SiW_{12}O_{40}$/SiO_2	160–220	180	5.0 (H_2)	0.09 (WHSV)	23.3	[119]
Pt-$H_3PMo_{12}O_{40}$/SiO_2	160–240	180	5.0 (H_2)	0.09 (WHSV)	2.1	[120]
Pt-$H_3PW_{12}O_{40}$/SiO_2	160–240	180	5.0 (H_2)	0.09 (WHSV)	8.4	[120]
Pt-$H_4SiW_{12}O_{40}$/SiO_2	160–240	180	5.0 (H_2)	0.09 (WHSV)	11.6	[120]
Pt/WO_3/Al_2O_3	240–300	260	0.1 (H_2)	0.14 (WHSV)	13.8	[139]
Pt-WO_3/SBA-15	150–250	210	0.1 (H_2)	1.02 (WHSV)	36.1	[140]
Pt/$AlPO_4$	150–280	260	0.1 (H_2)	1.02 (WHSV)	35.4	[141]
Pt/H-MOR	150–250	225	0.1 (H_2)	1.02 (WHSV)	46.1	[143]
Pt-Cu/H-MOR	150–240	210	0.1 (H_2)	1.02 (WHSV)	52.6	[143]
Pt/S-MMT	160–220	200	0.1 (H_2)	1.02 (WHSV)	58.2	[144]
Cu-$H_4SiW_{12}O_{40}$/SiO_2	180–230	210	0.36 (H_2)	0.08 (WHSV)	21.7	[155]

SV—space velocity; $Y_{1,3\text{-PG}}$—yield to 1,3-PG.

4.5. Effect of Pressure

The effect of pressure was studied using batch reactors (Table 11) and continuous flow reactors (Table 12).

Table 11. The effect of pressure in batch reactors using different catalysts.

Catalyst	Range (MPa)	$P_{optimum}$ (MPa)	T (°C)	m_{gly}/m_c	t (h)	$Y_{1,3\text{-PG}}$ (%)	Ref.
Ir-ReO_x/SiO_2	2.0–8.0 (H_2)	8.0 (H_2)	120	26.8	36	38.0	[60]
Pt/WO_x/Al_2O_3	5.0–9.0 (H_2)	9.0 (H_2)	200	6.0	4	38.5	[66]
IrO_x/H-ZSM-5	2.0–8.0 (H_2)	8.0 (H_2)	180	2.4	24	23.9	[82]
Ir-ReO_x/H-ZSM-5	2.0–8.0 (H_2)	8.0 (H_2)	220	42.0	4	2.7	[83]
Pt/WO_3/TiO_2/SiO_2	4.5–6.0 (H_2)	5.5 (H_2)	180	2.0	12	7.7	[97]
Pt/Au/WO_3	1.0–5.0 (H_2)	5.0 (H_2)	155	2.0	12	22.5	[101]
Pt/W+Al/SBA-15	4.0–8.0 (H_2)	6.0 (H_2)	160	1.5	12	33.0	[107]
Pt-Ru/WO_x/Al_2O_3	7.0–11.0 (H_2)	9.0 (H_2)	170	3.0	36	38.9	[114]
Pt/WO_x/S-TiO_2	0.5–6.0 (H_2)	4.0 (H_2)	120	1.3	4	36.0	[117]
Ni-Zr/H-β	2.1–8.3 (H_2)	4.1 (H_2)	200	40.0	10	10.8	[165]
Pt-WO_x/SAPO-34	3.0–6.0 (H_2)	6.0 (H_2)	210	5.0	80	12.0	[166]
Pt/WO_3/Al_2O_3/ SiO_2	2.0–7.0 (H_2)	6.0 (H_2)	160	1.5	12	26.6	[167]

m_{gly}/m_c—glycerol/catalyst mass ratio; $Y_{1,3\text{-PG}}$—yield to 1,3-PG.

Table 12. The effect of pressure in continuous flow reactors using different catalysts.

Catalyst	Range (MPa)	$P_{optimum}$ (MPa)	T (°C)	SV (h^{-1})	$Y_{1,3\text{-PG}}$ (%)	Ref.
$Pt/WO_3/ZrO_2$	2.0–5.0 (H_2)	4.0 (H_2)	130	0.25 (LHSV)	32.0	[62]
$Pt\text{-}H_4SiW_{12}O_{40}/SiO_2$	3.0–6.0 (H_2)	6.0 (H_2)	200	0.045 (WHSV)	31.4	[118]
$Cu\text{-}H_4SiW_{12}O_{40}/SiO_2$	0.1–0.54 (H_2)	0.54 (H_2)	210	0.10 (WHSV)	26.8	[155]

SV—space velocity; $Y_{1,3\text{-PG}}$—yield to 1,3-PG.

In the liquid phase, using batch reactors, it has been reported that an increase in H_2 pressure generates an increase in glycerol conversion as well as an increase in selectivity to 1,3-PG, using catalysts based on noble metals such as Pt [66,97,101,107,114,117,166,167] and Ir [60,82,83] and non-noble metals such as Ni [165].

The effect of pressure on the conversion and selectivity was also tested in the liquid phase using continuous flow reactors of the trickle bed type and the results obtained were similar to those reported in batch reactors [62]. In general, the results obtained have been attributed to a higher solubility of H_2 in the liquid phase, which allows for hydrogenation of the intermediate in the formation of 1,3-PG.

Increasing the pressure generates two benefits. On one hand, it allows the liquid phase condition to be maintained, and on the other hand, it increases the H_2 solubility, improving the selectivity to 1,3-PG. However, reactors operating at higher pressures presuppose not only a higher fixed cost associated with the equipment, but also a higher operating cost and potential safety risks during H_2 handling [47,164].

Very few articles have been published in which the effect of pressure has been studied when the reaction is conducted in the vapor phase, and they report an increase in the conversion and selectivity at 1,3-PG [118,155] due to the effect of pressure.

4.6. Effect of H_2 Flow

Table 13 shows the results of the H_2 flux study in both the liquid phase (trickle bed reactors) and vapor phase (fixed bed reactors) conditions by using different catalytic systems.

Table 13. The effect of H_2 flow in continuous flow reactors.

Catalyst	Range ($cm^3\ min^{-1}$)	H_2 $Flow_{optimum}$ ($cm^3\ min^{-1}$)	P (MPa)	T (°C)	SV (h^{-1})	$Y_{1,3\text{-PG}}$ (%)	Ref.
$Pt\text{-}WO_3/SBA\text{-}15$	40–100	80	0.1 (H_2)	210	1.02 (WHSV)	36.1	[140]
$Pt/AlPO_4$	60–140	140	0.1 (H_2)	260	1.02 (WHSV)	35.4	[141]
Pt/H-MOR	20–80	60	0.1 (H_2)	225	1.02 (WHSV)	46.1	[142]
Pt-Cu/MOR	40–100	80	0.1 (H_2)	210	1.02 (WHSV)	52.6	[143]
Pt/S-MMT	30–90	70	0.1 (H_2)	200	1.02 (WHSV)	58.2	[144]

SV—space velocity; $Y_{1,3\text{-PG}}$—yield to 1,3-PG.

The results have indicated that an increase in H_2 flux generates an increase in glycerol conversion due to increased H_2 availability at the catalytic surface, which generates the increased hydrogenation of reaction intermediates to form 1,3-PG. It has been observed that in some cases, the selectivity to 1,3-PG increases with increasing H_2 flux up to a certain point, after which it decreases due to the generation of side products [140,141,143].

4.7. Effect of Reaction Time

The effect of reaction time has been studied by several authors using batch reactors operating in the liquid phase condition (Table 14).

Table 14. The effect of reaction time in the liquid phase using batch reactors.

Catalyst	Range (h)	$t_{optimum}$ (h)	T (°C)	P (MPa)	m_{gly}/m_c	$Y_{1,3\text{-PG}}$ (%)	Ref.
Ir-ReO_x/SiO_2	1–48	36	120	8.0 (H_2)	26.7	38.0	[59]
Co-Ir nanorods	2–16	12	200	3.0 (H_2)	66.7	20.8	[77]
Ru-Ir-ReO_x/SiO_2	4–24	24	120	8.0 (H_2)	26.7	30.3	[80]
IrO_x/H-ZSM-5	6–48	24	180	8.0 (H_2)	2.4	23.9	[82]
Ir-ReO_x/H-ZSM-5	1–8	8	220	4.0 (H_2)	42.0	2.8	[83]
Ir-ReO_x/SiO_2	6–48	24	120	8.0 (H_2)	20.0	17.5	[89]
Pt/$WO_3/TiO_2/SiO_2$	6–24	12	180	5.5 (H_2)	2.0	7.7	[97]
Pt/W+Al/SBA-15	8–24	12	160	6.0 (H_2)	1.5	33.0	[107]
Pt/WO_x/Ta_2O_5	1–24	24	160	5.0 (H_2)	9.0	29.6	[109]
Pt-Ru/WO_x/Al_2O_3	3–36	36	170	9.0 (H_2)	3.0	38.9	[114]
Pt/W-MCFs	6–24	24	150	4.0 (H_2)	3.0	65.0	[116]
Ni-Zr/H-β	5–15	10	200	4.1 (H_2)	40.0	10.8	[165]
Pt-WO_x/SAPO-34	5–80	80	210	6.0 (H_2)	5.0	12.0	[166]
Pt/WO_3/Al_2O_3/ SiO_2	2–20	12	160	6.0 (H_2)	1.5	26.6	[167]

m_{gly}/m_c—glycerol/catalyst mass ratio; $Y_{1,3\text{-PG}}$—yield to 1,3-PG.

Naturally, the conversion of glycerol in batch reactors increases as the reaction time increases. This effect was reported for several catalytic systems based on noble metals such as Pt [97,107,109,114,116,166,167] and Ir [59,80,82,83,89], and on non-noble metals such as Ni [165] and Co [77].

As the conversion increases, there is a decrease in selectivity to 1,3-PG due to the generation of side products such as 1-POH and propane. Since the conversion increases as the reaction time increases, the selectivity at 1,3-PG decreases, and there is an optimum time to obtain the maximum yield to these products.

4.8. Effect of Space Velocity

For continuous flow reactors, both in the liquid phase [118] and in the vapor phase condition [139,140,142,144,155], the special velocity (WHSV) has been studied using different catalytic systems (Table 15).

Table 15. The effect of space velocity in continuous flow reactors.

Catalyst	Range (h^{-1})	$SV_{optimum}$ (h^{-1})	P (MPa)	T (°C)	$Y_{1,3\text{-PG}}$ (%)	Ref.
Pt-$H_4SiW_{12}O_{40}/SiO_2$	0.03–0.15	0.045 (WHSV)	5.0 (H_2)	200	22.0	[118]
Pt/WO_3/Al_2O_3	0.09–0.14	0.14 (WHSV)	0.1 (H_2)	260	13.8	[139]
Pt-WO_3/SBA-15	1.02–4.08	1.02 (WHSV)	0.1 (H_2)	210	36.1	[140]
Pt/H-MOR	1.02–4.08	1.02 (WHSV)	0.1 (H_2)	225	46.1	[142]
Pt-Cu/H-MOR	1.02–4.08	1.02 (WHSV)	0.1 (H_2)	210	52.6	[143]
Pt/S-MMT	1.02–4.08	1.02 (WHSV)	0.1 (H_2)	200	58.2	[144]
Cu-$H_4SiW_{12}O_{40}/SiO_2$	0.025–0.12	0.065 (WHSV)	0.36 (H_2)	190	17.8	[155]

SV—space velocity; $Y_{1,3\text{-PG}}$—yield to 1,3-PG.

It has been reported that high WHSV values lead to lower conversions due to low contact times [118,139,140,142,144]. In some cases, high WHSV values have led to obtaining high selectivity to 1,3-PG [118], while in other cases, the selectivity values have been low [140,142–144,155] due to the formation of side products due to high contact times. In a

number of studies, it has been indicated that there is an optimum WHSV value for which the yield to glycols is the maximum [118,155].

5. Stability and Reusability of Catalysts

From previous sections, it can be concluded that Ir and Pt based catalysts are promising for the formation of 1,3-PG, in particular, those consisting of Ir-ReO_x/SiO_2 and Pt/WO_x supported on ZrO_2, SBA-15, and Al_2O_3.

In this section, we discuss the stability of such catalytic systems and the possibility of their reuse in successive reaction cycles, given their potential use for an industrial application.

5.1. Ir-ReO_x/SiO_2 Catalysts

Luo et al. reported the stability of Ir-ReO_x/SiO_2 catalysts in liquid-phase continuous flow reactors employed in the form of egg-shell pellets. The catalytic thickness in these systems was controlled using an ethanol solution with different concentrations (20–30 wt.%) to perform the impregnation, first with the H_2IrCl_6 precursor and then with the NH_4ReO_4 precursor.

The catalyst showed a conversion of 60% with a selectivity to 1,3-PG of 31% at 130 °C and 8 MPa H_2. After 36 h of reaction, the glycerol conversion reached a maximum (~65%) and then progressively decreased to reach half that value only at 468 h of reaction. In the first 36 h of reaction, the selectivity to 1,3-PG increased from 31 to 40% and after 500 h of reaction, the yield to 1,3-PG only decreased from 19 to 13%. The cause of deactivation in these catalysts was the agglomeration and sintering of the Ir particles, together with a loss in the interfacial area of the sites and their acidity [127].

5.2. Pt/WO_x/ZrO_2 Catalysts

Wang et al. tested $Pt/WO_x/ZrO_2$ catalysts in a continuous flow reactor at 150 °C and 4 MPa H_2 using 40 wt.% glycerol solutions. Their results showed that the catalyst was stable for 200 h when the water content was 20 wt.% (i.e., with 80 wt.% glycerol solutions). With more dilute solutions (40, 60 wt.%), the catalyst undergoes deactivation, showing a drop in conversion of almost 50% after 200 h of reaction.

This phenomenon was attributed to the loss of W by leaching, which is favored in the presence of water. By modifying the catalyst with Mg (0.5 wt.%), the authors avoided the deactivation phenomenon, making the catalyst stable for 400 h under the same reaction conditions.

The presence of Mg decreased the degree of polymerization of the WO_x species and also increased the stability of the W species on the ZrO_2 surface, avoiding the loss of W by leaching and therefore obtaining a more stable catalyst.

Moreover, among their results, Wang et al. proved that monoclinic ZrO_2 was more stable as a support than tetragonal ZrO_2, since the latter tends to form monoclinic ZrO_2 under the hydrothermal conditions of the reaction [127].

In order to improve the stability, Zhu et al. added $Li_2B_4O_7$ to the $Pt/WO_x/ZrO_2$ catalyst in the 0.5–2 wt.% range, which favored the dispersion of the Pt particles and increased the total number of acid sites, increasing the interaction between the metal phase and the support. At 150 °C and 4 MPa H_2, the catalyst with 1 wt.% $Li_2B_4O_7$ (Pt-1LiB/WZr) allowed for the most stable catalyst with an average yield to 1,3-PG of 45% being stable for more than 200 h to be obtained [126].

The authors further studied the effect of the WHSV on the catalytic stability over the Pt-1LiB/WZr catalyst. The glycerol conversion was relatively high and stable when the WHSV was equal to 0.1 h^{-1} and 0.2 h^{-1}. However, as the WHSV increased to 0.3 h^{-1}, glycerol conversion decreased significantly with time evolution. The higher stability was attributed to the fact that $Li_2B_4O_7$ could restrain the reduction of tetragonal zirconium after hydrothermal treatment and reaction by strengthening the interaction between the active components and support.

Another Li modifier, based on a partial replacement of a Keggin acid ($H_2Li_2SiW_{12}O_{40}$), was also used to improve the stability of $Pt/WO_x/ZrO_2$ catalysts. At 180 °C and 5 MPa H_2 using 10 wt.% glycerol solutions, this catalyst was stable for 120 h of reaction in a continuous flow reactor operating in the liquid phase. The characterization revealed a preservation of the Keggin structure as well as of the Pt particles [119].

5.3. Pt/WO$_x$/SBA-15 Catalysts

The $Pt/WO_x/SBA$-15 catalysts were tested in batch reactors operating in the liquid phase and were relatively stable at 150 °C and 4 MPa H_2 after four reaction cycles of 30 h in the presence of 30 wt.% glycerol solutions. The results showed a slight decrease in conversion (~3%), which was attributed to the loss of catalytic material between one reaction cycle and the next. In all cases, the selectivity to 1,3-PG remained invariant (~70%) [67].

In the vapor phase condition at 210 °C and 0.1 MPa H_2, employing continuous flow reactors, Priya et al. also observed a slight drop in conversion (~5%), but with a decrease in selectivity to 1,3-PG being more pronounced (~8%) (Figure 20). In this case, the authors reported the formation of carbonaceous deposits on the catalytic surface, probably due to the higher severity of the operating condition [140].

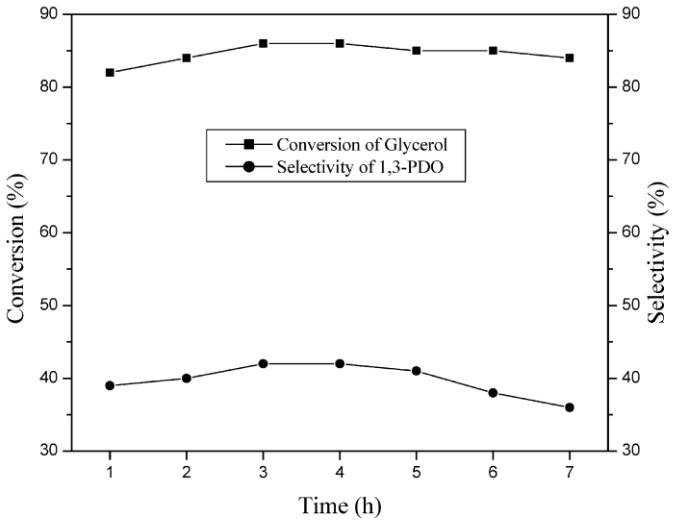

Figure 20. The glycerol conversion and selectivity to 1,3-PG employing $Pt/WO_x/SBA$-15 catalysts. Reaction conditions: 210 °C, 0.1 MPa H_2, 1.02 h^{-1} WHSV. Reproduced from [140] with permission from the American Chemical Society (ACS).

5.4. Pt/WO$_x$/Al$_2$O$_3$ Catalysts

Lei et al. studied the stability of $Pt/WO_x/Al_2O_3$ catalysts in a liquid phase continuous flow reactor at 180 °C and 5 MPa H_2 using 50 wt.% glycerol solutions. Their results initially showed a glycerol conversion of 57% with a selectivity to 1,3-PG of 40%. After 100 h of reaction, the conversion decreased to ~45% and began to decrease steadily to 25% conversion at 600 h of reaction, after which time it remained constant. The selectivity to 1,3-PG, on the other hand, remained unchanged for 700 h of reaction. The characterization results revealed a preservation in the structure of the WO_x/Al_2O_3 support but an agglomeration of the Pt particles, leading to an increase in particle size from 1.9 to 3.1 nm. This increase in particle size led to a decrease in the Brønsted acid sites created at the Pt–WO_x interface, causing catalyst deactivation [168].

Numpilai et al. carried out tests with $Pt/WO_x/Al_2O_3$ catalysts in batch reactors operating in the liquid phase at 220 °C and 6 MPa H_2 using 30 wt.% glycerol solutions and 5 h reaction time (Figure 21).

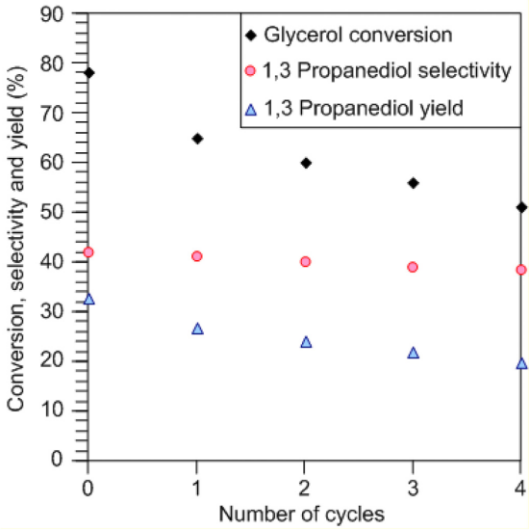

Figure 21. The glycerol conversion, selectivity, and yield to 1,3-PG employing $Pt/WO_x/Al_2O_3$ catalysts. Reaction conditions: 220 °C, 6 MPa H_2, 30 wt.% glycerol solution, 5 h. Reproduced from [104] with permission from the American Chemical Society (ACS).

The results showed that even regenerating the catalyst in H_2 flow at 300 °C after each use, the yield to 1,3-PG decreased from 31 to 19% after the fourth reaction cycle. The characterization results indicated the formation of carbon deposits on the catalytic surface, which would cause the deactivation phenomenon [104].

In contrast to the previously obtained results, Yan et al. tested the $Pt/Al\text{-}WO_x$ catalysts in batch reactors at 140 °C and 3 MPa H_2 using 5 wt.% glycerol solutions and observed no apparent catalyst deactivation (Figure 22).

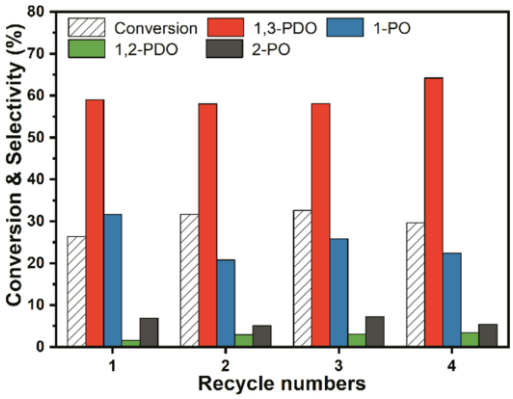

Figure 22. The glycerol conversion and selectivity to liquid products by employing the $Pt/Al\text{-}WO_x$ catalyst. Reaction conditions: 140 °C, 3 MPa H_2, 5 wt.% glycerol solution, 4 cycles of 12 h. Reproduced from [98] with permission from Elsevier.

The glycerol conversion and selectivity to 1,3-PG were maintained after four cycles of 12 h reaction each [98]. The addition of alumina as a promoter improved the catalytic properties. The characterization revealed that the high activity and selectivity of the $Pt/Al\text{-}WO_x$ catalyst was a result of the increased amount of oxygen vacancies in the in situ generation of WO_x species, which enhanced the selective adsorption of glycerol and in situ Brønsted acid sites for the selective activation of secondary C–O bonds, which greatly increases the hydrogenolysis yield.

For the $Pt\text{-}Au/WO_x/Al_2O_3$ catalysts, which became even more active by modification of the metal phase, Wang et al. also observed a drop in conversion from 41 to 35% after four reaction cycles of 12 h each at 180 °C and 5 MPa H_2 using 10 wt.% glycerol solutions.

The results showed that the introduction of a very small amount of Au (up to 0.1 wt.%) into the Pt/W/Al catalyst led to an increase in the yield to 1,3-PG (Figure 23).

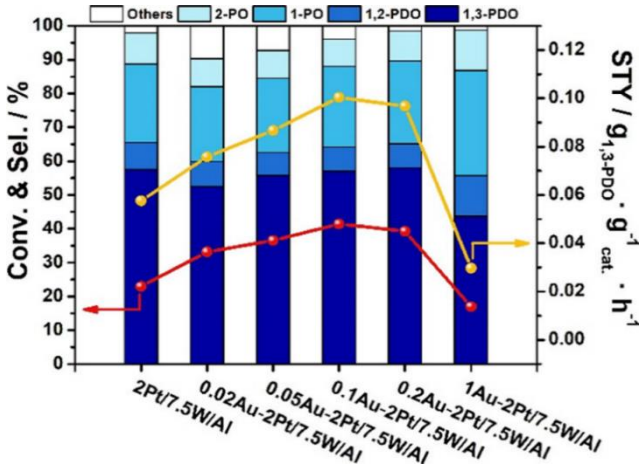

Figure 23. The performance of the Pt-Au/WO_x/Al_2O_3 catalysts (%Au = 0, 0.02, 0.05, 0.1, 0.2, 1). Reaction conditions: 180 °C, 5 MPa H_2, 10 wt.% glycerol solutions, 12 h. Reproduced from [115] with permission from the American Chemical Society (ACS).

Structural characterization reveals that Au likely exists as single atoms and binds to WO_x, forming Au–WO_x clusters that interact with Pt at the periphery of the Pt nanoparticles. The presence of Au alleviates the Pt-WOx SMSI by electron transfer from W to Au, thus allowing a more exposed Pt surface, hence enhancing the H spillover ability, and the latter is positively related to the formation of strong Brønsted acid sites responsible for the attack of the secondary C–O bond of glycerol.

The selectivity to 1,3-PG remains practically constant after four reaction cycles (Figure 24), and the small decrease in activity can be attributed to a joint effect of Pt particle agglomeration with the formation of coke deposits [115].

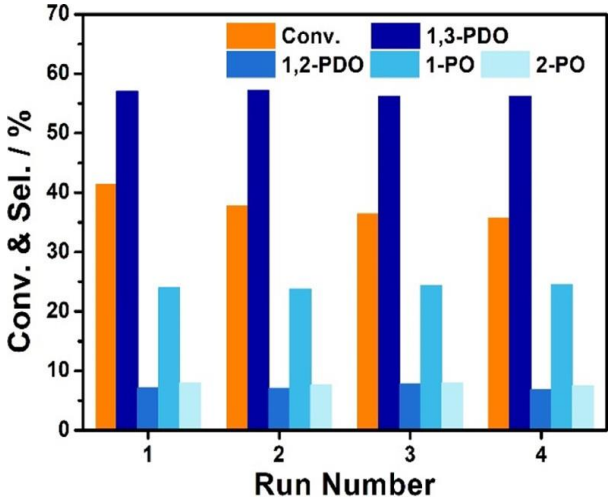

Figure 24. The glycerol conversion and selectivity to liquid products employing Pt-Au/WO_x/Al_2O_3 catalysts. Reaction conditions: 180 °C, 5 MPa H_2, 10 wt.% glycerol solutions, four cycles of 12 h. Reproduced from [115] with permission from the American Chemical Society (ACS).

6. Conclusions, Future Work, and Perspectives

The synthesis of 1,3-PG from glycerol obtained as a by-product in biodiesel production offers an attractive alternative route to those currently implemented in the petrochemical industry.

However, the steric hindrance of the secondary –OH group in the glycerol molecule makes hydrogenolysis to 1,3-PG more difficult than the hydrogenolysis of glycerol to 1,2-PG. Of the four reaction mechanisms leading to the formation of 1,3-PG by glycerol hydrogenolysis, the dehydration–hydrogenation mechanism and the direct mechanism of hydrogenolysis have been the most widely reported.

The glycerol hydrogenolysis reaction can be carried out in batch reactors or flow reactors operating in the liquid phase or in flow reactors operating in the vapor phase. Experience shows that the highest yields to 1,3-PG are obtained by operating in the liquid phase, with batch reactors and flow reactors being the best alternatives. The selection of the optimum operating condition in these reactors involves determining the temperature, pressure, reaction time, space velocity, H_2 flow, and concentration of glycerol, water, and eventually some solvent to maximize the yield at 1,3-PG, as appropriate.

Glycerol hydrogenolysis is a catalyst structure-sensitive reaction, requiring a metal for the activation of the H_2 molecule coupled with an oxyphilic promoter for the activation of the secondary hydroxyl group of the glycerol molecule. Pt-based catalysts supported on WO_x and heteropolyacids, and other systems based on Ir, Rh modified with ReO_x, in addition to some catalysts based on non-noble metals, have been reported. In the case of catalysts based on Pt and heteropolyacids, the presence of Brønsted acid sites favors the formation of the intermediate 3-HPA, which is then hydrogenated on the metal sites to form 1,3-PG, giving priority in this case to the dehydration–hydrogenation mechanism. On the other hand, in the catalytic systems based on WO_x and ReO_x, the generation of H^+ and H^- species intervene in the formation of alkoxide-type intermediates that favor the formation of 1,3-PG by means of a direct mechanism of hydrogenolysis.

Of all the catalysts studied thus far, it is possible to establish the following order of activity, taking into account the yields at 1,3-PG at the optimum reaction condition:

$$Pt/WO_x/AlOOH\ (66\%) > Pt/W\text{-}MCFs\ (65\%) > Pt/WO_x/SBA\text{-}15\ (61\%) > Pt/WO_x/ZrO_2\ (49\%) > Ir\text{-}ReO_x/SiO_2\ (38\%)$$

The results indicate that it is possible to produce 1,3-PG with yields of 38–66% in the range of 120–180 °C and 4–8 MPa H_2 operating in batch reactors in the liquid phase condition.

The stability analysis indicates that the hydrothermal condition of the reaction affects the structural stability of the supports (Al_2O_3, ZrO_2, SiO_2), being required for its stabilization by some thermal method or the incorporation of other elements (Li, Mg). On the other hand, the sintering by agglomeration of Pt metal particles, the loss by leaching of W species, and the formation of carbonaceous deposits have been identified as the main mechanisms of deactivation of the catalysts studied.

The yields at 1,3-PG obtained with current catalytic systems (38–66%) suggest that the formation of 1,3-PG is a disadvantage with respect to other hydrogenolysis products such as 1,2-PG. From a thermodynamic point of view, it has been reported that the formation of 3-HPA, intermediate in the formation of 1,3-PG, is thermodynamically unstable but kinetically stable, while for acetol, an intermediate in the formation of 1,2-PG, exactly the opposite occurs. This aspect is key for the design of a suitable catalyst, so it is necessary to have thermodynamic studies in the liquid phase to establish the values of conversion and selectivity to 1,3-PG to determine whether its formation is limited by equilibrium, considering, in addition, other side products in the hydrogenolysis reaction.

The design of better catalysts should be based on finishing the right set of textural, acidic, and structural properties that allow for the values reported by thermodynamics to be reached. In this sense, catalytic systems with adequate density and type of acid site, high dispersion of the metal phase, and good stability in the hydrothermal condition of the reaction are required. Due to the costs of metal phases based on noble metals, the optimization of the metal content should be a factor to be taken into account in the design of these catalysts, or their partial replacement by other less expensive metal phases.

In order to design reactors with industrial application, kinetic studies should be carried out for the formation of 1,3-PG, involving the possibility of using crude glycerol as

feedstock. In addition, techno-economic and environmental impact studies would be useful for the analysis of the process in the framework of the design of glycerol biorefineries.

Author Contributions: Conceptualization, M.N.G. and F.P.; Methodology, M.N.G.; Validation, M.N.G., F.P. and N.N.N.; Formal analysis, M.N.G. and F.P.; Investigation, M.N.G.; Resources, N.N.N.; Data curation, F.P.; Writing—original draft preparation, M.N.G.; Writing—review and editing, F.P.; Visualization, M.N.G. and F.P.; Supervision, N.N.N.; Project administration, N.N.N.; Funding acquisition, N.N.N. All authors have read and agreed to the published version of the manuscript.

Funding: This research was funded by the Consejo Nacional de Investigaciones Científicas y Técnicas (CONICET), grant number PIP 0065, and the University of La Plata (UNLP), grant number I-248.

Data Availability Statement: Data reported was taken from papers included in the references.

Acknowledgments: M.N.G. thanks the University of La Plata (UNLP) for awarding him the 2019 Young Research Grant.

Conflicts of Interest: The authors declare no conflict of interest.

References

1. Corma, A.; Iborra, A.; Velty, A. Chemical Routes for the Transformation of Biomass into Chemicals. *Chem. Rev.* **2007**, *107*, 2411–2502. [CrossRef] [PubMed]
2. Moreira Neto, J.; Komesu, A.; Da Silva Martins, L.H.; Gonçalves, V.O.O.; Rochade Oliveira, J.A.; Rai, M. Third generation biofuels: An overview. In *Sustainable Bioenergy*; Elsevier, B.V.: Amsterdam, The Netherlands, 2019; Chapter 10, pp. 283–298, ISBN 9780128176542. [CrossRef]
3. Quispe, C.A.G.; Coronado, C.J.R.; Carvalho, A.J., Jr. Glycerol: Production, consumption, prices, characterization and new trends in combustion. *Renew. Sustain. Energy Rev.* **2013**, *27*, 475–493. [CrossRef]
4. Carriquiry, M.A. A comparative analyisis of the development of the United States and European Union biodiesel industries. *AgEcon* **2007**, bp070051. [CrossRef]
5. OCDE-FAO. Biocombustibles. In *Perspectivas Agrícolas 2017–2026*; OCDE Publishing: Paris, France, 2018. Available online: https://www.fao.org/3/BT092s/BT092s.pdf (accessed on 23 June 2022).
6. Bianchi, C.L.; Canton, P.; Dimitratos, N.; Porta, F.; Prati, L. Methanol Adsorption and Oxidation on Gold, Platinum and Gold-Platinum Bimetallic Clusters: A Case Study on Au6, Pt6 and Au3Pt3 Clusters Using Density Functional Theory. *Catal. Today* **2005**, *102–103*, 203–212. [CrossRef]
7. Hosseini, S.A. Nanocatalysts for biodiesel production. *Arab. J. Chem.* **2022**, *15*, 104152. [CrossRef]
8. Meher, L.C.; Sagar, D.V.; Naik, S.N. Technical aspects of biodiesel production by transesterification—A review. *Renew. Sustain. Energy Rev.* **2006**, *10*, 248–268. [CrossRef]
9. Pagliaro, M.; Rossi, M. *The Future of Glycerol*; Royal Society of Chemistry (RSC): Cambridge, UK, 2010; ISBN 978-1-84973-046-4.
10. Fonseca Amaral, P.F.; Ferreira, T.F.; Cardoso Fontes, G.; Zarur Coelho, M.A. Glycerol valorization: New biotechnological routes. *Food Bioprod. Processing* **2009**, *87*, 179–186. [CrossRef]
11. Available online: https://www.trademap.org/Country_SelProduct_TS.aspx?nvpm=3%7c%7c%7c%7c%7c1520%7c%7c%7c4%7c1%7c1%7c2%7c2%7c1%7c2%7c3%7c1%7c1 (accessed on 23 June 2022).
12. Anitha, M.; Kamarudin, S.K.; Kofli, N.T. The potential of glycerol as a value-added commodity. *Chem. Eng. J.* **2016**, *295*, 119–130. [CrossRef]
13. Jérome, F.; Kharchafi, G.; Adam, J.; Barrault, I. "One pot" and selective synthesis of monoglycerides over homogeneous and heterogeneous guanidinecatalysts. *Green Chem.* **2004**, *6*, 72–74. [CrossRef]
14. Melero, J.A.; Vicente, G.; Morales, G.; Paniagua, M.; Moreno, J.M.; Roldán, R.; Ezquerro, A.; Pérez, C. Acid-catalyzed etherification of bio-glycerol and isobutylene over sulfonic mesostructured sílicas. *Appl. Catal. A Gen.* **2008**, *346*, 44–51. [CrossRef]
15. Buffoni, I.N.; Gatti, M.N.; Santori, G.F.; Pompeo, F.; Nichio, N.N. Hydrogen from glycerol steam reforming with a platinum catalyst supported on a SiO_2-C composite. *Int. J. Hydrogen Energy* **2017**, *42*, 12967–12977. [CrossRef]
16. Almena, A.; Martín, M. Technoeconomic Analysis of the Production of Epichlorohydrin from Glycerol. *Ind. Eng. Chem. Res.* **2016**, *55*, 3226–3238. [CrossRef]
17. Li, J.; Wang, T. Chemical equilibrium of glycerol carbonate synthesis from glycerol. *J. Chem. Thermodyn.* **2011**, *43*, 731–736. [CrossRef]
18. Cavani, F.; Guidetti, S.; Marinelli, L.; Piccinini, M.; Ghedini, E.; Signoretto, M. Unexpected events in sulfated zirconia catalyst during glycerol-to-acrolein conversion. *Appl. Catal. B Environ.* **2011**, *100*, 197–204. [CrossRef]
19. Gatti, M.N.; Pompeo, F.; Santori, G.F.; Nichio, N.N. Bio-propylene glycol by liquid phase hydrogenolysis of glycerol with Ni/SiO_2-C catalysts. *Catal. Today* **2017**, *296*, 26–34. [CrossRef]
20. Available online: www.alibaba.com (accessed on 23 June 2022).
21. Market Research Future, 1,3-Propanediol Market Research Report—Forecast to 2023. 2020. Available online: https://www.marketresearchfuture.com/reports/1-3-propanediol-market-5722 (accessed on 23 June 2022).

22. Million Insights, 1,3-Propanediol (PDO) Market to Be Driven by Rising Infiltration of Polyurethane & High Demand for Polyesters Till 2022 | Million Insights. 2020. Available online: https://www.millioninsights.com/industry-reports/1-3-propanediol-pdo-market?utm_source=prnewswire%26utm_medium=referral%26utm_campaign=prn_09Jan2020_pdo_rd2 (accessed on 23 June 2022).
23. Vivek, N.; Pandey, A.; Binod, P. An efficient aqueous two phases systems using dual inorganic electrolytes to separate 1,3-propanediol from the fermented broth. *Bioresour. Technol.* **2018**, *254*, 239–246. [CrossRef]
24. Vivek, N.; Pandey, A.; Binod, P. Chapter 31—Production and applications of 1,3-propanediol. In *Current Developments in Biotechnology and Bioengineering*; Elsevier, B.V.: Amsterdam, The Netherlands, 2017; pp. 719–738, ISBN 9780444636621. [CrossRef]
25. Tjahjasari, D.; Kaeding, T.; Zeng, A.P. 1,3-propanediol and polytrimethyleneterephthalate. In *Comprehensive Biotechnology*; Elsevier, B.V.: Amsterdam, The Netherlands, 2011; pp. 229–242. [CrossRef]
26. Nakagawa, Y.; Tomishige, K. Heterogeneous catalysis of the glycerol hydrogenolysis. *Catal. Sci. Technol.* **2011**, *1*, 179–190. [CrossRef]
27. Gallezot, P. Process options for converting renewable feedstocks to bioproducts. *Green Chem.* **2007**, *9*, 295–302. [CrossRef]
28. West, R.M.; Kunkes, E.L.; Simonetti, D.A.; Dumesic, J.A. Catalytic conversion of biomass-derived carbohydrates to fuels and chemicals by formation and upgrading of mono-functional hydrocarbon intermediates. *Catal. Today* **2009**, *147*, 115–125. [CrossRef]
29. Knifton, J.F.; James, T.G.; Allen, K.D.; Weider, P.R.; Powell, J.B.; Slaugh, L.H. One-Step Production of Propanedol from Ethylene Oxide and Syngas with a Catalyst. U.S. Patent 6,576,802, 10 June 2003.
30. Haas, T.; Arntz, D. Process for the Preparation of 1,3-Propanediol. U.S. Patent 5,364,987, 15 November 1994.
31. Hilaly, A.K.; Binder, T.P. Method of Recovering 1,3-Propanediol from Fermentation Broth. U.S. Patent 6,479,716, 19 September 2002.
32. Nakamura, C.E.; Gatenby, A.A.; Hsu, A.K.-H.; La Reau, R.D.; Haynie, S.L.; Diaz-Torres, M.; Trimbur, D.E.; Whited, G.M.; Nagarajan, V.; Payne, M.S.; et al. Method for the Production of 1,3-Propanediol by Recombinant Microorganisms. U.S. Patent 6,013,494, 11 January 2000.
33. Biebl, H. Glycerol fermentation of 1,3-propanediol by Clostridium butyricum. Measurement of product inhibition by use of a pH-auxostat. *Appl. Microbiol. Biotechnol.* **1991**, *35*, 701–705. [CrossRef]
34. Günzel, B.; Yonsel, S.; Deckwer, W.-D. Fermentative production of 1,3-propanediol from glycerol by Clostridium butyricum up to a scale of 2 m^3. *Appl. Microbiol. Biotechnol.* **1991**, *36*, 289–294. [CrossRef]
35. Boenigk, R.; Bowien, S.; Gottschalk, G. Fermentation of glycerol to 1,3-propanediol in continuous cultures of Citrobacter freundii. *Appl. Microbiol. Biotechnol.* **1993**, *38*, 453–457. [CrossRef]
36. Barbirato, F.; Camarasaclaret, C.; Grivet, J.P.; Bories, A. Glycerol fermentation by a new 1,3-propanediol-producing microorganism:Enterobacter agglomerans. *Appl. Microbiol. Biotechnol.* **1995**, *43*, 786–793. [CrossRef]
37. Cameron, D.C.; Altaras, N.E.; Hoffman, M.L.; Shaw, A.J. Metabolic Engineering of Propanediol Pathways. *Biotechnol. Prog.* **1998**, *14*, 116–125. [CrossRef] [PubMed]
38. Himmi, E.H.; Bories, A.; Barbirato, F. Nutrient requirements for glycerol conversion to 1,3-propanediol. *Clostridium Butyricum Bioresour. Technol.* **1999**, *67*, 123–128. [CrossRef]
39. Nimlos, M.R.; Blanksby, S.J.; Qian, X.; Himmel, M.E.; Johnson, D.K. Mechanisms of Glycerol Dehydration. *J. Phys. Chem. A* **2006**, *110*, 6145–6156. [CrossRef] [PubMed]
40. Feng, J.; Xu, B.; Liu, D.; Xiong, W.; Wang, J. Production of 1,3-Propanediol by Catalytic Hydrogenolysis of Glycerol. *Adv. Mater. Res.* **2013**, *791–793*, 16–19. [CrossRef]
41. Nakagawa, Y.; Tamura, M.; Tomishige, K. Catalytic materials for the hydrogenolysis of glycerol to 1,3-propanediol. *J. Mater. Chem. A* **2014**, *2*, 6688–6702. [CrossRef]
42. Wang, J.; Yang, M.; Wang, A. Selective hydrogenolysis of glycerol to 1,3-propanediol over Pt-W based catalysts. *Chin. J. Catal.* **2020**, *41*, 1311–1319. [CrossRef]
43. Wu, F.; Jiang, H.; Zhu, X.; Lu, R.; Shi, L.; Lu, F. Effect of Tungsten Species on Selective Hydrogenolysis of Glycerol to 1,3-Propanediol. *ChemSusChem* **2021**, *14*, 569–581. [CrossRef]
44. Dias da Silva Ruy, A.; De Brito Alves, R.M.; Reis Hewer, T.L.; De Aguiar Pontes, D.; Sena Gomes Teixeira, L.; Magalhaes Pontes, L.A. Catalysts for glycerol hydrogenolysis to 1,3-propanediol: A review of chemical routes and market. *Catal Today* **2021**, *381*, 243–253. [CrossRef]
45. Zhang, D.; Zhang, Q.; Zhou, Z.; Li, Z.; Meng, K.; Fang, T.; You, Z.; Zhang, G.; Yin, B.; Shen, J.; et al. Hydrogenolysis of Glycerol to 1,3-Propanediol: Are Spatial and Electronic Configuration of "Metal-Solid Acid" Interface Key for Active and Durable Catalysts? *ChemCatChem* **2022**, *14*, 202101316. [CrossRef]
46. Montassier, C.; Giraud, D.; Barbier, J. Rolyol conversion by liquid phase heterogeneous catalysis over metals. *Stud. Surf. Sci. Catal.* **1988**, *41*, 165–170. [CrossRef]
47. Dasari, M.A.; Kiatsimkul, P.; Sutterlin, W.R.; Suppes, G.J. Low-pressure hydrogenolysis of glycerol to propylene glycol. *Appl. Catal. A Gen.* **2005**, *281*, 225–231. [CrossRef]
48. Maglinao, R.L.; He, B.B. Verification of propylene glycol preparation from glycerol via the acetol pathway by in situ hydrogenolysis. *Biofuels* **2012**, *3*, 675–682. [CrossRef]
49. Yfanti, L.; Lemonidou, A.A. Mechanistic study of liquid phase glycerol hydrodeoxygenation with in-situ generated hydrogen. *J. Catal.* **2018**, *368*, 98–111. [CrossRef]

50. Feng, J.; Wang, J.; Zhou, Y.; Fu, H.; Chen, H.; Li, X. Effect of Base Additives on the Selective Hydrogenolysis of Glycerol over Ru/TiO2 Catalyst. *Chem. Lett.* **2007**, *36*, 1274–1275. [CrossRef]
51. Miyazawa, T.; Kusunoki, Y.; Kunimori, K.; Tomishige, K. Glycerol conversion in the aqueous solution under hydrogen over Ru/C + an ion-exchange resin and its reaction mechanism. *J. Catal.* **2006**, *240*, 213–221. [CrossRef]
52. Guan, J.; Wang, X.C.; Wang, X.Y.; Mu, X.D. Thermodynamics of glycerol hydrogenolysis to propanediols over supported copper clusters: Insights from first-principles study. *Sci. China Chem.* **2013**, *56*, 763–772. [CrossRef]
53. Zeng, A.; Biebl, H. Bulk Chemicals from Biotechnology: The Case of 1,3-Propanediol Production and the New Trends. *Adv. Biochem. Eng. Biotechnol.* **2002**, *74*, 237–257. [CrossRef]
54. Perosa, A.; Tundo, P. Selective Hydrogenolysis of Glycerol with Raney Nickel. *Ind. Eng. Chem. Res.* **2005**, *44*, 8535–8537. [CrossRef]
55. Furikado, I.; Miyazawa, T.; Koso, S.; Shimao, A.; Kunimori, K.; Tomishige, K. Catalytic performance of Rh/SiO_2 in glycerol reaction under hydrogen. *Green Chem.* **2007**, *9*, 582–588. [CrossRef]
56. Kusunoki, Y.; Miyazawa, T.; Kunimori, K.; Tomishige, K. Highly active metal–acid bifunctional catalyst system for hydrogenolysis of glycerol under mild reaction conditions. *Catal. Commun.* **2005**, *6*, 645–649. [CrossRef]
57. Chaminand, J.; Djakovitch, L.; Gallezot, P.; Marion, P.; Pinel, C.; Rosier, C. Glycerol hydrogenolysis on heterogeneous catalysts. *Green Chem.* **2004**, *6*, 359–361. [CrossRef]
58. Shinmi, Y.; Koso, S.; Kubota, T.; Nakagawa, Y.; Tomishige, K. Modification of Rh/SiO_2 catalyst for the hydrogenolysis of glycerol in water. *Appl. Catal. B Environ.* **2010**, *94*, 318–326. [CrossRef]
59. Nakagawa, Y.; Shinmi, Y.; Koso, S.; Tomishige, K. Direct hydrogenolysis of glycerol into 1,3-propanediol over rhenium-modified iridium catalyst. *J. Catal.* **2010**, *272*, 191–194. [CrossRef]
60. Amada, Y.; Shinmi, Y.; Koso, S.; Kubota, T.; Nakagawa, Y.; Tomishige, K. Reaction mechanism of the glycerol hydrogenolysis to 1,3-propanediol over $Ir–ReOx/SiO_2$ catalyst. *Appl. Catal. B Environ.* **2011**, *105*, 117–127. [CrossRef]
61. Guan, J.; Chen, X.; Peng, G.; Wang, X.; Cao, Q.; Lan, Z.; Mu, X. Role of ReOx in Re modified Rh/ZrO_2 and Ir/ZrO_2 catalysts in glycerol hydrogenolysis: Insights from first principles study. *Chin. J. Catal.* **2013**, *34*, 1656–1666. [CrossRef]
62. Qin, L.Z.; Song, M.J.; Chen, C.L. Aqueous-phase deoxygenation of glycerol to 1,3-propanediol over $Pt/WO_3/ZrO_2$ catalysts in a fixed-bed reactor. *Green Chem.* **2010**, *12*, 1466–1472. [CrossRef]
63. Liu, L.; Zhang, Y.; Wang, A.; Zhang, T. Mesoporous WO_3 Supported Pt Catalyst for Hydrogenolysis of Glycerol to 1,3-Propanediol. *Chin. J. Catal.* **2012**, *33*, 1257–1261. [CrossRef]
64. Arundhathi, R.; Mizugaki, T.; Mitsudome, T.; Jitsukawa, K.; Kaneda, K. Highly Selective Hydrogenolysis of Glycerol to 1,3-Propanediol over a Boehmite-Supported Platinum/Tungsten Catalyst. *ChemSusChem* **2013**, *6*, 1345–1347. [CrossRef] [PubMed]
65. García-Fernández, S.; Gandarias, I.; Requies, J.; Güemez, M.B.; Bennici, S.; Auroux, A.; Arias, P.L. New approaches to the $Pt/WO_x/Al_2O_3$ catalytic system behavior for the selective glycerol hydrogenolysis to 1,3-propanediol. *J. Catal.* **2015**, *323*, 65–75. [CrossRef]
66. García-Fernández, S.; Gandarias, I.; Requies, J.; Soulimani, F.; Arias, P.L.; Weckhuysen, B.M. The role of tungsten oxide in the selective hydrogenolysis of glycerol to 1,3-propanediol over $Pt/WO_x/Al_2O_3$. *Appl. Catal. B Environ.* **2017**, *204*, 260–272. [CrossRef]
67. Fan, Y.; Cheng, S.; Wang, H.; Ye, D.; Xie, S.; Pei, Y.; Hu, H.; Hua, W.; Li, Z.H.; Qiao, M.; et al. Nanoparticulate Pt on mesoporous SBA-15 doped with extremely low amount of W as highly selective catalyst for glycerol hydrogenolysis to 1,3-propanediol. *Green Chem.* **2017**, *19*, 2174–2183. [CrossRef]
68. Chia, M.; Pagan-Torres, Y.J.; Hibbitts, D.; Tan, Q.; Pham, H.N.; Datye, A.K.; Neurock, M.; Davis, R.J.; Dumesic, J.A. Selective Hydrogenolysis of Polyols and Cyclic Ethers over Bifunctional Surface Sites on Rhodium_Rhenium Catalysts. *J. Am. Chem. Soc.* **2011**, *133*, 12675–12689. [CrossRef]
69. Wang, S.; Liu, H. Selective hydrogenolysis of glycerol to propylene glycol on Cu–ZnO catalysts. *Catal. Lett.* **2007**, *117*, 62–67. [CrossRef]
70. Gebretsadik, F.B.; Llorca, J.; Salagre, P.; Cesteros, Y. Hydrogenolysis of glycidol as alternative route to obtain selectively 1,3-propanediol using MO_x modified Ni-Cu catalysts supported on acid mesoporous saponite. *ChemCatChem* **2017**, *9*, 3670–3680. [CrossRef]
71. Che, T.M. Production of Propanediols. U.S. Patent 4,642,394, 10 February 1987.
72. Drent, E.; Jager, W.W. Hydrogenolysis of Glycerol. U.S. Patent 6,080,898, 27 June 2000.
73. Schlaf, M.; Ghosh, P.; Fagan, P.J.; Hauptman, E.; Bullock, R.M. Metal-catalyzed selective deoxygenation of diols to alcohols. *Angew. Chem. Int. Ed.* **2001**, *40*, 3887–3890. [CrossRef]
74. Alhanash, A.; Kozhevnikova, E.F.; Kozhevnikov, I.V. Hydrogenolysis of Glycerol to Propanediol Over Ru: Polyoxometalate Bifunctional Catalyst. *Catal. Lett.* **2008**, *120*, 307–311. [CrossRef]
75. Shimao, A.; Koso, S.; Ueda, N.; Shinmi, Y.; Furikado, I.; Tomishige, K. Promoting Effect of Re Addition to Rh/SiO_2 on Glycerol Hydrogenolysis. *Chem. Lett.* **2009**, *38*, 540–541. [CrossRef]
76. Pamphile-Adrián, A.J.; Florez-Rodriguez, P.P.; Pires, M.H.M.; Perez, G.; Passos, F.B. Selective hydrogenolysis of glycerol over Ir-Ni bimetallic catalysts. *Catal. Today* **2017**, *289*, 302–308. [CrossRef]
77. Liu, Q.; Cao, X.; Wang, T.; Wang, C.; Zhang, Q.; Ma, L. Synthesis of shape controllable cobalt nanoparticles and the shape dependent performance in glycerol hydrogenolysis. *RSC Adv.* **2015**, *5*, 4861–4871. [CrossRef]

78. Nakagawa, Y.; Ning, X.; Amada, Y.; Tomishige, K. Solid acid co-catalyst for the hydrogenolysis of glycerol to 1,3-propanediol over Ir-ReO_x/SiO_2. *Appl. Catal. A Gen.* **2012**, *433–434*, 128–134. [CrossRef]
79. Liu, L.; Kawakami, S.; Nakagawa, Y.; Tamura, M.; Tomishige, K. Highly Active Iridium- Rhenium Catalyst Condensed on Silica Support for Hydrogenolysis of Glycerol to 1,3-Propanediol. *Appl. Catal. B. Environ.* **2019**, *256*, 117775. [CrossRef]
80. Tamura, M.; Amada, Y.; Liu, S.; Yuan, Z.; Nakagawa, Y.; Tomishige, K. Promoting effect of Ru on Ir-ReO_x/SiO_2 catalyst in hydrogenolysis of glycerol. *J. Mol. Catal. A Chem.* **2014**, *388–389*, 177–187. [CrossRef]
81. Liu, L.; Asano, T.; Nakagawa, Y.; Tamura, M.; Okumura, K.; Tomishige, K. Selective Hydrogenolysis of Glycerol to 1,3-Propanediol over Rhenium-Oxide-Modified Iridium Nanoparticles Coating Rutile Titania Support. *ACS Catal.* **2019**, *9*, 10913–10930. [CrossRef]
82. Wan, X.; Zhang, Q.; Zhu, M.; Zhao, Y.; Liu, Y.; Zhou, C.; Yang, Y.; Cao, Y. Interface synergy between IrOx and H-ZSM-5 in selective C–O hydrogenolysis of glycerol toward 1,3-propanediol. *J. Catal.* **2019**, *375*, 339–350. [CrossRef]
83. Chanklang, S.; Mondach, W.; Somchuea, P.; Witoon, T.; Chareonpanich, M.; Faungnawakij, K.; Seubsai, A. Hydrogenolysis of glycerol to 1,3-propanediol over H-ZSM-5-supported iridium and rhenium oxide catalysts. *Catal. Today* **2022**, *397–399*, 356–364. [CrossRef]
84. Deng, C.; Leng, L.; Zhou, J.; Zhou, X.; Yuan, W. Effects of pretreatment temperature on bimetallic Ir-Re catalysts for glycerol hydrogenolysis. *Chin. J. Catal.* **2015**, *36*, 1750–1758. [CrossRef]
85. Deng, C.; Leng, L.; Duan, X.; Zhou, J.; Zhou, X.; Yuan, W. Support effect on the bimetallic structure of Ir–Re catalysts and theirperformances in glycerol hydrogenolysis. *J. Mol. Catal. A Chem.* **2015**, *410*, 81–88. [CrossRef]
86. Gilkey, M.J.; Brady, C.; Vlachos, D.C.; Xu, B. Characterization of Oxidation States in Metal/Metal Oxide Catalysts in Liquid-Phase Hydrogenation Reactions with a Trickle Bed Reactor. *Ind. Eng. Chem. Res.* **2018**, *57*, 5591–5598. [CrossRef]
87. Amada, Y.; Watanabe, H.; Tamura, M.; Nakagawa, Y.; Okumura, K.; Tomishige, K.; Phys, J. Structure of ReOx Clusters Attached on the Ir Metal Surface in Ir-ReO_x/SiO_2 for the Hydrogenolysis Reaction. *Chem. C* **2012**, *116*, 23503–23514. [CrossRef]
88. Lan, M.A.; Yuming, L.; Dehua, H. Glycerol Hydrogenolysis to Propanediols over Ru-Re/SiO_2: Acidity of Catalyst and Role of Re. *Chin. J. Catal.* **2011**, *32*, 872–876. [CrossRef]
89. Varghese, J.J.; Cao, L.; Robertson, C.; Yang, Y.; Gladden, L.F.; Lapkin, A.A.; Mushrif, S.H. Synergistic Contribution of the Acidic Metal Oxide−Metal Couple and Solvent Environment in the Selective Hydrogenolysis of Glycerol: A Combined Experimental and Computational Study Using ReOx−Ir as the Catalyst. *ACS Catal.* **2019**, *9*, 485–503. [CrossRef]
90. Deng, C.; Duan, X.; Zhou, J.; Zhou, X.G.; Yuan, W.; Scott, S.L. Ir-Re alloy as a highly active catalyst for the hydrogenolysis of glycerol to 1,3-propanediol. *Catal. Sci. Technol.* **2015**, *5*, 1540–1547. [CrossRef]
91. Kurosaka, T.; Maruyama, H.; Naribayashi, I.; Sasaki, Y. Production of 1,3-propanediol by hydrogenolysis of glycerol catalyzed by Pt/WO_3/ZrO_2. *Catal. Commun.* **2008**, *9*, 1360–1363. [CrossRef]
92. Daniel, O.M.; De La Riva, A.; Kunkes, E.L.; Datye, A.K.; Dumesic, J.A.; Davis, R.J. X-ray Absorption Spectroscopy of Bimetallic Pt–Re Catalysts for Hydrogenolysis of Glycerol to Propanediols. *ChemCatChem* **2010**, *2*, 1107–1114. [CrossRef]
93. Falcone, D.D.; Hack, J.H.; Klyushin, A.Y.; Knop-Gericke, A.; Schlögl, R.; Davis, R.J. Evidence for the Bifunctional Nature of Pt−Re Catalysts for Selective Glycerol Hydrogenolysis. *ACS Catal.* **2015**, *5*, 5679–5695. [CrossRef]
94. Dam, J.T.; Djanashvili, K.; Kapteijn, F.; Hanefeld, U. Pt/Al_2O_3 Catalyzed 1,3-Propanediol Formation from Glycerol using Tungsten Additives. *ChemCatChem* **2013**, *5*, 497–505. [CrossRef]
95. Mai, C.T.Q.; Ng, F.T.T. Effect of Metals on the Hydrogenolysis of Glycerol to Higher Value Sustainable and Green Chemicals Using a Supported HSiW Catalyst. *Org. Process Res. Dev.* **2016**, *20*, 1774–1780. [CrossRef]
96. Gu, M.; Shen, Z.; Yang, L.; Peng, B.; Dong, W.; Zhang, W.; Zhang, Y. The Effect of Catalytic Structure Modification on Hydrogenolysis of Glycerol to 1,3-Propanediol over Platinum Nanoparticles and Ordered Mesoporous Alumina Assembled Catalysts. *Ind. Eng. Chem. Res.* **2017**, *56*, 13572–13581. [CrossRef]
97. Gong, L.F.; Lu, Y.; Ding, Y.; Lin, R.; Li, J.; Dong, W.; Wang, T.; Chen, W. Selective hydrogenolysis of glycerol to 1,3-propanediol over a Pt/$WO_3/TiO_2/SiO_2$ catalyst in aqueous media. *Appl. Catal. A Gen.* **2010**, *390*, 119–126. [CrossRef]
98. Yang, M.; Wu, K.; Sun, S.; Ren, Y. Regulating oxygen defects via atomically dispersed alumina on Pt/WOx catalyst for enhanced hydrogenolysis of glycerol to 1,3-propanediol. *Appl. Catal. B Environ.* **2022**, *307*, 121207. [CrossRef]
99. Wang, J.; Lei, N.; Yang, C.; Su, Y.; Zhao, X.; Wang, A. Effect of promoters on the selective hydrogenolysis of glycerol over Pt/W-containing catalysts. *Chin. J. Catal.* **2016**, *37*, 1513–1519. [CrossRef]
100. Zhao, X.; Wang, J.; Yang, M.; Lei, N.; Li, L.; Hou, B.; Miao, S.; Pan, X.; Wang, A.; Zhang, T. Selective Hydrogenolysis of Glycerol to 1,3-Propanediol: Manipulating the Frustrated Lewis Pairs by Introducing Gold to Pt/WOx. *ChemSusChem* **2017**, *10*, 819–824. [CrossRef]
101. Yang, C.; Zhang, F.; Lei, N.; Yang, M.; Liu, F.; Miao, Z.; Sun, Y.; Zhao, X.; Wang, A. Understanding the Promotional Effect of Au on Pt/WO_3 in the Hydrogenolysis of Glycerol to 1,3-Propanediol. *Chin. J. Catal.* **2018**, *39*, 1366–1372. [CrossRef]
102. Fan, Y.; Cheng, S.; Wang, H.; Tian, J.; Xie, S.; Pei, Y.; Qiao, M.; Zong, B. Pt–WO_x on monoclinic or tetrahedral ZrO_2: Crystal phase effect ofzirconia on glycerol hydrogenolysis to 1,3-propanediol. *Appl. Catal. B Environ.* **2017**, *217*, 331–341. [CrossRef]
103. Saelee, T.; Limsoonthakul, P.; Aphichoksiri, P.; Rittiruam, M.; Lerdpongsiripaisarn, M.; Miyake, T.; Yamashita, H.; Mori, K.; Kuwahara, Y.; Praserthdam, S.; et al. Experimental and computational study on roles of WO_x promoting strong metal support promoter interaction in Pt catalysts during glycerol hydrogenolysis. *Sci. Rep.* **2021**, *11*, 530. [CrossRef]

104. Numpilai, T.; Cheng, C.K.; Seubsai, A.; Faungnawakij, K.; Limtrakul, J.; Witoon, T. Sustainable utilization of waste glycerol for 1,3-propanediol production over $Pt/WO_x/Al_2O_3$ catalysts: Effects of catalyst pore sizes and optimization of synthesis conditions. *Environ. Pollut.* **2021**, *272*, 116029. [CrossRef]
105. Jarauta-Córdoba, C.; Bengoechea, M.O.; Agirrezabal-Telleria, I.; Arias, P.L.; Gandarias, I. Insights into the Nature of the Active Sites of $Pt\text{-}WO_x/Al_2O_3$ Catalysts for Glycerol Hydrogenolysis into 1,3-Propanediol. *Catalysts* **2021**, *11*, 1171. [CrossRef]
106. Zhao, B.; Liang, Y.; Liu, L.; He, Q.; Dong, J.X. Facilitating $Pt\text{-}WO_x$ Species Interaction for Efficient Glycerol Hydrogenolysis to 1,3-Propanediol. *ChemCatChem* **2021**, *13*, 3695–3705. [CrossRef]
107. Feng, S.; Zhao, B.; Liang, Y.; Liu, L.; Dong, J. Improving Selectivity to 1,3-Propanediol for Glycerol Hydrogenolysis Using W- and Al-Incorporated SBA-15 as Support for Pt Nanoparticles. *Ind. Eng. Chem. Res.* **2019**, *58*, 2661–2671. [CrossRef]
108. Zhao, B.; Liang, Y.; Liu, L.; He, Q.; Dong, J. Discovering positively charged Pt for enhanced hydrogenolysis of glycerol to 1,3-propanediol. *Green Chem.* **2020**, *22*, 8254–8259. [CrossRef]
109. Zhao, B.; Liang, Y.; Yan, W.; Liu, L.; Dong, J. A Facile Approach to Tune WO_x Species Combining Pt Catalyst for Enhanced Catalytic Performance in Glycerol Hydrogenolysis. *Ind. Eng. Chem. Res.* **2021**, *60*, 12534–12544. [CrossRef]
110. Oh, J.; Dash, S.; Lee, H. Selective conversion of glycerol to 1,3-propanediol using Pt-sulfated zirconia. *Green Chem.* **2011**, *13*, 2004–2007. [CrossRef]
111. Zhou, W.; Luo, J.; Wang, Y.; Liu, J.; Zhao, Y.; Wang, S.; Ma, X. WO_x Domain Size, Acid Properties and Mechanistic Aspects of Glycerol Hydrogenolysis over $Pt/WO_x/ZrO_2$. *Appl. Catal. B Environ.* **2019**, *242*, 410–421. [CrossRef]
112. Zhao, J.; Hou, B.; Guo, H.; Jia, L.; Niu, P.; Chen, C.; Xi, H.; Li, D.; Zhang, J. Insight into the Influence of WO_x-Support Interaction over Pt/W/SiZr Catalysts on 1,3-Propanediol Synthesis from Glycerol. *ChemCatChem* **2022**, *14*, 202200341. [CrossRef]
113. Bhowmik, S.; Enjamuri, N.; Darbha, S. Hydrogenolysis of glycerol in an aqueous medium over Pt/WO_3/zirconium phosphate catalysts studied by 1H NMR spectroscopy. *New J. Chem.* **2021**, *45*, 5013. [CrossRef]
114. Wen, Y.; Shen, W.; Li, Y.; Fang, Y. Promoting effect of Ru in the $Pt\text{-}Ru/WO_x/Al_2O_3$ catalyst for the selective hydrogenolysis of glycerol to 1,3-propanediol, Reaction Kinetics. *Mech. Catal.* **2021**, *132*, 219–233. [CrossRef]
115. Wang, B.; Liu, F.; Guan, W.; Wang, A.; Zhang, T. Promoting the Effect of Au on the Selective Hydrogenolysis of Glycerol to 1,3-Propanediol over the $Pt/WO_x/Al_2O_3$ Catalyst. *ACS Sustain. Chem. Eng.* **2021**, *9*, 5705–5715. [CrossRef]
116. Cheng, S.; Fan, Y.; Zhang, X.; Zeng, Y.; Xie, S.; Pei, Y.; Zeng, G.; Qiao, M.; Zong, B. Tungsten-doped siliceous mesocellular foams-supported platinum catalyst for glycerol hydrogenolysis to 1,3-propanediol. *Appl. Catal. B Environ.* **2021**, *297*, 120428. [CrossRef]
117. Zhou, Z.; Jia, H.; Guo, Y.; Wang, Y.; Liu, X.; Xia, Q.; Li, X.; Wang, Y. The Promotional Effect of Sulfates on TiO_2 Supported $Pt\text{-}WO_x$ Catalyst for Hydrogenolysis of Glycerol. *ChemCatChem* **2021**, *13*, 3953–3959. [CrossRef]
118. Zhu, S.; Zhu, Y.; Hao, S.; Chen, L.; Zhang, B.; Li, Y. Aqueous-Phase Hydrogenolysis of Glycerol to 1,3-propanediol Over $Pt\text{-}H_4SiW_{12}O_{40}/SiO_2$. *Catal. Lett.* **2012**, *142*, 267–274. [CrossRef]
119. Zhu, S.; Gao, X.; Zhu, Y.; Zhu, Y.; Xiang, X.; Hu, C.; Li, Y. Alkaline metals modified $Pt\text{–}H_4SiW_{12}O_{40}/ZrO_2$ catalysts for the selective hydrogenolysis of glycerol to 1,3-propanediol. *Appl. Catal. B Environ.* **2013**, *140–141*, 60–67. [CrossRef]
120. Zhu, S.; Qiu, Y.; Zhu, Y.; Hao, S.; Zheng, H.; Li, Y. Hydrogenolysis of glycerol to 1,3-propanediol over bifunctional catalysts containing Pt and heteropolyacids. *Catal. Today* **2013**, *212*, 120–126. [CrossRef]
121. Zhu, S.; Gao, X.; Zhu, Y.; Li, Y. Promoting effect of WO_x on selective hydrogenolysis of glycerol to 1,3-propanediol over bifunctional $Pt\text{–}WO_x/Al_2O_3$ catalysts. *J. Mol. Catal. A Chem.* **2015**, *398*, 391–398. [CrossRef]
122. Xu, W.; Niu, P.; Guo, H.; Jia, L.; Li, D. Study on the performance of platinum and tungsten bifunctional catalyst supported on Al_2O_3 in the hydrogenolysis of glycerol to 1,3-propanediol. *Fuel Chem. Technol.* **2021**, *49*, 1270–1280. [CrossRef]
123. Xu, W.; Niu, P.; Guo, H.; Jia, L.; Li, D. Hydrogenolysis of glycerol to 1,3-propanediol over a Al_2O_3-supported platinum tungsten catalyst with two-dimensional open structure. *React. Kinet. Mech. Catal.* **2021**, *133*, 173–189. [CrossRef]
124. Zhu, S.; Gao, X.; Zhu, Y.; Cui, J.; Zheng, H.; Li, Y. SiO_2 promoted $Pt/WO_x/ZrO_2$ catalysts for the selective hydrogenolysisof glycerol to 1,3-propanediol. *Appl. Catal. B Environ.* **2014**, *158–159*, 391–399. [CrossRef]
125. Xi, Z.; Hong, Z.; Huang, F.; Zhu, Z.; Jia, W.; Li, J. Hydrogenolysis of Glycerol on the $ZrO_2\text{-}TiO_2$ Supported $Pt\text{-}WO_x$ Catalyst. *Catalysts* **2020**, *10*, 312. [CrossRef]
126. Zhu, M.; Chen, C. Hydrogenolysis of Glycerol to 1,3-Propanediol over $La_2B_4O_7$-Modified Tungsten-Zirconium Composite Oxide Supported Platinum Catalyst. *React. Kinet. Mech. Catal.* **2018**, *124*, 683–699. [CrossRef]
127. Wang, C.; Chen, C. Stabilized Hydrogenolysis of Glycerol to 1,3-Propanediol over Mg Modified $Pt/WO_x\text{-}ZrO_2$ Catalysts. *React. Kinet. Mech. Catal.* **2019**, *128*, 461–477. [CrossRef]
128. Lei, N.; Zhao, X.; Hou, B.; Yang, M.; Zhou, M.; Liu, F.; Wang, A.; Zhang, T. Effective Hydrogenolysis of Glycerol to 1,3-Propanediol over Metal-Acid Concerted $Pt/WO_x/Al_2O_3$ Catalysts. *ChemCatChem* **2019**, *11*, 3903–3912. [CrossRef]
129. Wang, J.; Zhao, X.; Lei, N.; Li, L.; Zhang, L.; Xu, S.; Miao, S.; Pan, X.; Wang, A.; Zhang, T. Hydrogenolysis of Glycerol to 1,3-propanediol under Low Hydrogen Pressure over WO_x-Supported Single/Pseudo- Single Atom Pt Catalyst. *ChemSusChem* **2016**, *9*, 784–790. [CrossRef] [PubMed]
130. Hino, M.; Arata, K. Synthesis of solid superacid of tungsten oxide supported on zirconia and its catalytic action for reactions of butane and pentane. *Chem. Commun.* **1988**, *18*, 1259–1260. [CrossRef]
131. Chen, X.; Chen, C.; Xu, N.; Mou, C. Ga-Promoted Tungstated Zirconia Catalyst for n-Butane Isomerization. *Catal. Lett.* **2003**, *85*, 177–182. [CrossRef]

132. Chen, X.; Chen, C.; Xu, N.; Mou, C. Al- and Ga-promoted WO_3/ZrO_2 strong solid acid catalysts and their catalytic activities in *n*-butane isomerization. *Catal. Today* **2004**, *93–95*, 129–134. [CrossRef]
133. Chen, X.; Du, Y.; Chen, C.; Xu, N.; Mou, C. Highly active and stable n-pentane isomerization catalysts without noble metal containing: Al- or Ga-promoted tungstated zirconia. *Catal. Lett.* **2006**, *187*, 111–193. [CrossRef]
134. Triwahyono, S.; Yamada, T.; Hattori, H. IR study of acid sites on WO_3–ZrO_2 and Pt/WO_3–ZrO_2. *Appl. Catal. A Gen.* **2003**, *242*, 101–109. [CrossRef]
135. Triwahyono, S.; Jalil, A.A.; Hattori, H. Study of Hydrogen Adsorption on Pt/WO_3-ZrO_2 through Pt Sites. *J. Nat. Gas Chem.* **2007**, *16*, 252–257. [CrossRef]
136. Feng, J.; Xu, B. Reaction mechanisms for the heterogeneous hydrogenolysis of biomass-derived glycerol to propanediols. *Prog. React. Kinet. Mech.* **2014**, *39*, 1–15. [CrossRef]
137. Nakagawa, Y.; Tamura, M.; Tomishige, K. Perspective on catalyst development for glycerol reduction to C3 chemicals with molecular hydrogen. *Res. Chem. Intermed.* **2018**, *44*, 3879–3903. [CrossRef]
138. García-Fernandez, S.; Gandarias, I.; Tejido-Núñez, Y.; Requies, J.; Arias, P.L. Influence of the support of bimetallic Pt-WO_x catalysts on the 1,3-propanediol formation from glycerol. *ChemCatChem* **2017**, *9*, 4508–4519. [CrossRef]
139. Edake, M.; Dalil, M.; Mahboub, M.J.D.; Dubois, J.L.; Patience, G.S. Catalytic glycerol hydrogenolysis to 1,3-propanediol in a gas–Solid fluidized bed. *RSC Adv.* **2017**, *7*, 3853–3860. [CrossRef]
140. Priya, S.S.; Kumar, V.P.; Kantam, M.L.; Bhargava, S.K.; Srikanth, A.; Chary, K.V.R. High Efficiency Conversion of Glycerol to 1,3-Propanediol Using a Novel Platinum−Tungsten Catalyst Supported on SBA-15. *Ind. Eng. Chem. Res.* **2015**, *54*, 9104–9115. [CrossRef]
141. Priya, S.S.; Kumar, V.P.; Kantam, M.L.; Bhargava, S.K.; Chary, K.V.R. Catalytic performance of $Pt/AlPO_4$ catalysts for selective hydrogenolysis of glycerol to 1,3-propanediol in the vapour phase. *RSC Adv.* **2014**, *4*, 51893–51903. [CrossRef]
142. Priya, S.S.; Bhanuchander, P.; Kumar, V.P.; Dumbre, D.K.; Periasamy, S.R.; Bhargava, S.K.; Kantam, M.L.; Chary, K.V.R. Platinum Supported on H-Mordenite: A Highly Efficient Catalyst for Selective Hydrogenolysis of Glycerol to 1,3-Propanediol. *ACS Sustain. Chem. Eng.* **2016**, *4*, 1212–1222. [CrossRef]
143. Priya, S.S.; Bhanuchander, P.; Kumar, V.P.; Bhargava, S.K.; Chary, K.V.R. Activity and Selectivity of Platinum−Copper Bimetallic Catalysts Supported on Mordenite for Glycerol Hydrogenolysis to 1,3-Propanediol. *Ind. Eng. Chem. Res.* **2016**, *55*, 4461–4472. [CrossRef]
144. Priya, S.S.; Kandasamy, S.; Bhattacharya, S. Turning Biodiesel Waste Glycerol into 1,3- Propanediol: Catalytic Performance of Sulphuric Acid-Activated Montmorillonite Supported Platinum Catalysts in Glycerol Hydrogenolysis. *Sci. Rep.* **2018**, *8*, 7484. [CrossRef]
145. Gandarias, I.; Arias, P.L.; Requies, J.; El Doukkali, M.; Güemez, M.B. Liquid-phase glycerol hydrogenolysis to 1,2-propanediol under nitrogen pressure using 2-propanol as hydrogen source. *J. Catal.* **2011**, *282*, 237–247. [CrossRef]
146. Gandarias, I.; Arias, P.L.; Fernandez, S.G.; Requies, J.; Doukkali, M.E.; Guemez, M.B. Hydrogenolysis through catalytic transfer hydrogenation: Glycerol conversion to 1,2-propanediol. *Catal. Today* **2012**, *195*, 22–31. [CrossRef]
147. Zhou, C.H.; Deng, K.; Di Serio, M.; Xiao, S.; Tong, D.S.; Li, L.; Lin, C.X.; Beltramini, J.; Zhang, H.; Yu, W.H. Cleaner hydrothermal hydrogenolysis of glycerol to 1,2-propanediol over Cu/oxide catalysts without addition of external hydrogen. *Mol. Catal.* **2017**, *432*, 274–284. [CrossRef]
148. Rode, C.V.; Ghalwadkar, A.A.; Mane, R.B.; Hengne, A.M.; Jadkar, S.T.; Biradar, N.S. Selective Hydrogenolysis of Glycerol to 1,2-Propanediol: Comparison of Batch and Continuous Process Operations. *Org. Process Res. Dev.* **2010**, *14*, 1385–1392. [CrossRef]
149. Jean, D.; Nohair, B.; Bergeron, J.Y.; Kaliaguine, S. Hydrogenolysis of Glycerol over Cu/ZnO-Based Catalysts: Influence of Transport Phenomena Using the Madon−Boudart Criterion. *Ind. Eng. Chem. Res.* **2014**, *53*, 18740–18749. [CrossRef]
150. Hu, J.; Liu, X.; Fan, Y.; Xie, S.; Pei, Y.; Qiao, M.; Fan, K.; Zhang, X.; Zong, B. Physically mixed ZnO and skeletal NiMo for one-pot reforming-hydrogenolysis of glycerol to 1,2-propanediol. *Chin. J. Catal.* **2013**, *34*, 1020–1026. [CrossRef]
151. Rajkhowa, T.; Marin, G.B.; Thybaut, J.W. A comprehensive kinetic model for Cu catalyzed liquid phase glycerolhydrogenolysis. *Appl. Catal. B Environ.* **2017**, *205*, 469–480. [CrossRef]
152. Cai, F.; Song, X.; Wu, Y.; Zhang, J.; Xiao, G. Selective Hydrogenolysis of Glycerol over Acid-Modified Co−Al Catalysts in a Fixed-Bed Flow Reactor. *ACS Sustain. Chem. Eng.* **2018**, *6*, 110–118. [CrossRef]
153. Chiu, C.; Tekeei, A.; Sutterlin, W.R.; Ronco, J.M.; Suppes, G.J. Low-Pressure Packed-Bed Gas Phase Conversion of Glycerol to Acetol. *AIChE J.* **2008**, *54*, 2457–2463. [CrossRef]
154. Maglinao, R.L.; He, B.B. Catalytic Thermochemical Conversion of Glycerol to Simple and Polyhydric Alcohols Using Raney Nickel Catalyst. *Ind. Eng. Chem. Res.* **2011**, *50*, 6028–6033. [CrossRef]
155. Huang, L.; Zhu, Y.; Zheng, H.; Ding, G.; Li, Y. Direct Conversion of Glycerol into 1,3-Propanediol over Cu-$H_4SiW_{12}O_{40}/SiO_2$ in Vapor Phase. *Catal. Lett.* **2009**, *131*, 312–320. [CrossRef]
156. Van Ryneveld, E.; Mahomed, A.S.; Van Heerden, P.S.; Friedrich, H.B. Direct Hydrogenolysis of Highly Concentrated Glycerol Solutions Over Supported Ru, Pd and Pt Catalyst Systems. *Catal. Lett.* **2011**, *141*, 958–967. [CrossRef]
157. Gandarias, I.; Arias, P.L.; Agirrezabal-Telleria, I. Economic Assessment for the Production of 1,2-Propanediol from Bioglycerol Hydrogenolysis Using Molecular Hydrogen or Hydrogen Donor Molecules. *Environ. Prog. Sustain. Energy* **2015**, *35*, 447–454. [CrossRef]

158. Vasiliadou, E.S.; Lemonidou, A.A. Kinetic study of liquid-phase glycerol hydrogenolysis over Cu/SiO_2 catalyst. *Chem. Eng. J.* **2013**, *231*, 103–112. [CrossRef]
159. Cai, F.; Pan, D.; Ibrahim, J.J.; Zhang, J.; Xiao, G. Hydrogenolysis of glycerol over supported bimetallic Ni/Cu catalysts with and without external hydrogen addition in a fixed-bed flow reactor. *Appl. Catal. A Gen.* **2018**, *564*, 172–182. [CrossRef]
160. Gandarias, I.; Requies, J.; Arias, P.L.; Armbruster, U.; Martin, A. Liquid-phase glycerol hydrogenolysis by formic acid over $Ni–Cu/Al_2O_3$ catalysts. *J. Catal.* **2012**, *290*, 79–89. [CrossRef]
161. Zhu, W.; Cai, F.F.; Wang, Y.; Sang, S.Y.; Xiao, G.M. Hydrogenolysis of glycerol to propanediols over supported Ag–Cu catalysts. *Chem. Pap.* **2017**, *71*, 763–773. [CrossRef]
162. Pudi, S.M.; Biswas, P.; Kumar, S.; Sarkar, B. Selective Hydrogenolysis of Glycerol to 1,2-Propanediol Over Bimetallic Cu-Ni Catalysts Supported on γ-Al2O3. *J. Braz. Chem. Soc.* **2015**, *26*, 1551–1564. [CrossRef]
163. Gong, L.F.; Lu, Y.; Ding, Y.; Lin, R.; Li, J.; Dong, W.; Wang, T.; Chen, W. Solvent Effect on Selective Dehydroxylation of Glycerol to 1,3-Propanediol over a $Pt/WO_3/ZrO_2$ Catalyst. *Chin. J. Catal.* **2009**, *30*, 1189–1191. [CrossRef]
164. Sun, P.; Zhang, W.; Yu, X.; Zhang, J.; Xu, N.; Zhang, Z.; Liu, M.; Zhang, D.; Zhang, G.; Liu, Z.; et al. Hydrogenolysis of Glycerol to Propylene Glycol: Energy, Tech-Economic, and Environmental Studies. *Front. Chem.* **2022**, *9*, 778579. [CrossRef]
165. Kant, A.; He, Y.; Jawad, A.; Li, X.; Rezaei, F.; Smith, J.D.; Rownaghi, A.A. Hydrogenolysis of glycerol over Ni, Cu, Zn, and Zr supported on H-beta. *Chem. Eng. J.* **2017**, *317*, 1–8. [CrossRef]
166. Shi, G.; Xu, J.; Song, Z.; Cao, Z.; Jin, K.; Xu, S.; Yan, X. Selective hydrogenolysis of glycerol to 1,3-propanediol over Pt-WOx/SAPO-34 catalysts. *Mol. Catal.* **2018**, *456*, 22–30. [CrossRef]
167. Feng, S.; Zhao, B.; Liu, L.; Dong, J. Platinum Supported on WO_3-Doped Aluminosilicate: A Highly Efficient Catalyst for Selective Hydrogenolysis of Glycerol to 1,3-Propanediol. *Ind. Eng. Chem. Res.* **2017**, *56*, 11065–11074. [CrossRef]
168. Lei, N.; Miao, Z.; Liu, F.; Wang, H.; Pan, X.; Wang, A.; Zhang, T. Understanding the deactivation behavior of $Pt/WO_3/Al_2O_3$ catalyst in the glycerol hydrogenolysis reaction. *Chin. J. Catal.* **2020**, *41*, 1261–1267. [CrossRef]